# Interrogating the interplay between matrix topology, matrix stiffness and aortic smooth muscle cell function

**Teclahymanot Afewerki**

**4578767**

Thesis submission for the degree of Doctor of Philosophy (PhD.)

**September 2022**

Supervisors: Dr Derek Warren and Prof Samuel Fountain

University of East Anglia

School of Pharmacy

Norwich

# Declaration

I declare that the work undertaken in this thesis is my original work, except were acknowledged in the text.

**Teclino Afewerki**

UEA,

School of Pharmacy

I am dedicating this thesis to God Almighty my creator, wisdom, my strong pillar and to my increasable wife and my wonderful children for their understanding and patience, especially my Raei for showing tremendous interest in my research. I also want to dedicate this to my parents- especially my late father who inspired me to dream big and encouraged me to follow my dreams.

# Acknowledgements

I would like to thank God the Almighty for the abundant mercy and grace. Life hasn't been easy, but God's Grace has always kept me grounded.

I would also like to thank my incredible supervisor, Dr Derek Warren, first of all for taking the chance to have me as your PhD student even though my conditions weren't favourable. I can't appreciate you enough for your inconceivable level of fortitude to deal with all my unconventional issues- that you haven't seen before, for standing up for me, and for bringing me this far. I have learned so much more from your leadership, support, and guidance than from all the experience I built over the years. Your unwavering belief that I can do this gave me the courage to come back and finish what I started. You made me feel valued, comfortable, and confident when I was at my lowest. I couldn't have asked for a better mentor during my turbulent days. I haven't enough words to express how grateful I am.

I would also like to thank my secondary supervisor, Prof Samuel Fountain, for our limited encounters. Because of COVID, group meetings were hindered but some of the communications in the lab and the guidance you gave me were very helpful.

I would also like to acknowledge the British Heart Foundation for the financial support and the university of East Anglia for the opportunity to pursue my dream in research science.

I would also like to thank Dr Philip Wilson for his patience, commitment, and dedication to troubleshooting issues with the microscopes through the pandemic. I appreciate your efforts to discover the things that troubled me the most and reassure me that it was problems with the microscopes and not my inability to use them. It won't have been possible to finish without your intervention.

I would also like to extend my gratitude to Dr Sultan Ahmed, for your friendship, guidance, and patience. Thank you for going above and beyond to show me everything that I needed to know in the lab from day one. The late nights in the lab and imaging suites, your extremely competitive aspirations, the silly mistakes, and failed experiments we laughed about and the subjects we touched outside science are memories I will forever cherish. I hope you are winning in everything that you set out to do.

I'm grateful for the support and guidance I received from my first and only postdoc Dr Robert Johnson. I am exceptionally grateful for your help when I was struggling with the loss of my daughter- Aklesia and for your thought-provoking engagements with my progress. I appreciate your friendly and gentle guidance and support in writing my thesis. I would also like

## Access Condition and Agreement

Each deposit in UEA Digital Repository is protected by copyright and other intellectual property rights, and duplication or sale of all or part of any of the Data Collections is not permitted, except that material may be duplicated by you for your research use or for educational purposes in electronic or print form. You must obtain permission from the copyright holder, usually the author, for any other use. Exceptions only apply where a deposit may be explicitly provided under a stated licence, such as a Creative Commons licence or Open Government licence.

Electronic or print copies may not be offered, whether for sale or otherwise to anyone, unless explicitly stated under a Creative Commons or Open Government license. Unauthorised reproduction, editing or reformatting for resale purposes is explicitly prohibited (except where approved by the copyright holder themselves) and UEA reserves the right to take immediate 'take down' action on behalf of the copyright and/or rights holder if this Access condition of the UEA Digital Repository is breached. Any material in this database has been supplied on the understanding that it is copyright material and that no quotation from the material may be published without proper acknowledgement.

# Glossary of Abbreviations

| | |
|---|---|
| ACE | Angiotensin converting enzyme |
| ADP | Adenosine diphosphate |
| Ang II | Angiotensin II |
| APES | 3-Amonopropyltriethoxysilane |
| AR | Aspect ratio |
| Arp2/3 | Actin-related proteins 2 and 3 |
| ATP | Adenosine triphosphate |
| BSA | Bovine Serum Albumin |
| C | Control |
| CA | Cell area |
| $Ca^{2+}$ | Calcium |
| cAMP | Cyclic adenosine monophosphate |
| Co | Colchicine |
| CT | Computerized topography |
| CVD | Cardiovascular disease |
| D | Demecolcine |
| DAG | Diacylglycerol |
| ECM | Extracellular Matrix |
| F-Actin | Filamentous actin |
| FAK | Focal adhesion kinase |
| FTTC | Fourier transform attraction cytometry |
| G | GSM-Tx-4 |
| GAP | GTPase activating protein |
| GDF | GDI displacement factor |
| GDI | Guanine nucleotide dissociation inhibitor |
| GDP | Guanosine diphosphate |
| GEF | Guanine nucleotide exchange factor |
| GEF-H1 | Rho guanine nucleotide exchange factor 1 |
| GPCR | G protein-coupled receptors |
| GRV | Grooved hydrogels |
| GRV | Grooved PAHs |

| | |
|---|---|
| GTP | Guanosine triphosphate |
| HAOSMC | Human aortic smooth muscle cells |
| HMG-CoA | Hydroxy-3-methylutaryl coenzyme A |
| ILK | Integrin-linked kinase |
| IP3 | Inositol triphosphate |
| ITF | Integrated traction force |
| MACF1 | Microtubule-actin cross-linking factor 1 |
| MAPKs | Mitogen-activated protein kinases |
| mDia | Mammalian homolog of diaphanous |
| MLC | Myosin light chain |
| MLCK | Myosin light chain kinase |
| MRCK | Myotonic dystrophy-related Cdc42-binding kinases |
| MRI | Magnetic resonance imaging |
| MTF | Maximal traction force |
| NAT10 | N-Acetyltransferase 10 |
| NM-myosin-II | Non-muscle myosin II |
| NP-40 | NONIDET P-40 |
| PAH | Polyacrylamide hydrogel |
| PAK | P21-activated kinase |
| PBS | Phosphate-buffered saline |
| PDGF | Platelet-derived growth factor |
| PIP2 | Phosphatidylinositol 4,5-biphosphate |
| PIV | Practical image velocimetry |
| PKA | Protein kinase A |
| PKB | Protein kinase B, also known as Akt (serine/threonine-specific protein kinase) |
| PKC | Protein kinase C |
| PKG | Protein kinase G |
| PLC | Phospholipase C |
| pMLC | Phosphatase myosin light chain |
| PTM | Post-translational modification |
| PWV | Pulse wave velocity |
| R | Remodelin |
| ROCK | Rho-associated coiled-coil kinase |

| | |
|---|---|
| ROI | Region of interest |
| RTKs | Receptor tyrosine kinases |
| SAC | Systolic arterial compliance |
| SAC | Stretch activated ion channel |
| SMT | Smooth PAHs |
| SM-Myosin II | Smooth muscle myosin II |
| T | Tubastatin |
| TFM | Traction force microscopy |
| TEMED | Tetramethyl ethylenediamine |
| TS | Traction stress |
| VEGF | Vascular epithelial growth factor |
| VSMC | Vascular smooth muscle cells |
| WASP | Wiskott-Aldrich syndrome protein |

# Abstract

Vascular smooth muscle cells (VSMCs) are the predominant cell type in the arterial wall and normally adopt a quiescent, contractile phenotype to regulate vascular tone. VSMCs are exposed to multiple mechanical cues, including stretch and matrix stiffness, which regulate VSMC contraction. Recent studies have shown that extracellular matrix (ECM) topology and stiffness influence the migration of a variety of cell types. Whilst we have extensive knowledge of how soluble factors regulate VSMC function, our understanding of the importance of matrix-derived cues is limited.

In this study we use polyacrylamide hydrogels (PAHs) of physiological and pathological stiffness, to investigate the interplay between matrix topology, matrix stiffness and VSMC function. To mimic the in vivo features of VSMCs ECM, we used 3D printed micropatterns to develop grooved PAHs, and cells were cultured on smooth and grooved PAHs. VSMCs grown on grooved hydrogels of physiological stiffness were spindle-shaped, less spread than those grown on smooth hydrogels showing fried egg morphology.

Traction force microscopy revealed that VSMCs on the grooved hydrogels of physiological stiffness generated enhanced traction stress compared to their counterparts on smooth hydrogels. VSMCs on grooved hydrogels of pathological stiffness still generated enhanced traction stress however, they displayed similar spreading to VSMCs grown on smooth hydrogels. We also investigated the migrational capacity of VSMCs. VSMCs on grooved hydrogels of physiological stiffness displayed a reduced migrational capacity compared to their counterparts on smooth hydrogels. However, VSMC migrational capacity remained unaltered between grooved and smooth hydrogels of pathological stiffness. Finally, we tested the proliferation rate of VSMCs and the VSMCs on grooved showed a significantly lower proliferation rate than those on smooth PASs, on both healthy and aged/diseased stiffness.

We also investigated the role of novel regulators of VSMCs, however, because previous studies cultured cells on plastic or glass, the information we found wasn't much help and we started with little understanding of their mechanism of action. We found out that the novel regulators of VSMCs' function we used behave differently in different stiffness and topology. Hence, our data demonstrate that matrix topology and stiffness differentially regulate VSMC function and novel regulators respond differently to matrix alteration.

# Table of Contents

# Table of Figures

# List of Tables

# Chapter 1: Introduction

## 1.1 The cardiovascular system

The cardiovascular system consists of the heart, a muscular pump that forces the blood around the body, and the blood vessels, a closed system that includes arteries, veins, and capillaries. The circulatory system has two main distinctive but interconnected forms. The systemic circulatory system, with the primary task of transporting nutrition and oxygen-rich blood to the parts of the body; and the pulmonary circulatory system, moves blood between the heart and the lungs, where oxygenated blood comes into the heart and sends deoxygenated blood back to the lungs.

The closed system must work effectively for blood circulation to be complete. Any complication that affects either the heart or blood vessels has the general term cardiovascular disease (CVD). Many complications of the cardiovascular system such as heart failure, heart valve disease, congenital heart disease, coronary artery disease, cardiomyopathy, arrhythmias, aortic disease, and vascular disease are generally called CVDs. The focus of my thesis will be blood vessels, in particular the large elastic arteries like the aorta.

## 1.2 Arterial structure and function

The body contains three main types of arteries, namely, 1) the elastic arteries that carry blood away from the heart; 2) the muscular arteries that are rich in smooth fibres and are less elastic; and 3) the branches that become arterioles, distributing blood through the extensive network of capillaries [1].

The main artery we are discussing here is the largest artery known as the aorta. The primary job of the aorta is to efficiently carry blood away from the heart. The aortic wall has a trilaminar structure, consisting of tunica adventitia, media and intima (Figure 1.1) [2].

The third outer layer is called tunica adventitia and it is composed of loose connective tissues predominantly composed of fibroblasts, collagen and elastic fibres rich ECM [3]. The adventitia is essential for maintaining the aortic diameter, aortic integrity, and resisting dissection [4,5]. The tunica media is the middle layer of the arterial walls, which is composed of smooth muscle cells and structural proteins (collagen and elastin fibres) that form the ECM [4]. Elastic fibres provide elasticity that allows the arteries to stretch and change shape in response to changes in blood pressure that is exerted on the walls as a direct effect of the

pumping of blood from the heart.
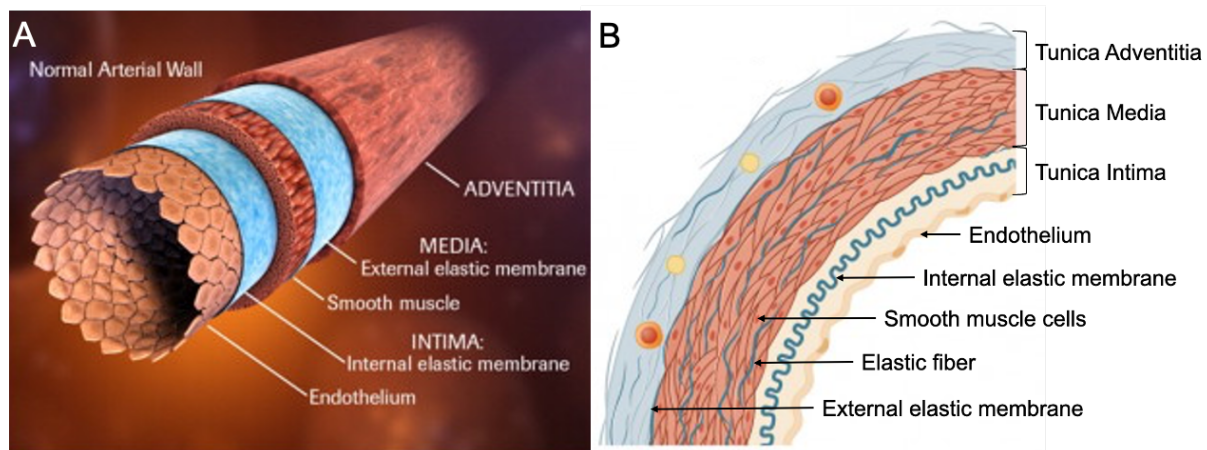


**Figure 1. 1 A diagram illustrat***of Arterial wall. Diagram* **(A)** *shows* the general structure of a healthy artery and **(B)** *shows* cross section of an artery. Adopted from (6)(7)

Non-elastic collagen-I fibres provide tensile strength to the arterial wall [6]. The vascular smooth muscle cells (VSMCs) reside within the medial layer and undergo contraction, which causes vasoconstriction, or relaxation, which causes vasodilation. Hence, tunica media is the thickest layer and most of the mechanical properties of the aorta can be attributed to the strong collagen component and stretchable elastin components within this layer along the contractile activity of the VSMCs.

The inner layer of the arterial walls is called the tunica intima, which is composed of an elastic membrane lining and one cell layer of endothelial cells. This layer is directly subjected to the blood flow on its free surface and its inner side is attached to the basement membrane. This layer allows the movement of biologically active molecules between the tissues and vasculature. Moreover, it senses alterations to the environment, such as cellular damage, and helps dictate the activities of VSMCs.

## 1.3 An overview of cardiovascular disease

Cardiovascular disease (CVD) is the single largest cause of death after age 65 years of age and is the second-highest cause of mortality in the UK. This makes CVD the most prevalent risk factor for health worldwide and places a heavy burden on the well-being of the population in developing countries [7,8]. Most CVD shares multiple risk factors such as age, obesity, lifestyle, and genetic and environmental factors [9]. Other prevalent risk factors that are

mutually observed in developed and developing countries with ageing populations include hypercholesterolemia, hypertension and atherosclerosis [10]. Currently, healthy people who are at risk of getting CVD are being advised to make radical changes to their lifestyle and diet. In general, statins, 3-hydroxy-3-methylgluaryl coenzyme A (HMG-CoA) inhibitors which lower cholesterol, are frequently prescribed. Even though most CVD can be attenuated by risk reduction factors, ageing is an inevitable process and a better understanding of its impact on cardiovascular health will augment our ability to effectively treat this disease [11].

### 1.3.1 Ageing and CVD

Across all cardiovascular diseases, ageing is the largest risk factor and by 2030, more than 20% of the population will be 65 years or older [11]. This is evident from the statistics that 50% the CVD-related deaths are attributed to the population at a later age [12]. As a result of arterial age, the vasculature undergoes structural and functional alteration, which commonly leads to the stiffening of the arteries in particular the aorta [9][13]. This change in aortic stiffness leads to a lack of dynamicity of the arterial walls [14]. For a long time, the prevalence of CVD was thought to be due to the reduction of vascular compliance, which is the ability of blood vessels to distend and increase volume with increasing transmural pressure [15].

### 1.3.2 Ageing, arterial alteration and its implication in CVD

The largest artery, the aorta, which is about a foot long and an inch in diameter, is subjected to high systolic blood volume and pressure [16]. The aorta has four sections- the ascending, thoracic (descending), aortic arch and abdominal aorta. The medial layer of the aorta is rich in elastin and collagen. Elastin and collagen are crucial for the elasticity of the aorta when it is exposed to low and high pressures respectively, where elasticity provides the aorta with the ability to maintain stable flow to distal organs [17–19]. The dynamics of the aorta make it a key player in maintaining the continuous oxygen supply to the tissues and regulation of blood flow to the peripheries [17].

With age and CVD such as arteriosclerosis, the aorta reduces its compliance and results in clinically increased aortic pulse pressure and systolic arterial pressure [20]. This results in a reduction of compliance and labours the left ventricle to pump the desired blood volume across the altered arterial-resistant aortic wall. As a result, the left ventricle undergoes temporary compensatory mechanisms by prolonging systolic contraction and adjusting the

end-systolic volume [21] [22]. This adjustment leads to the increase in the density of muscle mass of the left ventricle termed ventricular hypertrophy [23,24]. Furthermore, a compensated cardiovascular system leads to increased heart rate and stroke volume and cardiac malfunction.

### 1.3.3 Arterial compliance and CVD

Complications anywhere across the aorta could lead to aortic aneurysm, aortic dissection, aortic insufficiency/regurgitation, and aortic atherosclerosis [17,20]. Aortic compliance can be determined using Artificial Intelligence, systolic arterial compliance (SAC), computerised tomography (CT) scan, pulse wave velocity (PWV), MRI scan and other invasive and non-invasive diagnostic measures [25,26]. It is worth noting that arterial trees respond to ageing varyingly depending on the location and mechanical property of the blood vessel [21].

Healthy aortae have the fundamental property of dampening blood pressure plausibility, ensuring adaptive blood flow through the arteries [27]. However, during ageing and after injury the aorta loses its plasticity and becomes rigid [20]. When that happens, the change in systolic blood volume faces elevated resistance, and the same amount of blood must flow through at a higher speed. Hence, aortic compliance is the ability of the aortic walls to expand when filled with blood volume, maintaining the pressure on the arterial wall and the speed of blood reaching the vasculatures. Compliance (C) can be expressed mathematically as aortic volume ( V) and change in aortic pulse pressure ($\Delta P$); (C = $\Delta V/\Delta P$) **(Figure 1.2B)**.

Reduced compliance is caused via augmented arterial wall stiffness which results in increased vascular stiffness[28]. This predictive biomarker has been shown in patients with developing hypertension, atherosclerosis and diabetes mellitus among other CVDs [29]. In these conditions, the high pulse pressure is unable to expand the stiffened arterial wall, resulting in a faster pulse velocity that leads to and damages the microcirculation of vital organs [30]. PWV has arguably remained the optimal method to measure arterial stiffness and a relatively low PWV has been shown in healthy individuals [31]. Individuals with a higher likelihood of CVD and heart failure have previously presented elevated pulse pressures and increased PWV [32]. Despite the intensive research in cardiovascular disease over the past 100 years, the aetiology remains mostly obscure. Nevertheless, arterial stiffness is considered a predictive value of

cardiovascular events resulting in reduced arterial compliance [9] [29].
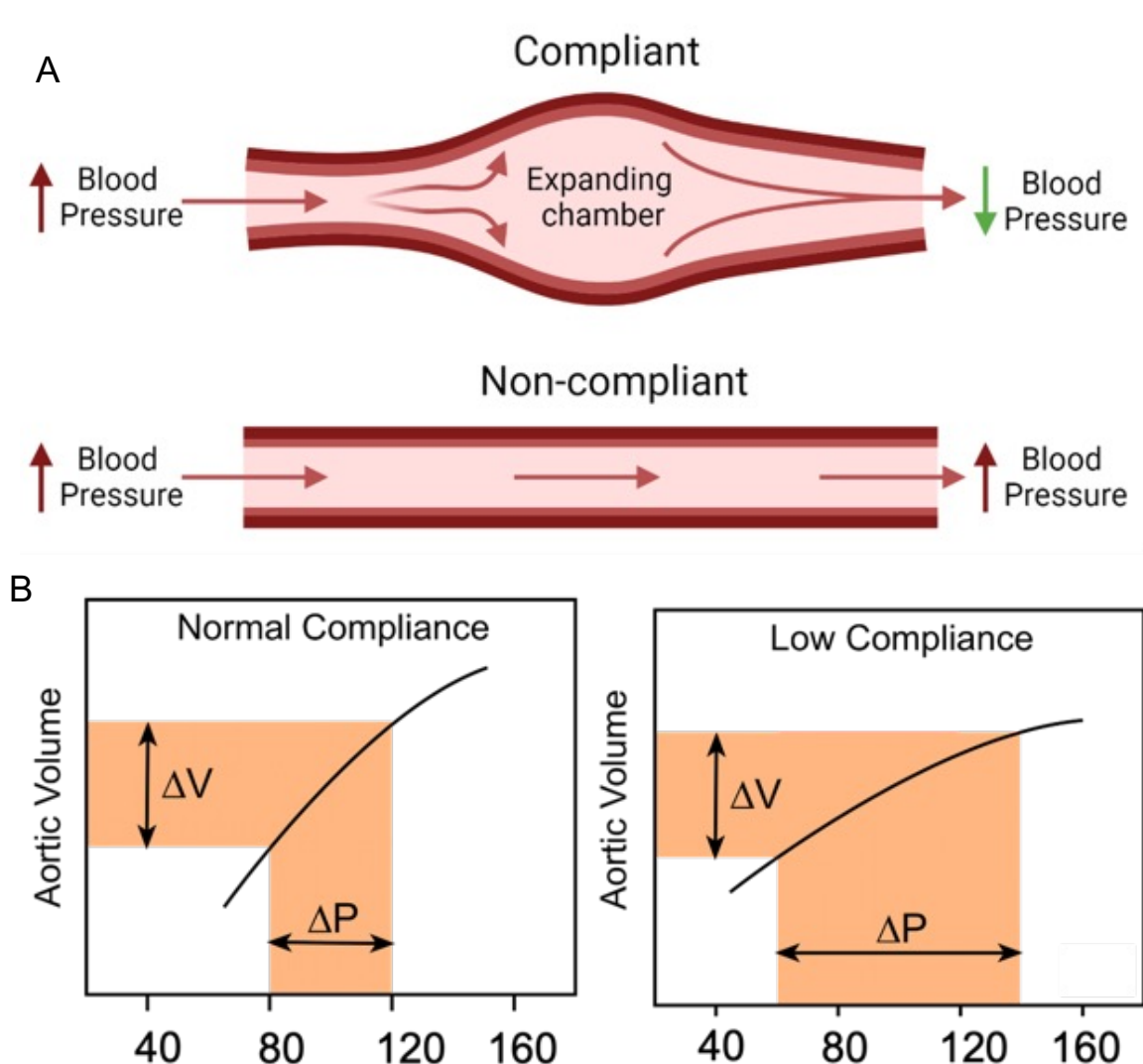


**Figure 1. 2: Schematic representation aortic compliance.** Diagram showing **(A)** complaint and non-compliant artery and **(B)** this diagram illustrates the relationship change in aortic volume ( DV) and change in aortic pulse pressure (DP) in a normal-compliance artery and in low-compliance artery. Diagram B Adopted from Cardiovascular Physiology Concepts (30)

The composition of the ECM is comprised of various structural glycoproteins such as fibronectin, laminin, vitronectin and thrombospondin [33]. However, among those, collagen and elastin have presented themselves as the key structural proteins that determine the compliance of the aortic wall [32]. The ECM undergoes remodelling during ageing and CVD, and collagen and elastin levels have been shown to increase and diminish, respectively. This results in decreased elasticity and increased stiffness of the aortic wall **(Figure 1.2A)**.

## 1.4 VSMC function and phenotype

### 1.4.1 VSMC function

Within physiological conditions, VSMCs exist in a quiescent contractile state and use actomyosin-generated force to regulate the vascular tone [34]. As blood pulse travels through the aorta, VSMCs are stretched, resulting in the activation of stretch-activated ion channels that facilitate $Ca^{2+}$ entry and VSMC contraction [35]. In addition to this mechanically regulated VSMC contraction, soluble factors, including angiotensin II, bind to receptors and activate the release of $Ca^{2+}$ from intracellular stores to promote VSMC contraction [36]. A balance between the mechanical and soluble regulation of VSMC contraction determines aortic compliance and tone, resulting in controlled organ blood flow and pressure [37].

### 1.4.2 VSMC contractile marker proteins and CVD

VSMCs within the medial layer of the healthy aortic wall are quiescent and their main role is to maintain vascular tone via contraction. However, VSMCs are also capable of repairing the injured vessel wall by migrating, proliferating and adjusting the ECM content [38,39]. VSMC proliferation, migration and ECM remodelling are all prevalent in aortic CVDs. A key unanswered question is how VSMCs can regulate these distinct functions and switch between quiescence/contraction and proliferation/migration

Within a healthy adult aorta, VSMCs express genes required for efficient contraction, α-smooth muscle (SM)-actin-(SMA), γ- smooth muscle (SM)-actins, SM22α (also known as transgelin), SM-myosin heavy chain (SM-MHC), high molecular weight caldesmon (h-caldesmon) and calponin [40] [41]. VSMCs have high plasticity and can de-differentiate into a synthetic-proliferative and migratory- phenotype during vessel injury or in an aged/diseased state [42]. Those phenotypical switches of de-differentiated VSMCs are characterised by reduced expression of the contractile marker proteins, increased non-muscle myosin II (NM-myosin II) upregulation ECM protein synthesis and VSMCs migrate from the tunica media to the tunica intima, where the cells are unable to regulate vascular tone as effectively [40,43]. This is caused by mechanical/biochemical signals typically associated with the development and CVDs such as atherosclerosis and hypertension. Signals that promote VSMC phenotypic modulation include growth factors, mitogens, inflammatory mediators and mechanical stimuli [44]. Synthetic phenotype modulation is associated with a variety of changes that increase

VSMC migration and proliferation capacity, which are characteristic of VSMCs in the aged/diseased state [7].

### 1.4.3 VSMC remodelling

One of the key factors used to determine vascular system health is vascular ageing, which lays a trend toward progressive remodelling and stiffening of the vasculature [45]. Blood pressure hemodynamic, change in ECM and other blood-born signalling molecules govern the structure and function of the different layers of the arterial walls [46]. In a pathological vascular system such as atherosclerosis, vascular walls undergo remodelling by alterations driven by changing VSMC and endothelial cell function [47]. Those changes in VSMCs between healthy and pathological environments are seen as contractile or synthetic phenotype switches [48]. Hence, VSMCs exhibit an extraordinary capacity to undergo phenotypic switches. Furthermore, mature differentiated VSMCs enable the vascular wall to function in a highly regulated manner and functionally adapt to extracellular stimuli from the ECM [48,49].

### 1.4.4 Arterial stiffness and CVD

In healthy aortae, the mechanical properties of the ECM and the mechanical forces from the blood flow determine the function of the VSMCs [50,51]. Though the exact mechanism is unknown, during ageing, VSMCs de-differentiate and express increased ECM proteins [52]. The increased expression of ECM proteins along with many other factors increases the tensile strength and stiffness of the extracellular mechanics [53]. VSMCs respond to the increased stiffness of the ECM by enhanced actomyosin-driven contractile forces [54]. This elevated traction stress by VSMCs results in arterial stiffness, predictive of arterial ageing and onset of CVD [55]. There has been a wealth of research on the topic of arterial stiffness and that ECM is a key regulator of VSMCs, yet further extensive research is required to investigate the force generation of VSMCs in response to the change in ECM stiffness and how that applies in healthy and aged/diseased arterial wall [7,9,56].

Conventionally, most in vitro experiments cultured isolated VSCMs on glass or plastic materials, where those materials are a thousand times stiffer than of the arterial wall. Hence, the data acquired from those experiments have not been entirely reflective of what goes on inside the body. In the recent past, a more practical technique that is easy to tailor to desired stiffness has been developed with polyacrylamide hydrogels (PAHs) [57]. Studies using PAHs substrate to investigate the role of matrix stiffness in regulating VSMCs characteristics have identified that matrix stiffness is a key regulator of VSMCs phenotype [7]. Increased matrix

stiffness was found to promote VSMC migration and proliferation and significantly decrease traction stress generation [58].

## 1.5 VSMC cytoskeletal networks

The cytoskeleton is a multifunctional component of VSMCs, that consists of a highly dynamic network of 3D spaced structures of filamentous proteins [59]. These structures provide a collaborative framework to maintain cellular organisation, mediate communication and transport mechanism, morphological support and network for the generation and transduction of mechanical forces [60]. Three components are unique, yet interdependently constitute the cytoskeleton, namely the microfilaments, intermediate filaments, and microtubules **(Figure 1.3)**.

### 1.5.1 Microfilaments

Microfilaments, also called thin filaments, are polymers of the most abundant protein in the cell called actin. Actin filaments are two-stranded helical polymers of monomeric globular actin units, that are about 7nm in diameter. Actin filaments act as major signal transducers and are critical for a cellular responses such as cell motility and traction force generation [61]. There are three isotopes of actin; α, β and γ actin, where the α-actin is the most abundant actin [62].

### 1.5.2 Intermediate filaments

Intermediate filaments are composed of many different proteins such as keratin, vimentin, desmin and lamin [63]. Intermediate filaments are about 12 nm in diameter, named after their size, as they are larger than the actin filament and smaller than the microtubules which are about 23 nm in diameter [63]. The main function of intermediate filaments is to bear tension, provide support and maintain cell shape integrity [64].

The three types of filaments found in the cytoskeleton are distinguished by their size and structure, and the protein subunit of which they are made.
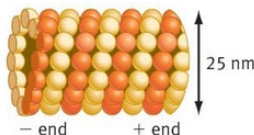
| | Structure | Subunits | Functions |
|---|---|---|---|
| **Actin filaments (microfilaments)** | Strands in double helix, 7 nm, − end + end | Actin | • maintain cell shape by resisting tension (pull)<br>• move cells via muscle contraction or cell crawling<br>• divide animal cells in two<br>• move organelles and cytoplasm in plants, fungi, and animals |
| **Intermediate filaments** | Fibers wound into thicker cables, 10 nm | Keratin or vimentin or lamin or others | • maintain cell shape by resisting tension (pull)<br>• anchor nucleus and some other organelles |
| **Microtubules** | Hollow tube, 25 nm, − end + end | α- and β-tubulin dimers | • maintain cell shape by resisting compression (push)<br>• move cells via flagella or cilia<br>• move chromosomes during cell division<br>• assist formation of cell plate during plant cell division<br>• move organelles<br>• provide tracks for intracellular transport |

**Figure 1. 3: Summary table of cytoskeleton**, adopted from Cell (68)

### 1.5.3 Microtubules

The microtubule is the largest component of the cytoskeleton with a 23 nm diameter. Microtubules are hollow and long tubes made of alpha and beta tubulin, that emanate from the centrosome, an organelle that organises tubulin at the microtubule organising centre (MTOC) [65]. Attributed to their dynamic instability (continuously cycle of growing and shrinking), their main function are cytokinesis, cell communication, transportation and cell motility [66].

## 1.6 Actomyosin and VSMC function

Vascular resistance is one of the indicators of cardiovascular health. Vascular resistance depends on a balance between contraction and relaxation of VSMCs [67]. The subcellular structures responsible for regulating the contractility of VSMCs are the smooth muscle myosin and actin filaments, regulated by receptors and mechanical stretch activation [68].

There are two synergetic pathways that lead to VSMCs contraction, the $Ca^{2+}$ dependent and $Ca^{2+}$ independent pathways **(Figure 1.4)** [69]. $Ca^{2+}$ dependent pathway involves the increased levels of $Ca^{2+}$ in the cytoplasm, where $Ca^{2+}$ influx into the intracellular space can be triggered by electrical, mechanical, and chemical stimuli or the release of $Ca^{2+}$ from the sarcoplasmic reticulum (SR) [70]. $Ca^{2+}$ entry from the extracellular space occurs via voltage-gated calcium channels (VGCC) or non-selective cation channels. This intracellular $Ca^{2+}$ concentration increase leads to $Ca^{2+}$/calmodulin-dependent activation of myosin light chain

kinase (MLCK), which phosphorylates the myosin light chain, enabling the interaction of myosin and actin [71]. The smooth muscle myosin head attaches to the actin filaments leading to the generation of contractile forces, which increases the arterial stiffness for the duration of the contraction [59,72]. The $Ca^{2+}$ sensitization of the contractile proteins is regulated by the Rho/Rho kinase pathway to block dephosphorylation of the light chain by myosin phosphatase to generate sustained contractile forces [73,74]. For VSMCs to relax, myosin phosphatase should be initiated and the $Ca^{2+}$ concentration in the cytosol has to drop [75].

VSMC contractile properties are classified as a tonic or phasic [7]. In phasic contractility, VSMCs force rapidly rises to a peak before falling to a lower steady-state level, whereas in tonic contractility, VSMCs force gradually rises to a sustained steady-state [76].
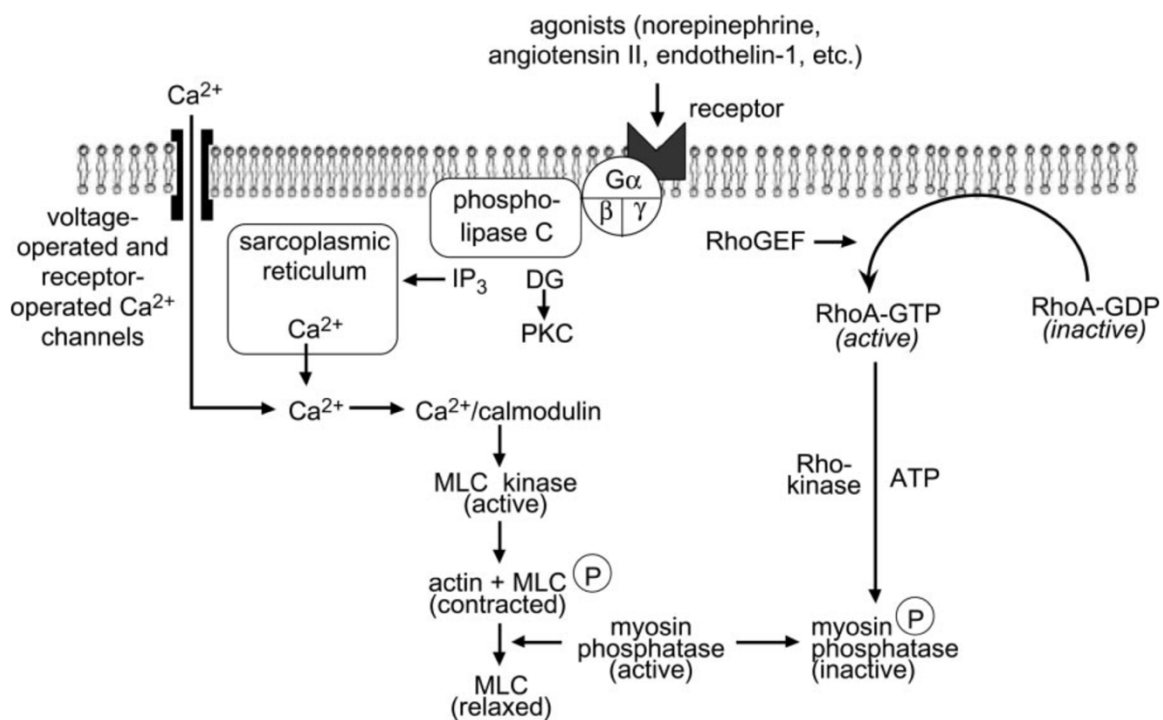


**Figure 1. 4: Diagram illustrating $Ca^{2+}$ dependent and $Ca^{2+}$ independent regulation of VSMCs contraction and their relation to phasic and tonic contraction**. Diagram adopted from smooth muscle contraction and relaxation(81)

## 1.7 Biochemical regulators of VSMC actomyosin activity

In vascular pathophysiology, haemodynamic factors are important regulators of VSMC function. Inside the body, VSMCs are subjected to the 3-D matrix and its interaction with the surroundings modulates the migration, proliferation, and contractility [77]. In return, VSMCs

actively contribute to vascular cell signalling via contact signalling, change in matrix production and extracellular vesicles [78]. Multiple signalling pathways are involved in the VSMC functional, phenotypic switching process characterised by differentiation, migration, and proliferation [40].

### 1.7.1 G-protein coupled receptors

G-protein coupled receptors (GPCRs) are receptors that are coupled to G-proteins. G-proteins are trimeric with α, β and $\gamma$ subunits on the intracellular side of the membrane connected by lipid anchors, that form the G-protein receptor system. When active, a conformation change causes the α-subunit to dissociate from β and γ subunits. For that to happen, G-proteins need to bind to G-protein coupled receptors (GPCRs). GPCRs span the plasma membrane and possess seven transmembrane domains. Upon ligand binding, the conformational change that leads to the α-subunit causes activation of various G-protein second messengers, which activate or inhibit multiple downstream target-proteins (Figure 1.5) [79–81].

In the resting state, the α-subunit of the G-proteins is bound to guanosine diphosphate (GDP). When a ligand binds to the GPCRs at the extracellular side of the cell membrane and causes a conformational change, it allows the α-subunit to activate by binding with guanosine triphosphate (GTP) and releasing the GDP. The α-subunit moves to the target protein and causes an increase or decrease in activity. The process is inactivated by GTPase - activation proteins (GAPs) which hydrolyses the GTP-α complex to GDP-α (reversing it to a resting state). This causes binds the α-subunit to bind back to the $\beta$ and $\gamma$ subunits [79,82].

The α-subunit of the G-protein is the key player in stimulating ($G_{\alpha s}$) or inhibiting ($G_{\alpha i}$) the activity of secondary messengers. The $G_{\alpha 12/13}$ subunit is important as they regulate actin cytoskeletal remodelling in cells. Furthermore, the $G_{\alpha 13}$ subunit is of particular importance as it is essential for a receptor tyrosine kinase (RTK), which induces migration [83]
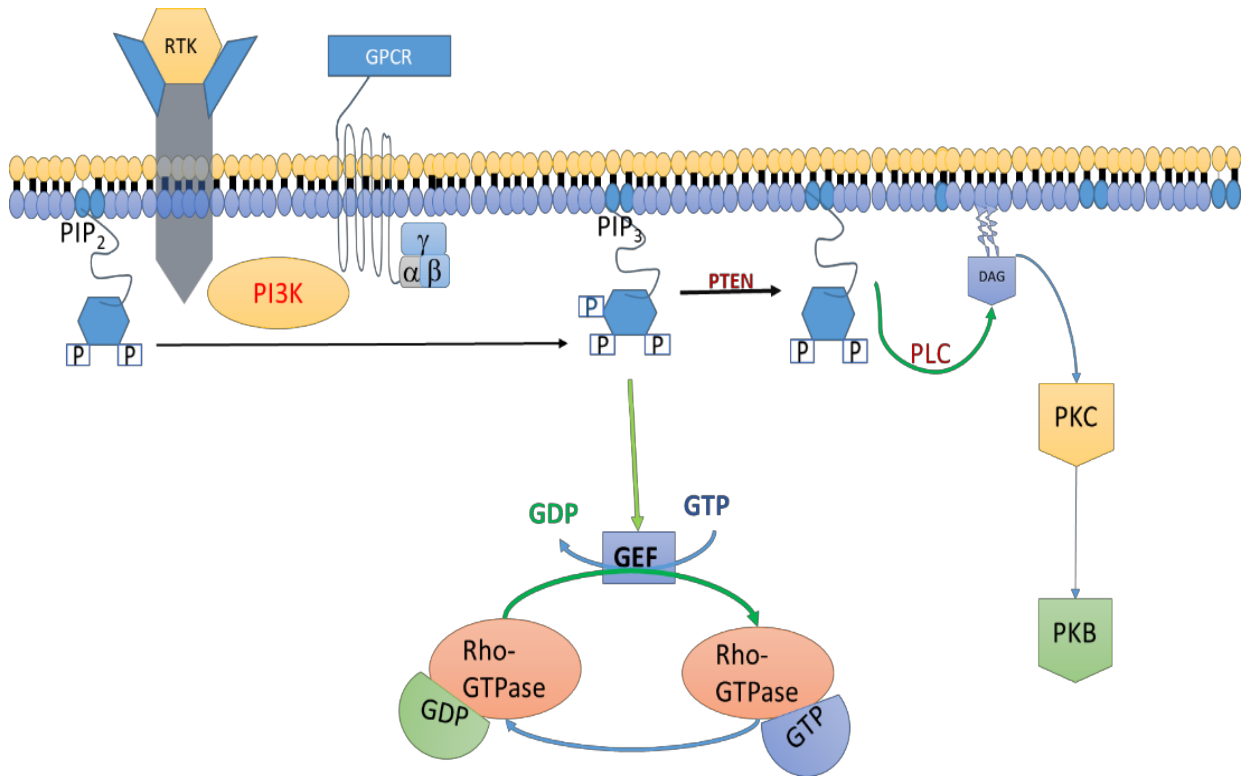
**Figure 1. 5: Schematic representation of GPCR signalling pathway through G proteins. GPCRs is a hetrotrimeric complex (α, β and γ subunits).** GPCR activation leads to the release of GDP by the $G_\alpha$ subunit and $G_{\beta\text{ and }\gamma}$ subunits and subsequent binding of GTP. $G_{\alpha q/11}$ subunit activates Phospholipase C (PLC) that hydrolyses phosphatidylinositol 4,5-biphosphate (PIP2) to diacyl glycerol (DAG) and inositol triphosphate (IP3). Diacylglycerol lives hanging on the intracellular side of the cell membrane and activates protein kinase C (PKC) and IP3 induces the effect of protein kinase B (PKB), which is important on cell migration. $G_{\alpha q12/13}$ subunit is key on activation of guanine nucleotide exchange (GEFs) for RhoA.

There are two main pathways important to the cytoskeletal reorganization-cyclic AMP (cAMP) dependent pathway and the phosphatidyl-inositol pathway [84]. Gαs/i's target the adenylyl cyclase enzyme which causes ATP to convert to cAMP. cAMP activates protein kinase A (PKA). Recent studies show that PKA plays an important role in the signalling loop that governs the protrusion-retraction cycle in migrating cells [80].

A different membrane-bound enzyme, phospholipase C (PLC) is triggered by Gαq and hydrolyses phosphatidylinositol 4,5-biphosphate (PIP2) to inositol 1,4,5-triphosphate (IP3) and diacylglycerol (DAG). IP3 is released into the cytosol and activates the release of $Ca^{2+}$ from the sarcoplasmic reticulum. Local cytosolic $Ca^{2+}$ pulses control adhesion and retraction around

the leading edge of migrating cells and are known to be high in the rear end of the cell and low in the leading edge of the cell. It also activates myosin light chain kinase (MLCK), which phosphorylates the myosin II increasing actomyosin activity and this is an oscillatory process. The contraction generated from the activation of myosin leads to the formation of focal adhesion complexes [85].

## 1.7.2 Rho GTPases

The Rho GTPase family is comprised of ~20 GTPases and exists as a subfamily of the Ras superfamily. They are well known to play a role in cell migration through various effectors as suggested by *in vitro* and *in vivo* studies performed over the past 20 years. The Rho proteins cycle between an active (GTP bound) form and an inactive (GDP bound) form as discussed above. They are regulated temporally using guanine-nucleotide-exchange factors (GEFs), GTPase-activating proteins (GAPs) and guanine-nucleotide-dissociation inhibitors (GDIs) [86]. GAPs inactivate GTPases by promoting hydrolysis of GTP into GDP, whereas GEFs prompt the exchange of GDP for GTP which triggers the enzymatic activity of the GTPase protein [84,87,88]. GDIs anchor the inactivated GTPase proteins within the cytoplasm, preventing interaction with the plasma membrane where it undergoes GDP/GTP exchange [87]. Of these 20 GTPase proteins, RhoA, Rac1 and Cdc42 have been heavily characterised to be essential in the regulation of the cell migration [89].

The activation of RhoA is facilitated via the Gα 12/13 subunits which bind to the p115 Rho GEF and stimulate the exchange of GDP/GTP. Once active, RhoA can activate its downstream targets, including Rho-associated protein kinase 1/2 (ROCK1/2). ROCK1/2 are major downstream RhoA effector proteins that belong to the protein kinase A, G and C family of serine/threonine kinases. ROCK1 and ROCK2 possess many similarities in both structure and function. Overall, they share a 65% identity in their amino acid sequence and can be seen to modulate mutual functions in endothelial, cardiac and smooth muscle cells **(Figure 1.6)** [90].
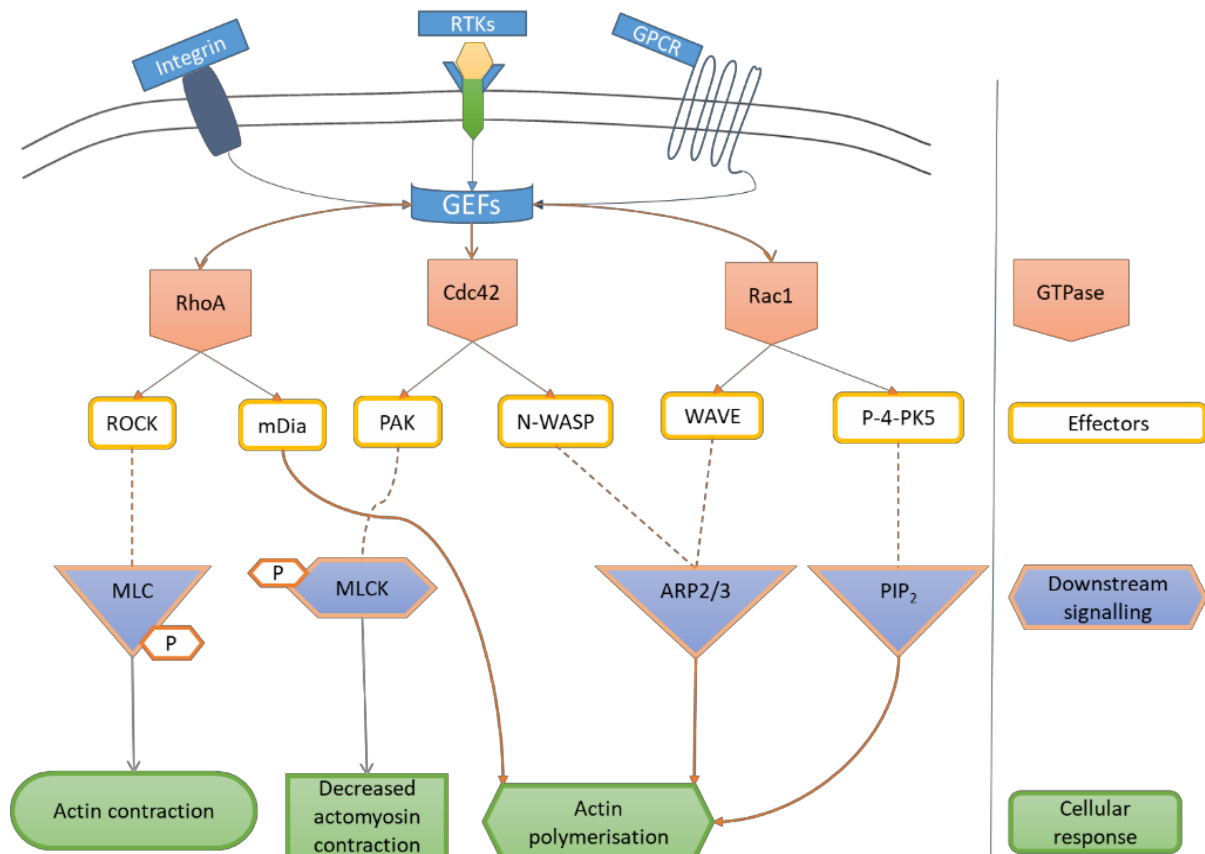
**Figure 1. 6: Diagram showing how Rho GTPases and the main pathway proteins mediate and regulate actin cytoskeleton.** Adapted from 'signalling networks of Rho GTPases in cell motility'(104)

Guanine nucleotide-exchange factors (GEFs) transduce GPCRs/RTKs induced activation of signalling (refer to Figure 1.6) and activate Rho GTPases-Cdc42, Rac1 and RhoA. In their activation Rho -GTPase bind to different effectors (RhoA to ROCK and mDia, Cdc42 to PAK and N-WASP and Rac1 to WAVE and P-4-PK5, and uses their effectors to pass the downstream signalling for different cellular response. RhoA is responsible for actin contraction via its effector ROCK, which phosphorylates downstream myosin light chain (MLC) and inhibits MLC dephosphorylation by inhibiting MLC phosphatases (pMLC) leading to actin-myosin contractility. On the contrary, the activation of p21 activating kinase (PAK), which is an effector of both Cdc42 and Rac, phosphorylates MLCK inactivates and inhibits MLC phosphorylation resulting in reduced actomyosin contraction. Cdc42 via activation of Wiskott-Aldrich syndrome protein (WASP); RhoA via activation of the mammalian homolog of diaphanous (mDia); and Rac1 via activation of WASP family verprolin homologous protein (WAVE) activate the actin related protein 2 and 3 (Arp2/3) complex result in actin polymerization.

However, there is evidence that there may be isoform-specific roles in these kinases. One example was shown in fibroblast cells, where knockdown of ROCK1 caused aberrant adhesion maturation and actin organisation [91]. Contrastingly, in prostate cancer cells, ROCK2 was shown to specifically regulate the migratory function of the cells [92]. Within CVD, there is differential regulation of cardiomyocytes by both kinases, with ROCK1 inducing apoptosis and ROCK2 causing hypertrophy of the cells [40]. The utilisation of more selective inhibitors is therefore required to identify further isoform-specific roles of the ROCK kinases [90].

ROCK1/2 activation affects cytoskeletal remodelling in two ways; it prevents actin depolymerisation, via inhibition of cofilin, and it can increase basal levels of phosphorylated myosin light chain, by inhibiting the activity of the myosin light chain phosphatase [93,94]. The regulation of cytoskeletal structure and actomyosin-generated traction force by RhoA plays an important role in VSMC migration [87].

Rac1 and Cdc42 also have multiple roles in cell migration. Cdc42 and Rac1 have been shown to regulate the formation of the filopodia and lamellipodia, respectively [89]. Lamellipodia formation via Rac1 is facilitated through Arp2/3 complex activation and the uncapping of actin filaments present at the cell membrane [87]. Conversely, Cdc42, via myotonic dystrophy-related Cdc42-binding kinases (MRCK), shows a similar mechanism to ROCK by inducing an increased myosin light chain phosphorylation [95]. In addition, both GTPases interact with and activate p21-activated kinase (PAK). Once active, PAK can increase the stabilisation of the microtubules as well as regulate cell polarity of the cell via the activation of the PIX/PAC complex [95].

Other agents most widely prescribed for the prevention and treatment of CVD are the cholesterol-lowering drugs, statins [96]. Statins act by inhibiting the 3-hydroxy-3-methylglutaryl-CoA (HMG-CoA) reductase, a key enzyme for the synthesis of endogenous cholesterol biosynthesis [97]. Statins inhibit the conversion of HMG-CoA to mevalonic acid and also block the biosynthesis of important intermediates; such as the isoprenoids farnesyl pyrophosphate (FPP) and geranylgeranyl pyrophosphate (GGPP) that affect many cellular processes [98,99]. Those intermediates regulate the small signalling proteins Ras, Rac and Rho on their signal transduction, growth of VSMC, apoptosis the regulation of vascular activity of NAD(P) H oxidase [100–102].

The GTPases have therefore presented themselves as a key regulator of the migratory process and more work is required in the crosstalk between various GTPases to further understand their dynamic regulation of cell migration.
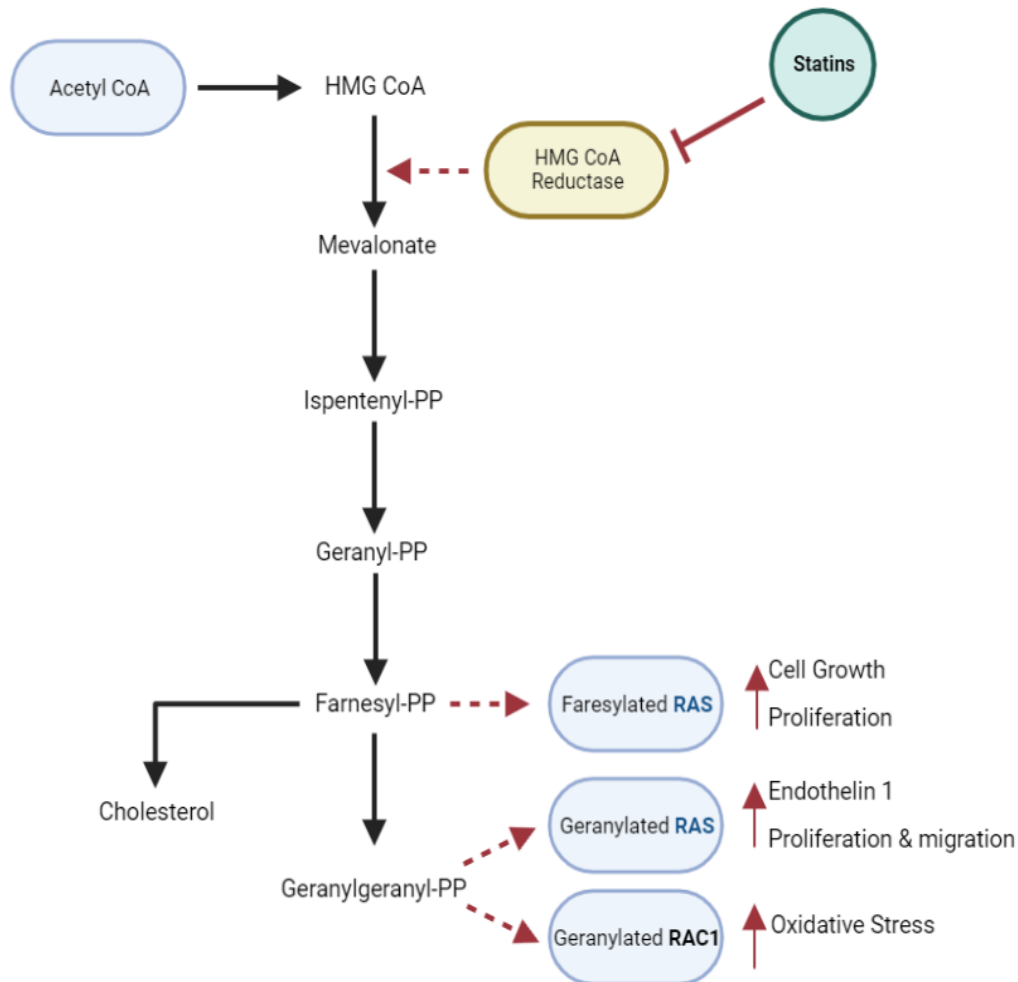
**Figure 1. 7: Illustration of statins blocking an important step in the activation of Rho GTPases** (Rho, Rac and Ras) in the post-translational isoprenylation. Adopted from Rho GTPases, statin and NO (101).

## F1.7.3 Stretch-activated ion channels (SAC) in VSMCs

Mechanical stimuli of VSMCs from the extracellular environment are translated to biochemical responses inside VSMCs and the process is called mechanotransduction[103]. Mechanotransduction is a crucial characteristic of VSMCs to properly maintain the dynamic changes required by the vasculatures [104]. The autoregulatory properties of small arteries and arterioles to intraluminal diameter in response to changes in intravascular pressure is primarily originated from mechanosensitive VSMCs [105]. Some of the key regulatory features of mechanotransduction are cellular functions such as contractility and phenotypic switch to migratory and proliferative activity [106]. This mechanical sensitivity is a property of voltage-gated

or ligand-gated channels, where the channels change shape between closed and open states, leading to increase mechanical stress in the membrane [107].

The membrane stress causes the reorganization of the cytoskeleton, expression of specific proteins responsible for post-translational modification and altered tension inside and outside VSMCs [108]. The biomechanical forces generated as the cytoskeleton reorganise is transmitted to the ECM via focal adhesion complex [109]. This makes mechanotransduction to be bidirectional, inside-out and outside-in biochemical apparatus [110]. In VSMCs the stretch-activated ion channels operate on tens of milliseconds pace, leading to increased ion transients and resulting in rapid intracellular alterations [111].

Transient receptor potential channels (TRPCs) are other groups of ion channels located on the plasma membrane of many cell types, which play a critical role in the regulation of membrane potential and $Ca^{2+}$ signalling of VSMCs [112]. They have also attracted attention as a key regulator of the VSMC phenotype modulation [113]. TRPCs are classified based on the amino acid sequence as canonical (TRP canonical, TRPC), vanilloid (TRPV), melastatin (TRPM), mucolipin TRP and ankyrin TRP [105].

Previous studies suggested that VSMC phenotype is manipulated by externally applied stretch, modulating cell shape, cytoplasmic organisation and intracellular processes leading to cell contraction, migration and proliferation [114]. In a healthy arterial wall, SACs myogenic response to the mechanical stimuli serves as a mechanical sensor [115,116]. Those SACs thoroughly regulate calcium inflex and generate normal traction stress to maintain arterial tone [117]. However, in an aged/diseased arterial wall, SAC gets activated causing a significant amount of calcium influx, which leads to depolymerization of the membrane to activate voltage-gated calcium channels and synergically generated increased traction stress [118].

Another mechanosensitive family are the Piezo non-selective cation channels consisting of the Piezo1 and Piezo2, with the former revealing roles in vascular development and blood pressure management [119]. Piezo1 is a relatively newly identified mechanosensitive non-selective ion channel, with is highly expressed within endothelial and smooth muscle cells, that play role in mediating blood vessels development and structural maintenance [120,121]. Its electrophysiological properties reveal an influx of $Na^+$, $Ca^+$ and $Mg^{2+}$ ions, with $Ca^{2+}$ showing favourable permeability. GsMTx4 reversibly antagonises piezo1 activation and blocks mechanically induced voltage-gated mechanosensitive currents [119]. Research has shown that treatment with GxMTx-4 abolishes the induction of cell current within HEK293 cells[122].

## 1.8 VSMC adhesions

Adhesions of VSMCs to the substrate alter the morphology, size and subcellular distribution of cytoskeletal components, yet, adequate cell adhesion to the ECM is essential for the proper function of VSMCs [123]. ECM is not only an anchoring substrate but also provides a suitable environment for biophysical activity [124]. VSMCs-ECM adhesion is mediated by integrin and interacts with the actin cytoskeleton inside the cell [125].

### 1.8.1 Integrins and focal adhesion

Integrins are within the type I family of transmembrane glycoproteins that mediate cell-matrix interactions. They are composed of three structural components: a large extracellular domain, a transmembrane domain, and a short cytoplasmic domain. Their heterodimeric (β and α subunit) isoforms allow them to have multiple compositions on the cell surface and to bind to various ECM proteins such as fibronectin and collagen [126]. The beta subunit of integrin links the ECM to the actin cytoskeleton. On the cytoplasmic face, adopter proteins, such as vinculin and talin, associate with the VSMC-matrix adhesion complex. These proteins serve to tether the integrin complex to the actin cytoskeleton. This allows for "outside-in" signalling which activates signalling pathways within the cell [7]. Those mechanical signals cause the rearrangement of the actin cytoskeleton during migration. Studies conducted in VSMCs of rat arteries showed integrin to be activated by platelet-derived growth factor (PDGF) which caused actin filaments to re-localize into the leading edge of the lamellipodia **(Figure 1.8)** [127].

Nascent cell-matrix adhesion formation at the leading edge of the cell requires; integrin ligation, integrin clustering, phosphorylation of proteins within the adhesion complex, and an intact actin filament meshwork [128]. Nascent adhesions are structurally small and either quickly disassemble or mature into much larger focal adhesions via an actomyosin-dependent process [129]. Matrix adhesion organisation is controlled by a wide range of kinases, including Src, focal adhesion kinase (FAK), mitogen-activated protein kinases (MAPKs) and phosphoinositide 3-kinases (PI3Ks) [130].

Integrin-linked kinase (ILK) is a serine-threonine protein kinase, with a molecular mass of ~50kDa [131]. It is an important component of the focal adhesion complex and is associated with paxillin, vinculin and FAK. It has been shown to activate PI3K and inhibit

glycogen synthase kinase-3β in vascular development through the modulation of downstream targets. ILK functions as a scaffold protein at VSMC -matrix adhesion sites and is composed of three subunits; the amino N-terminal domain, the central PH-like domain and the C-terminal kinase catalytic domain [129].

ILK co-localizes and interacts with several VSMC-matrix adhesion proteins, and such interactions coordinate actin polymerization and the stability of VSMC-matrix adhesions. It can also regulate the activation of Rac1 and Cdc42 by interacting with other proteins such as parvin. Previous work observed that ILK silenced cells showed slower wound closure due to decreased migration and proliferation. Hence, overexpression of wild-type ILK increased actin polarization and migration. However, there are opposing studies which present conflicting results about ILK's scaffolding and kinase functions and due to this, further work is required to conclude the different roles it may have on cell migration [132–134].

## 1.8.2 VSMC matrix adhesion and migration

Matrix adhesions are critical for VSMC motility. During VSMCs migration, VSMC-matrix adhesions assemble at the leading edge and disassemble at the trailing end. For protrusion of the lamellipodia/filopodia to be established, it needs to be physically linked to the surrounding environment. Within VSMCs, integrins act as the major receptor family that forms VSMC -matrix attachment fields[7].

In addition to the leading edge, VSMC- matrix adhesions at the rear must detach to allow the cell body to propel forward. This is required to prevent cell damage from occurring from the tension of the actomyosin-generated forces [95]. Several mechanisms regulating VSMC- matrix adhesion detachment have been identified. These include contractility-promoted release, where the NM-myosin II contractile force exceeds the strength of the VSMC -matrix adhesion [135]. Migration VSMCs de-differentiate into their synthetic phenotype and begin to remodel their ECM [43]. An example of this occurs within atherosclerotic lesions, where VSMCs display altered gene expression because of switching to their proliferative state. Analysis has shown that the fibrous plaques from these lesions contain a high concentration of collagen-I/III [136]. $Ca^{2+}$ levels also play an important role and activation of the phosphatase calcineurin, via a $Ca^{2+}$ -calmodulin-dependent mechanism, also promotes adhesion detachment.
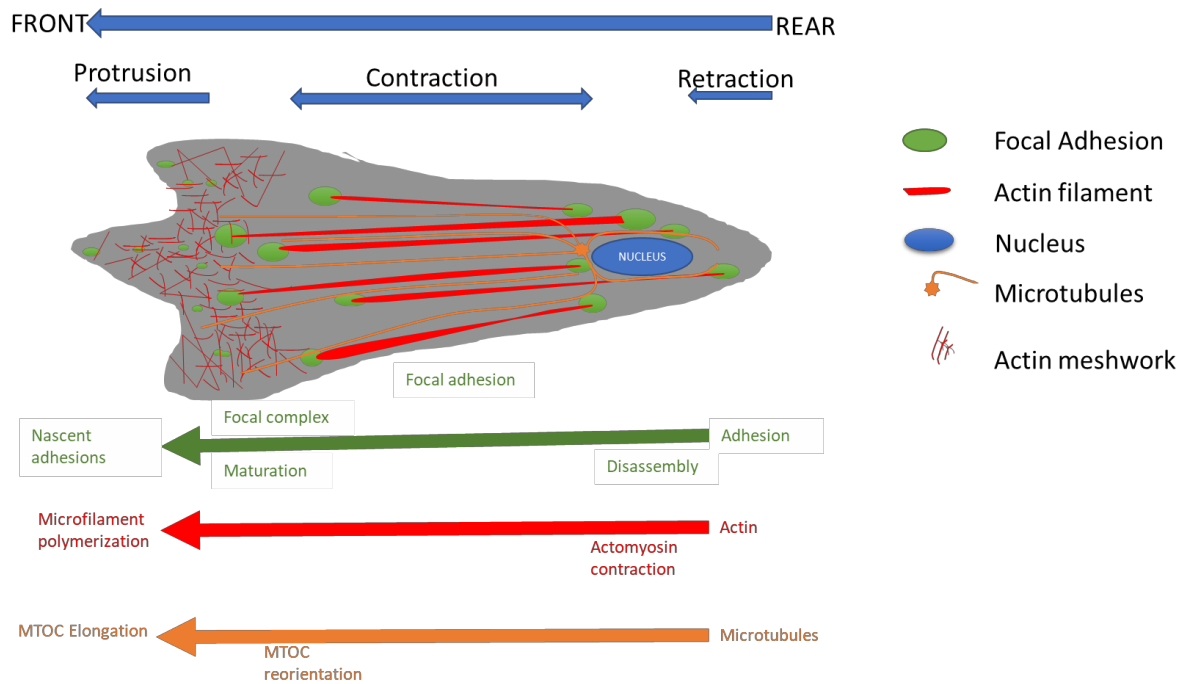
**Figure 1. 8: Schematic representation of the actin filament, focal adhesion, and microtubule organization of the cytoskeleton of a migrating cell VSMCs.** The diagram shows migrating cells with established front-rear polarity. The front of the cell is branched with actin meshwork, which supports leading edge protrusions. The newly formed focal adhesions are stabilized by nascent adhesions. Newly formed adhesion rapidly link to actin stress fibres and mature, that results in stable nascent adhesion and forward rolling motility. Focal adhesions disassemble through multiple mechanical cues, which allows the cell to perform effective displacement. The microtubules are organized in the direction of the cell migration and the Microtubule organizing centres (MOTCs) are localized in the front of the nucleus. Microtubules facilitate through all the remodelling of cytoskeleton in the leading edge of migrating cell. Adapted from Dale D. Tang and Brennan D. Gerlach (72).

Focal adhesion kinase is a tyrosine kinase whose structure is composed of an N-terminal FERM domain, a proline-rich region, and a C-terminal targeting domain. It has been implicated in the regulation of cell motility [137]. Phosphorylation of FAK in VSMCs has been observed in cases of both vascular injury and when stimulated with growth factors. Crystal structure analysis reveals that FAK is maintained in an inactive conformation via molecular interaction between the FERM domain and the catalytic domain [138]. Many research groups reported that

FAK works through its action as a scaffolding protein and also through direct phosphorylation of several other proteins such as talin, paxillin and N-WASP [139,140].

## 1.9 Microtubules

Microtubules form compression resistance sturts that are essential for cellular integrity and resist actomyosin-generated cellular stresses.

### 1.9.1 Microtubule dynamic instability

Microtubules are long, dynamic, cylindrical polymers with a diameter of around 25 nm, composed of a globular protein called tubulin- heterodimers consisting of two closely related polypeptides- α-tubulin and β-tubulin; and the γ-tubulin located at the centrosome, which is key for the nucleation of microtubule self-assembly [141]. 13 protofilaments of α/β-tubulin assemble forming a tubular structure, where new heterodimers are added on the plus/growing ends that are GTP-bound at β-tubulin caps. With the new addition of heterodimers, the GTP-bounded to β-tubulin hydrolysis to GDP and further addition (growth) occurs depending on the concentration of free heterodimers and other factors, and the microtubule further assembles or disassembles (Figure 1.9) [142,143]. They are responsible for the VSMCs morphology by creating an internal architecture through elaborate linkage(s) [144]. This spatial organisation of the VSMCs organelles in their morphology is key for polarity, cell migration, intercellular transport and cell division [145]. The higher-order system of the cytoskeleton is achieved by crosslinking accessory proteins such as tropomyosin, which facilitates long-term inward-out and outward-in dynamic contractile and compressive forces [146].
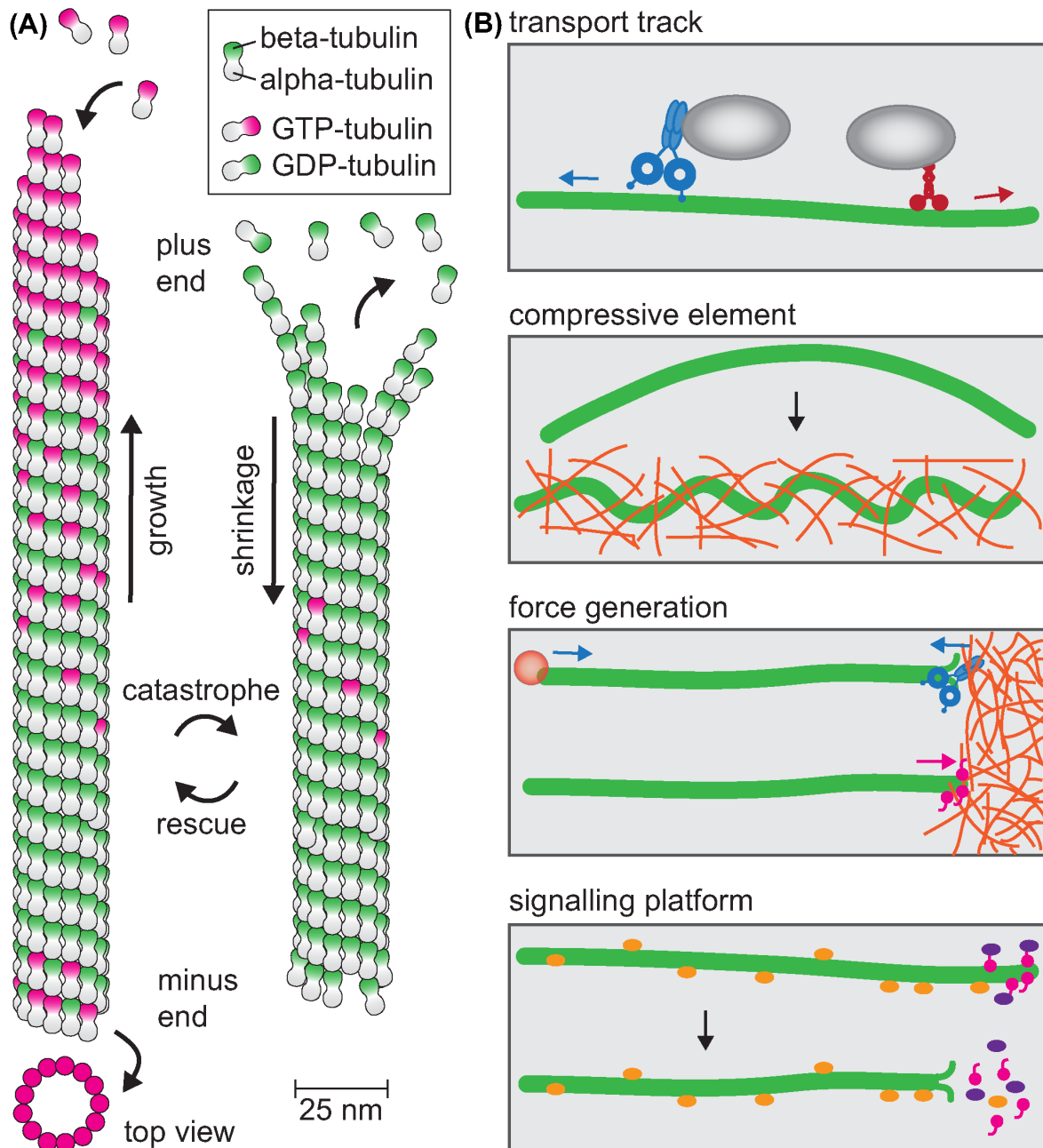
**Figure 1. 9: Illustration of microtubule organization.** Diagram shows **(A)** cycles of microtubule growth and shrinking, via a process known as dynamic instability; and **(B)** summary of microtubule functions in cells. These functions include intracellular transport, compression resistant struts and signalling scaffolds. Adapted from microtubules in the cell migration (141)

VSMCs sense their ECM, respond to the mechanical stimuli, and transduce the mechanical signals They respond by proliferating, differentiating, and migrating through the mechanotransduction process [147]. For example, during migration, cells reorganise their cytoskeleton to attain a morphological change that fits the directionality of their motion, producing a polarised cell with leading and trailing edges [148].

Microtubule dynamic instability (cycles of assembly and disassembly) and the actin filaments contribute to the overall morphology of cells about the activity they undergo [149]. Microtubules are thick, rigid structures, growing outwards from the centrosome in the centre of the cell called the microtubules organising centre (MTOC). They regulate the VSMCs morphology and contractility [146]. Previous work in our lab proposed that the microtubule ECM interaction balances the intracellular tension created by actomyosin-driven contractile forces [146].

## 1.9.2 Microtubules and VSMC migration

Microtubules play an important role in mesenchymal migration by providing an intracellular transport network for rapid directed transport of membrane vesicles, signalling molecules and other cytoskeletal components key to maintaining polarity and directionality of cell migration [150]. Asymmetry and microtubules' dynamics are important to support asymmetrically cellular activities necessary for the cell migration [151], where more microtubules extend to the front than the rear of migrating cells. The activity of the cell at the front includes selective capture and stabilization of microtubules whilst at the rear of the cell [152,153], selective support of persistent microtubule growth by local Rac1-dependent tubulin polymerization [154], inactivation of catastrophe factors such as stathmin [155] and asymmetric nucleation of the microtubule.

Within VSMCs, microtubules have also presented themselves as key modulator of cell migration. Cell polarisation is a prerequisite for directed cell migration, and microtubules assist in the polarization of the cell by reorienting themselves into a microtubule array facing toward the leading edge of the cell [156,157]. It does this via selective stabilisation of its plus end and this has been shown experimentally with the use of microtubule antagonists [72]. Dynamic instability of the microtubules is a requirement for migration and fibroblast cell lines whose microtubules were experimentally stabilised showed a decrease in the migration [158]. Microtubules have also shown a role, as mentioned before, in the disassembly of focal adhesions at the rear of the cell. Therefore, directed cell migration also depends on the dynamic regulation of microtubule function alongside actin polymerisation and adhesion turnover (Figure 1.10).

Small GTPases have shown roles in the regulation of microtubules. Examples are Rac1 and Cdc42 which can both decrease migration via microtubule stabilisation. Both Cdc42 and Rac1 activate PAK, which phosphorylates and subsequently inactivates stathmin. Stathmin is important in microtubule destabilisation and therefore Cdc42 and Rac1 increase the stability of microtubules during cell migration [159,160].
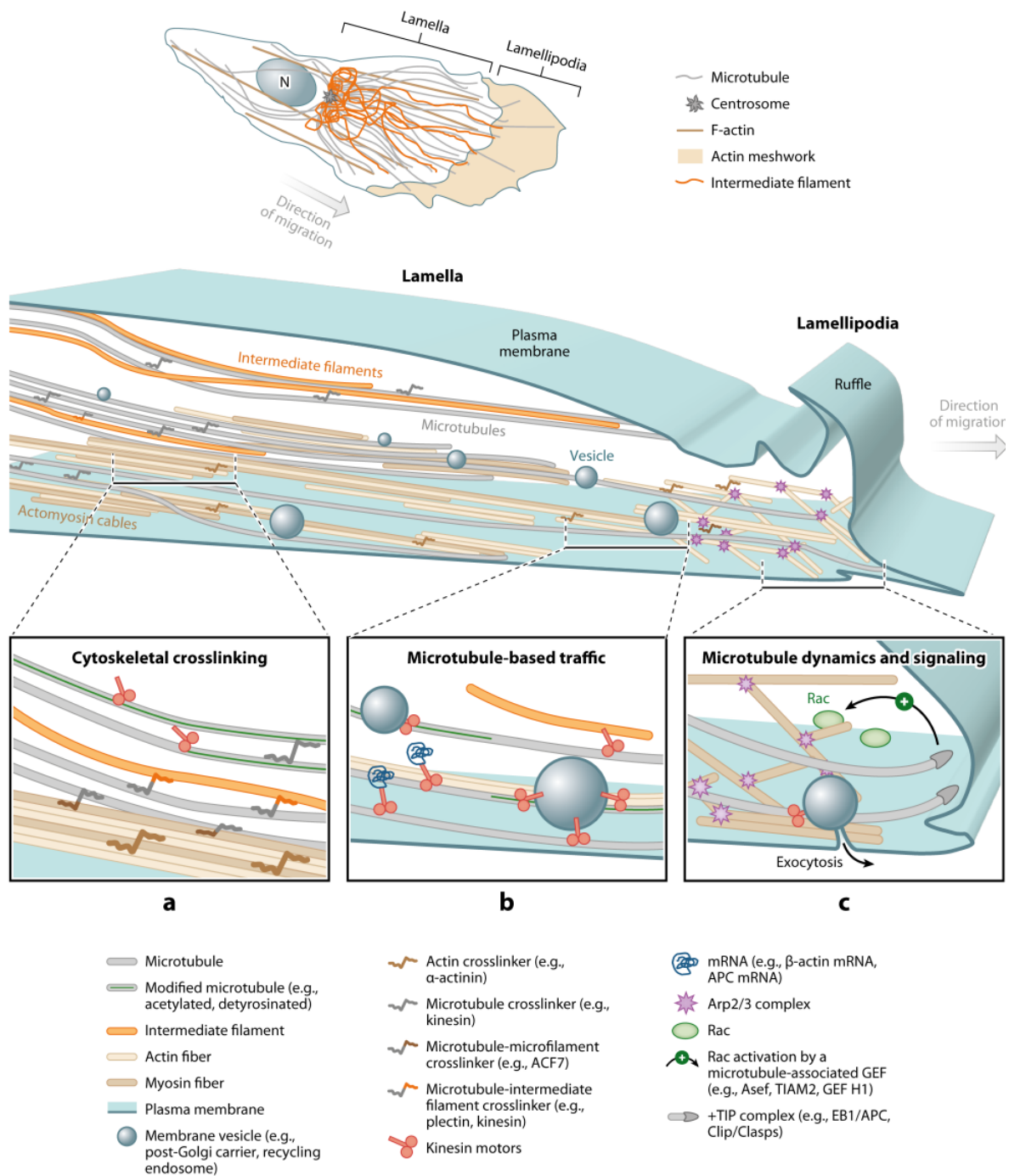
**Figure 1. 10: Illustration of microtubules in cell protrusion**. Adopted from Microtubules in cell migration (151)

### 1.9.3 Microtubules targeting agents

Given the widespread role of the cytoskeleton, it is an integral part of the cell's morphology and functionality, irregularity and defects within the cytoskeleton can lead to many serious dysfunction and disease. Studies showed that defects with the microtubules in the mitotic spindle are linked to chromosomal instability and subsequently lead to cancer [161,162]. Other disruptions of the microtubule function have been linked to neurodegenerative diseases and myopathies [163]. Furthermore, microtubule formation and function can be targeted by
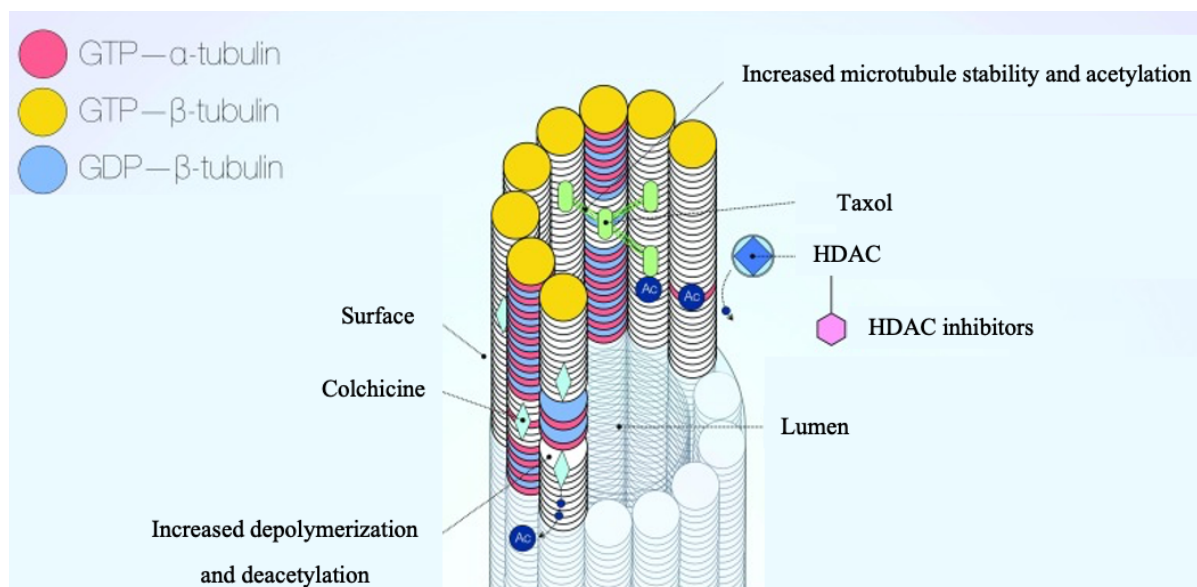


| Compound | Target | Molecular effect |
|---|---|---|
| Paclitaxel (Taxol) | Luminal β-tubulin | Conformational change at β-tubulin M-loop and increased microtubule acetylation |
| Colchicine | α-tubulin | Colchicine depolymerizes microtubules, decreases acetylation |
| Tubastatin | $Zn^{2+}$ dependent HDAC6 | Increase molecular acetylation |

**Figure 1. 11: Diagram illustrating tubulin binding sites and microtubule targeting drugs.** Adopted from Back to the tubule- microtubule dynamics in Parkinson's disease and the potential of combining tubulin-targeting anticancer therapeutics and immune therapy  (167)(164)

microorganisms for manipulation, such as HIV disrupting the microtubule network and microtubule motors-dynein as a key factor for the adenoviral entry into cells [164,165].

Among the most successful microtubule-targeted drugs are paclitaxel and colchicine, which work by suppressing the microtubule dynamics [166], which leads to mitotic block and apoptosis [167].

Microtubule inhibitors act by interfering with the dynamics of microtubule polymerization and depolymerisation. One group of inhibitors which include vinca alkaloid drugs such as vincristine and vinorelbine destabilise microtubule structure by binding to the β-tubulin subunit of the αβ-tubulin heterodimer and inhabiting polymerization of tubulin into microtubules. The second group of inhibitors such as paclitaxel promote stabilisation of the microtubule by binding to their distinct sites on the β-subunit located in the inner side of the microtubule lumen thereby inhibiting turbulent depolymerisation, resulting in a large stable and dysfunctional microtubule **(Figure 1.10)**. During cell division, this disruption of properly functioning microtubules causes the alignment of the chromosomes to fail and leads to cell cycle arrest at M-phase [168].

Hence, disrupting the microtubule dynamics are being used as a key target to develop many drugs as vascular disrupting agents (VDAs) alongside their cytotoxic activity. The benefit of those VDAs over the conventional cardiovascular disease treatment drugs such as angiogenesis inhibitors are the immediate vascular effects like decreased blood flow, vascular shutdown, increased interstitial pressure, reduced blood vessel diameter and vasculature permeability [169].

Microtubule targeting agents significantly reduce the migration speed of VSMCs. This is due to the microtubule stabilising effect of paclitaxel, which shifts the balance of microtubules to assembly, leading to numerous unorganised and decentralized microtubules inside the cytoplasm [170]. It's worth mentioning that both colchicine and paclitaxel inhibit cell division at the M phase, they involve different biological mechanisms and that is relevant to this observation [171]. Paclitaxel is believed to work via multiple pathways of inhibiting protein kinase activations such as the mitogen-activated protein kinases by reducing the growth factor-stimulated release of transcription factors [172]. Furthermore, some studies suggest that microtubule stabilising agents inhibit proliferation and migration as a result of some sort of microtubule-mediated sequestering and release mechanism [173].

### 1.9.4 Microtubules acetylation

The post-transitional modification (PTM) of histone is an important epigenetic regulatory process such as methylation, lipidation, glycosylation, ubiquitination and acetylation is a pivotal process in determining the structure, destination, function, activity of proteins and DNA binding affinity [174,175]. Microtubules undergo several PTM, one of which is tubulin acetylation, which is vital for survival of DNA damage and maintaining genome integrity [176,177].

Histone deacetylase 6 (HDAC6) is a cytoplasmic class II histone deacetylase that has specificity for non-histone proteins like α-tubulin [179]. HADC6 is involved in many cellular processes including protein degradation, cell motility and cell-cell interaction [180,181]. HADC6 is known to deacetylate α-tubulin to regulate microtubule stability and flexibility [182].

### 1.9.5 N-acetyltransferase 10 (NAT10) inhibition and VSMC function

N-acetyltransferase 10 (NAT10) are identified as a regulator of many cellular activities such as RNA stability and the translation process. Its deregulation is associated with many diseases including human immunodeficiency virus (HIV), cancer and Hutchinson-Gilford Progeria syndrome [183,184]. NAT10 promotes cell cycle progression through a proposed mechanism of the cyclinD1/CDK2/p21 axis [185] and is also shown to promote DNA damage response [186]. NAT10 must be predominantly distributed in the interphase and midbody during the telophase, where depletion of NAT10 induced defects in nucleolar assembly, cytokinesis and decreased acetylated α-tubulin-leading to G2/M cell cycle arrest [187].

NAT10 is a potential therapeutic target to treat different diseases for those reasons. Remodelin is a small molecule compound, which is the only known potent inhibitor of NAT10, shown to have a reverse effect on cell proliferation, cell invasion and migration under hypoxic conditions by blocking the epithelial-mesenchymal transition (EMT)[186 188–191]. Remodelin binds and interacts with the acetyl-CoA binding pocket of human NAT10.

### 1.9.6 Histone deacetylase 6 (HDAC6) inhibition and VSMCs

Histone acetylation and deacetylation are opposing activities of the class of transferase enzyme, histone acetylation transferase (HAT) and histone deacetyl transferase (HDACs), key for altered phenotypes and gene expressions. HDACs catalyse acetyl groups from lysine residues in histones and non-histone proteins, causing transcriptional repression. HDAC enzymes make one superfamily and have been categorised into four classes of I (HDACS 1/2/3 and 8), II (HDACs 4/5/6/7/9/10), III (HDACs, where they have seven signalling proteins-sirtuins (SIRT 1-7)) and IV [192]. Those processes are important for microtubule post-

translational modification of tubulin subunits [193]. Microtubules are affected by deacetylation leading to increased actomyosin forces [18,194]. This increased mechanical stress squashes the nucleus and physically induces DNA damage [195]. HDAC6 as a member of class IIb family has two active catalytic domains and unique physiological functions, which target specific substrates including α-tubulin. Guo *et al.,* identified that the protein levels of H3K23ac, H3K18ac, and H4K8ac were increased in VSMCs treated with the selective HDAC6 inhibitor tubastatin. The authors concluded that H3K23ac was the target of HDAC6 activity during VSMC dysfunction [196]. Hence, HDAC6 is a promising therapeutic target within cardiovascular diseases [192].

### 1.9.7 Actin-microtubule crosstalk in VSMC migration

The cytoskeleton is a unified system where the subcomponents co-regulate and function by leveraging their unique but interdependent filamentous networks. Each cytoskeleton can influence the other cytoskeletal components through direct interactions or cytoskeletal linkers or indirectly via signalling pathway [197,198]. Actin and microtubules share various cytoskeletal regulators and important proteins that mediate physical coupling that is key for cellular functions such as focal adhesion, contractility and motility [199]. The actin-microtubule-associated proteins regulate the small proteins GTPases, which in turn regulate both actin and microtubules, involve in the regulation of actin via their influence on regulating Rho GTPase (Figure 1.12) [199].

Microtubules influence actin polymerization through the microtubule-associated motors, that mediate intracellular transport of mRNA of proteins that regulate polarity in cell migration [200]. In turn, actin influences microtubule organization, where the retrograde flow of actin in lamellipodia results in a continuous backward transport of microtubules, causing them to buckle and break (Figure 1.12) [201,202]. The actin-microtubules crosstalk is important component of VSMC function [197], Some of the most important cellular activities include; mechanically cooperating in maintaining the integrity of cell morphology, traction force generation, controlling spindle position and orientation in cell division, cell to cell contact, lamellipodial protrusions, directional migration and others [199,200].
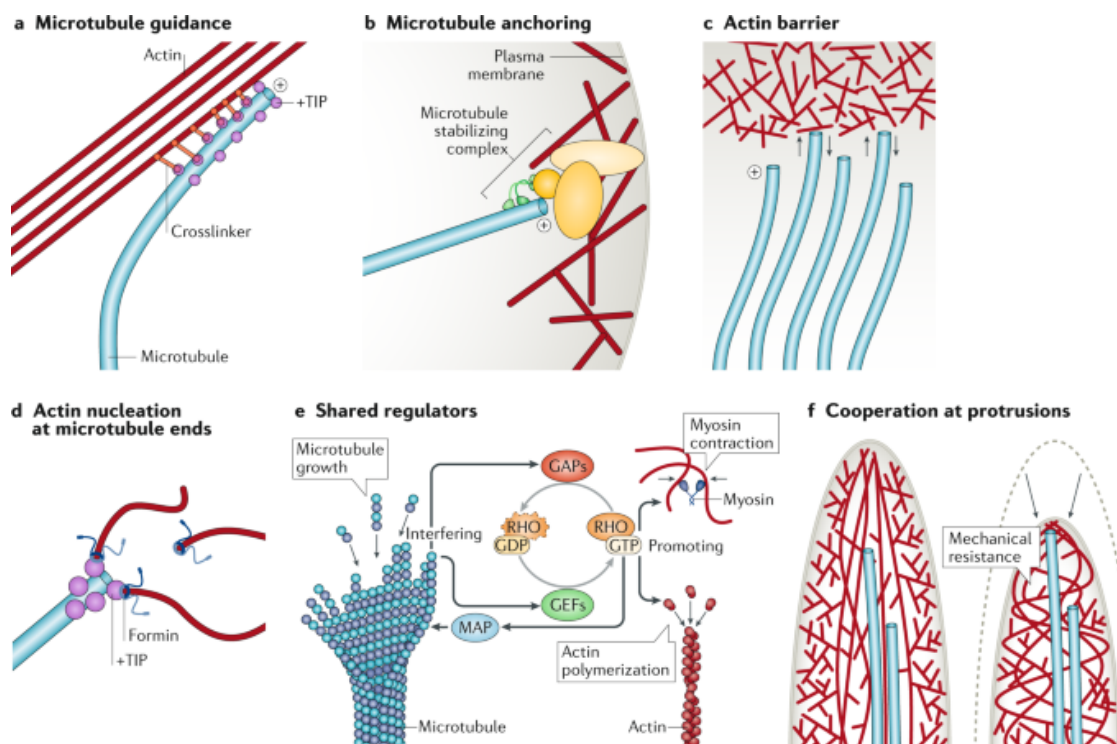


**Figure 1. 12: Illustration of actin-microtubule crosstalk**. Adopted from actin-microtubules crosstalk in cell biology (189)

## 1.10 VSMC migration

Several fundamental biological processes require cell migration, such as wound healing, embryonic development, pathological development and many others [203,204]. A precise understanding of the mechanism of cell migration has boosted many clinical interests in precision medicine, regenerative medicine and other novel therapeutic approaches [205]. There has been a remarkable process in uncovering cell motility and the factors, and mechanisms that influence cell migration and cell cycle in the cardiovascular biology [206]. Many studies investigating the VSMCs migration described the influence of soluble factors and emerging data is shading light on the impact of insoluble factors including ECM

characteristics [207].

Similarly, to other cell types, VSMC directional migration is initiated by external signals that stimulate receptors on the cell surface, causing multiple signalling cascades to occur that alter the cytoskeletal structure of the cell [208]. Typically, stimulation is initiated via G protein-coupled receptors and receptor tyrosine kinases (RTKs), which in turn activate several downstream components [80,209]. The migration process is cyclical, with external signalling inducing polarisation and filopodial projections, followed by lamellipodial projections extending from the cell [81] and this forms the leading edge of the cell. Nascent adhesions serve as anchor points for the newly formed protrusion to its ECM. These adhesions are associated with fare filamentous actin and actomyosin- a contractile force composed of the actin-myosin complex that forms within the cytoskeleton activity and pulls the cell body forward. Adhesions also serve as signalling conduits, allowing "inside-out" signalling by emitting the traction force generated by the cell. The force generated causes "outside-in" signalling to occur which further regulates the dynamics and maturation of the focal adhesions [95,210]. At the same time, adhesion disassembly and actomyosin activity detach and retract the rear of the cell, further propelling the cell body forward (Figure 1).

### 1.10.1 Actin polymerisation and VSMC migration

Actin polymerisation generates membrane protrusions at the leading edge of a cell during migration. Actin polymerisation requires nucleation which is the formation of multiple stable actin monomers. However, this is a rate-limiting step in the polymerisation process due to the instability of actin dimer intermediates along with the repressive activity of specific actin-binding proteins. To facilitate actin polymerisation and overcome this kinetic demand, cells employ a wide set of actin-nucleating proteins [211]. There are primarily two groups of actin polymerisation nucleators which are the Arp 2/3 complex and the formins, mDia1 and mDia2 [212]. mDia1 and mDia2 bind to the barbed end of actin filaments and polymerise actin linearly, to form thin cellular protrusions called filopodia. mDia1/2 are multi-domain proteins that function as dimers, utilising their formin homology domain 2 (FH2) to bind to globular actin monomers to nucleate actin. The protein profilin facilitates the polymerisation via interaction with the formin homology 1 (FH1) domain of mDia1/2 [213]. RhoA and Cdc42 regulate the mDia1 and mDia2, respectively [95].

### 1.10.2 2D vs 3D VSMCs migration

In vivo, the arterial wall is a complex biomechanical, biochemical, ECM composition and humoral factors of a 3D environment. and cells have to navigate through other VSMCs, collagen and elastin-dense structures [214]. As a result, VSMCs show a range of molecular and functional phenotypes in response to their complex environment [78]. In the arterial walls, VSMCs form a cell-to-cell and cell-ECM adhesion, forming a multilayer natural responsive and pliable representative of a normal arterial wall. Assessments of VSMCs conducted in multi-layered aggregates revealed reduced expression of genes associated with cell cycle control, cease proliferation and DNA replication and key differentiation markers of VSMCs such as decreased levels of mitogen-associated protein ERK1/2 and increased levels of autocrine TGGβ/SMAD2/3-mediated signalling (discussed in great detail in section 1.3.2 contractile marker proteins) [214].

However, in vitro, the culture of isolated VSMCs is conducted in a 2D environment, in 1000s fold of stiff flat glass or plastic [215]. Isolated VSMCs cultured in that unfavourable environment spread all over the glass/plastic and make multiple focal adhesions and become synthetic phenotypes, suggestive of their enhanced migratory capacity. This setup doesn't always reflect the organotypic organization and differentiation of VSMCs due to the loss of the contractile markers [216].

## 1.11 Project hypothesis and objectives

VSMCs are key components of the arterial walls, they play a crucial role in age-induced cardiovascular complications. We have celebrated 100 years of cardiovascular research and there has been remarkable advancement in understanding the underpinning science behind CVD. However, most of the research was carried out on glass or plastic, which are 1000s-fold in stiffness and don't represent arterial wall stiffness. We hypothesise that by developing PAHs that mimic the features of the blood vessels inside the body, we could unfold fundamental information in understanding the mechanisms and factors that influence VSMC behaviours in a healthy and aged/diseased environment. we set out to explore the following objective:

- ♦ Characterise VSMCs function in response to different matrix topologies and stiffness.

- ♦ To investigate the importance of microtubules in VSMC traction stress generation and migration.

♦ To test potential regulators of VSMCs migration on healthy and aged/diseased stiffness PAHs.

Those findings will help on uncovering the principles of VSMC function within the appropriate matrix stiffness and topology. This in turn will aid the endeavours of enhancing excising medicines or developing more effective therapeutic targets that prevent and/or treat CVD.

# Chapter 2: Materials and Methods

## 2.1 List of tables

**Table 2.1.1: Lab Consumable**

| Lab apparatus | Product number | Source |
|---|---|---|
| (3-Aminopropyl) triethoxysilane (APES) | A3678 | Sigma |
| 30 mm Coverslips | 631-0174 | VWR |
| 3D printed micropatterned Glass Slide | | University of Birmingham |
| 6 Well Plates | 130184 | Thermo Scientific |
| Acrylamide 40%/Electrophoresis | BP1404-250 | Fisher Scientific |
| Ammonium Persulfate (APS) | A3678 | Sigma |
| Bis-acrylamide 2% w/v/electrosphoresis | BP1402-1 | Fisher Scientific |
| Bovine Serum Albumin (BSA) | A2153 | Sigma |
| Collagen-1 | A1048301 | Thermo Scientific |
| DAKO Block | | |
| Dimethyl sulfoxide (DMSO) | D8418 | Sigma |
| Earle's Balanced Salt Solution | E6267 | Sigma |
| FluoSpheres$^{TM}$ Carboxylate-modified microspheres, 0.5 µm, red fluorescent (580/605), 2% solid | F8812 | Thermo Scientific |
| Glutaraldehyde solution | G6257 | Sigma |
| Hydrochloric Acid | | |
| Microscopic Slides with Ground Edges | 12373118 | Fisher Scientific |
| Mounting Media | H-1400 | Vector |
| Mounting Media + DAPI | H-1500 | Vector |
| Nonidet P- 40 (NP40), 10% w/v aqueous solution | 85124 | Thermo Scientific |
| Parafilm | P7793 | Sigma |
| Paraformaldehyde (PFA) | P6148 | Sigma |

**Table 2.1.1: Lab Consumable continued**

| | | |
|---|---|---|
| Phosphate Buffered Saline (PBS) | D8537 | Sigma |
| Smooth Muscle cell Basal Media | 132-500 | Sigma |
| Smooth Muscle cell Growth Media | 311-500 | Sigma |
| Smooth Muscle cell Growth Supplements | 311-GS | Sigma |
| Sulfo-SANPAH, primary amine-nitrophenylazide crosslinker | Ab145610 | Abcam |
| Tetramethylethylenediamine (TEMED) | 17919 | Thermo Scientific |
| Thermo Scientific™ BioLite Cell Culture Treated Flasks T25 | 11884235 | Fisher Scientific |
| Thermo Scientific™ BioLite Cell Culture Treated Flasks T75 | 11884235 | Fisher Scientific |
| Triton x-100 | X100 | Sigma |
| Trypsin-EDTA solution | T3924 | Sigma |

**Table 2.1.2: Compounds and concentrations**

| Compound | Source and product number | Working Concentration |
|---|---|---|
| Angiotensin II | Sigma A9525 | 0.01-100 µM (serial dilution) |
| Atorvastatin | Sigma PZ0001 | 0.5 µM |
| BrdU | Abcam Ab142567 | 10 µM |
| Colchicine | C9754 | 100 $\eta$M |
| Demecolcine | D1925 | 1 $\eta$M |
| GsMTx-4 | Abcam ab141871 | 0.5 µM |
| Mevastatin | Sigma 474705 | 1 µM |
| Paclitaxel | T7402 | 10 $\eta$M |
| Remodelin | Sigma SML112 | 1 µM and 100 µM |
| Simvastatin | Sigma 6196 | 1 µM |
| Tubastatin | Sigma 382187 | 1 µM |

**Table 2.1.3: Primary and Secondary Antibodies used for Immunofluorescence**

| Target | Source | Product Code | Host | Concentration used | Primary / Secondary |
|---|---|---|---|---|---|
| BrdU | Abcam | Ab1893 | Sheep | 9 ηg/μl | Primary |
| Mouse monoclonal anti-Lamin A/C | Sigma | SAB4200236 | Mouse | 10 ηg/μl | Primary |
| Anti-mouse Alexa fluor 488 | Thermo scientific | A-11001 | Goat | 5 ηg/μl | Secondary |
| Anti-sheep Alexa fluor 488 | Thermo scientific | A-11015 | Donkey | 4 ηg/μl | Secondary |
| Rhodamine Phalloidin | Thermo scientific | R415 | N/A | 1:400 | Secondary |

**Table 2.1.4: Lab Instrument**

| Instrument | Source |
|---|---|
| Benchtop UV Transilluminator | UVP |
| Magnetic Stirrer with Heating | Starlab |
| UV Cabinet | Fisher Scientific |
| Vortex | Starlab |
| Zeiss AxioPlan 2ie | Zeiss |
| Zeiss LSM980-Airyscan | Zeiss |
| Zeiss Observer 7 | Zeiss |

**Table 2.1.5 Composition of polyacrylamide hydrogel solutions**

| Solutions | 2 kPa | 12 kPa | 72 kPa |
|---|---|---|---|
| 40% Acrylamide solution | 6.25 ml | 3.75 ml | 5 ml |
| 2% Bis-acrylamide solution | 2 ml | 1.2 ml | 4 ml |
| dH20 | 41.75 ml | 15.05 ml | 11 ml |

## 2.2 Polyacrylamide Hydrogel Fabrication

### 2.2.1 Coverslip Activation

Coverslips (30 mm) were activated by applying a drop of (3-Aminopropyl) triethoxysilane (APES) for 3-5 minutes. Afterwards, coverslips were washed 3x with dH2O then fixed with 0.5% glutaraldehyde solution for 45 minutes. Coverslips were then washed 3x with dH2O and left to airdry overnight.

### 2.2.2 Hydrogel Fabrication

Polyacrylamide hydrogels of either 2 kPa, 12 kPa or 72 kPa stiffness were fabricated as follows. To the desired volume of polyacrylamide hydrogel solution (composition detailed in Table 2.5, 10% ammonium persulfate (1:100) and TEMED (1:1000) were added. Where required, red fluorescent (580/605) FluroSpheres (1:1000) were also added. The solution was briefly vortexed then 50 µl of the solution was added onto either a standard microscopy slide (smooth hydrogels) or an in-house 3D printed, ridged slide (grooved hydrogels) to which an activated coverslip (activated side down) was placed on top, and the hydrogel left to polymerise for 5-10 minutes. Hydrogels were gently removed from the slides and transferred to a 6-well plate and washed 3x with dH2O. Where live cell microscopy was being performed, hydrogels were glued to the base of the 6-well plate using nail polish to prevent excess movement during imaging.

### 2.2.3 Hydrogel Functionalisation

To enable attachment of ECM components and cells to the PAHs, they were first crosslinked with Sulfo-SANPAH (1:3000), which was activated by UV irradiation (365 nm) for 5 minutes. Prior to transferring the hydrogels to tissue culture, plates were UV sterilised for 30 minutes in a UV sterilisation cabinet. PAHs were subsequently washed with sterile PBS, then coated for 10 minutes at room temperature with 0.1 mg/ml collagen-I solution. After functionalisation with an ECM component, PAHs were again washed with sterile PBS before being ready for cell seeding.

## 2.3 Cell Culture

### 2.3.1 Routine Cell Culture

Healthy human aortic smooth muscle cells (HAOSMCs) (354-05A, Cell Applications Inc) used are commercially available. Cells between passages 5 and 9, were grown in smooth muscle growth media supplemented with additional growth supplements. Cells were incubated at 37 $^{\circ}$C with 5% CO2 and underwent routine passaging once cells reached 80% confluency. To passage cells, they were first washed with Earle's balanced salts solution (10 ml), then detached using trypsin (1.5 ml) and split (1:2) into fresh T75 flasks. For the rest of this thesis HAOSMCs will simply be referred to as VSMCs.

### 2.3.2 Experimental Seeding

For VSMC morphology (area/volume analysis), proliferation and contractility assay a confluent T75 underwent a 1:4 T75 flash split, with 1/4th of the flasks being seeded in VSMC growth media of a 6-well plate. Cells were maintained in growth media for morphology and proliferation assays, however for contractility assays once cells had adhered to the PAH, the media was replaced with VSMC basal media and left overnight to induce quiescence.

For traction stress and migration assays, a confluent T75 underwent a 1:6 T75 flask split, with 1/6th of the flasks being seeded in VSMCs growth media of 6-well plate. Cells were maintained in growth media for traction stress and migration assays and left overnight to adhere to the PAHs. For the traction stress assay, cells were taken to the microscope suit for imaging after the appropriate treatment. For the migration assay, cells were taken to the imaging suite, after treatment, left overnight for 12 hours of time-lapse imaging.

## 2.4 Immunofluorescence microscopy

### 2.4.1 Cell Staining

Following experimental treatment, cells were washed with PBS and fixed for 10 minutes with 4% paraformaldehyde at room temperature. Cells were then washed in PBS twice and permeabilised using 0.5% NP40 for 5 min at room temperature then blocked with 3% BSA/PBS for 1 hour at room temperature. Cells were incubated with primary antibodies, diluted in 3% BSA/PBS at 4 0C overnight. The following day, cells were washed with 3% BSA/PBS and incubated with secondary antibodies, diluted in 3% BSA/PBS, for 2 hours at room temperature in a dark cabinet. After staining, cells were washed three times in PBS then mounted onto a microscopy slide using mounting media. For details on the antibodies used and their concentrations please see Table 2.3.

### 2.4.2 Confocal Microscopy – Area & Volume Analysis

Following staining, images were captured at 20X on a Zeiss LSM980-Airyscan confocal microscope. For analysing volume, a Z-stack throughout the cell was captured at 1.4 μm interval. Cell area was measured using FIJI, open-source software [217], whilst cell volume was calculated using Volocity 6.3.

## 2.5 Traction Force Microscopy

Traction force Microscopy (TFM) was performed using the Zeiss Observer 7 live cell imaging system. Where the effects of a particular compound were being investigated, VSMCs were pre-treated with the compound for 1 hr prior to TFM being performed. Images were captured at 20x magnification at 2 minutes intervals. Images were captured before and after cell lysis, which was achieved by the addition of 0.5% Triton x-100 (100 ml). Bead displacement between the first and last time points was measured on FIJI [217] using the practical image velocimetry (PIV) plugin. The subsequent PIV file was used to generate a displacement field, by means of the Fourier transform attraction cytometry (FTTC) plugin. This displacement field was used to calculate the traction force magnitude and force fields generated by VSMCs. To determine the integrated (cell total) traction force, a Phase image of the cell was overlayed and used to generate a region of interest (ROI). Maximum traction force is reported as the largest force measured within the ROI of each cell.

## 2.6 Aspect ratio measurement

We also measured the aspect ratio, the ratio of the sizes of cells in different dimensions, which is also defined as the major axis length of the approximate ellipse/minor axis length of the approximate length. This is used to identify the deformation/elongation of the cells. A perfectly circular shape has an aspect ratio value of 1, and the value increases with increased deformation. To measure aspect ratio, cells were stained with rhodamine phalloidin, and ImageJ software was used process this data. Images were first converted to an 8-bit format and threshold adjusted to augment the ability to see the cells. The final step was to manually draw around individual cells using the freehand region of interest (ROI) function and adjust the scales according to the range of magnifications used. ImageJ provided processed data outputs of the images analysed.

## 2.7 Proliferation Assay

VSMCs were treated with BrdU (10 µM) overnight for 17 hrs. After treatment cells were washed twice with PBS before 10 minutes of 4% paraformaldehyde fixation. Cells were then incubated in 1 M HCl for 30 minutes followed by permeabilisation with 0.25% Triton/PBS for another 30 minutes. Finally, cells were blocked for 10 minutes at room temperature using DAKO™ Protein Block, Serum-Free. BrdU incorporation was achieved using the relevant primary and secondary antibodies, detailed in Table 2.3. Images were captured at 10x using a Zesis AxioPlan 2ie microscope.

## 2.8 Migration Assay

Cell migration was observed using the Zeiss Observer 7 live cell imaging system. Where the effect of a particular compound on the migratory potential of VSMCs was being investigated, VSMCs were treated with that compound for 1 hour (as detailed in Table 2.2) prior to imaging began. Images were captured at 20x magnification, over a 12-hour period, with images captured every 10 minutes. Time-lapse images were tracked FIJI (plugin →tracking → manual tracking) and data was analysed using chemotaxis, by using the chemotaxis tool plugin in FIJI, open-source software [217].

When tracking migrating cells, all cells were tracked until they left the frame, divided, or died. We also focused on tracking cells in the groove for the grooved PAH experiment, with

the same exclusion conditions as the smooth PAH experiment.

Directionality was calculated using the ImageJ plugin 'chemotaxis'. The system calculated the directionality of cells migrating with a preferred orientation, and the data was represented bya histogram peak at that orientation. The statistics generation by the plugin is explained in the ImageJ docs [218]. All directionality rose plot graphs display representative examples of the data obtained.

## 2.9 Contractility Assay

After being incubated in VSMC basal media overnight, thereby inducing VSMC quiescence, cells were then stimulated with the contractile agonist angiotensin II (between 0.01 µM to 100 µM). After 30 minutes, VSMC were fixed and processed for immunofluorescence microscopy as detailed in section 2.3. Imaging proceeds as previously, however for this assay cells were imaged in only 1 z-plain and only the cell/nuclear area was analysed.

## 2.10 Statistical Analysis

Data was collected from multiple replicates (N) of experiments, which is stated as an independent experiment in the figure legends. The number of cells analysed is denoted by (n).

Statistical significance of data analysed was performed using GraphPad -Prism 9 and it was determined based on the comparison of a set of data. To test for normal (Gaussian) distribution, a Shapiro-Wilk normality test was performed in prism to generate a QQ plot. This was performed on all data sets generated in the study. All data generated in the triplicate experiments displayed consistent spread of data between conditions. To determine the statistical significance between two groups of data, a paired Student t-test was performed. For data with multiple groups, statistical analysis was performed by subjecting the data to a One-way ANOVA, followed by Bonferroni's multiple comparison test. EC50 values of sigmoidal dose curves were derived through non-linear regression analysis. Error bars represent the standard error of the mean (SEM), with bar charts displaying the mean value. P values are represented as $*p = < 0.05$, $**p < 0.01$, $***p < 0.001$ and $****p < 0.0001$.

# Chapter 3: Matrix topology regulates VSMC morphology and function

## 3.1 Background

The Young's modulus of healthy large elastic arterial walls is between 10-20 kPa [219]. Arterial wall stiffness increases during ageing and cardiovascular disease progression. Traditionally, VSMCs have been grown on tissue culture plastic or glass, which is around 1000x stiffer than the healthy arterial wall. Recent developments in biomaterials and tissue engineering techniques have enabled the unique mechanical properties (elasticity) of blood vessels to be modelled in vitro. Previous studies conducted in our lab show that matrix stiffness plays a crucial role in modulating VSMC function. Arterial walls can distend to accommodate the increased blood volume in response to the pressure (the change in volume per change in pressure) is defined as arterial compliance [220]. During ageing/diseases, the arterials become stiff and lack compliance [221]. Our understanding of the mechanisms contributing to attenuated vascular compliance and its impact on VSMC function remains limited. Previous studies have shown that matrix stiffness regulates VSMC differentiation, proliferation and actomyosin-generated traction forces, yet we still do not understand the mechanisms that regulate VSMC response to matrix stiffness [146].

In addition to changes in matrix stiffness, changes in VSMC morphology are also observed between *in vivo* and *in vitro* conditions. VSMCs adopt a spindle-shaped morphology within the vessel wall [224]. However, when isolated and grown *in vitro*, VSMCs spread and adopt a morphology akin to that of a fried egg (Figure 3.1). Previous studies have shown that changes in VSMC morphology are associated with changes in function [225,226].

Current methods used to control VSMC morphology *in vitro* require specialised equipment and training, making them inaccessible to most VSMC labs [227]. Therefore, the development of an easy-to-fabricate system would potentially make *in vitro* findings more relevant to VSMC function *in vivo* [228].
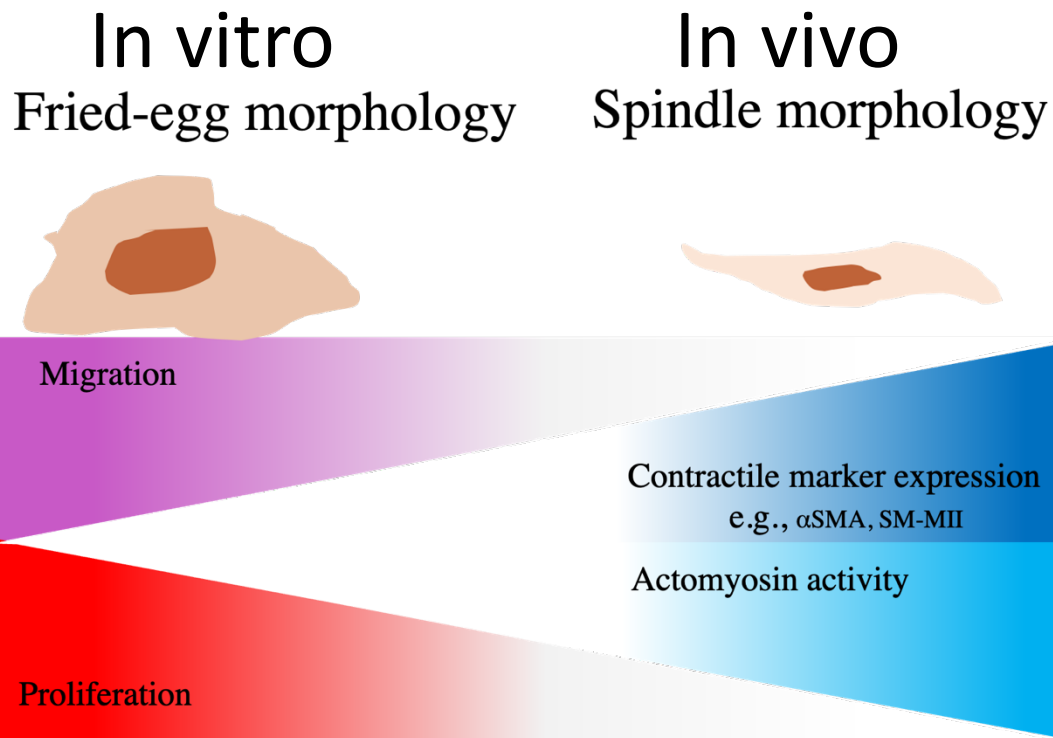
**Figure 3.1: Changes in VSMC morphology correspond with changes in VSMC phenotype**: *In vivo*, VSMCs adopt a spindle-shaped morphology, existing in a quiescent but contractile phenotype, expressing contractile markers including alpha-smooth muscle actin (αSMA) and smooth muscle myosin II (SM-MII). Once isolated and cultured on tissue culture glass or plastic, VSMCs dedifferentiate, down-regulating contractile marker expression whilst upregulating pathways that promote VSMC proliferation and migration.. adopted from mechanical programming of arterial smooth muscle cells in health and ageing (50).

### 3.1.1 Hypothesis

We hypothesise that changing the topology of our polyacrylamide hydrogels (PAHs) will promote VSMCs to adopt a more spindle-like morphology. We predict that this change in morphology will coincide with changes in VSMC traction stress, migration, and proliferation, with the VSMCs phenotype becoming more reminiscent of that observed *in vivo*.

### 3.1.2 Aim of the chapter

The objective of our experiments was to:

1. Validate an easy-to-fabricate method for regulating VSMC morphology.

2. Determine morphological changes caused by altering the ECM topology.

3. Test if changes in VSMCs morphology alter traction stress generation.

4. Determine if changes in VSMC morphology alter the migrational and proliferative capacities of VSMCs.

## 3.2 Methods

Smooth and grooved PAHs were fabricated as discussed in the materials and methods section (Chapter 2.2). Smooth PAHs are fabricated on a standard microscopy slide whilst grooved PAHs are fabricated on a custom-made micropatterned slide, imprinted with micrometre scale indentations (Figure 3.2A) [229]. Those microgroove PAH are used to generate a more physiological model of the human tissue and its microenvironment, that supports cell alignment like VSMCs inside the body, which gives us controlled in vitro cell culture of VSMCs' migration, proliferation, and traction force generation studies.

VSMCs were seeded onto collagen-I coated smooth and grooved PAHs at two different stiffnesses: 12 kPa to model healthy aortic wall stiffness and 72 kPa to model aged/diseased aortic wall stiffness). Smooth PAHs are fabricated on a standard microscopy slide whilst grooved PAHs are fabricated on a custom-made a micropatterned slide, imprinted with micrometre scale indentations (Figure 3.2A) [229]. VSMCs were seeded onto collagen-I coated smooth and grooved PAHs at two different stiffnesses: 12 kPa to model healthy aortic wall stiffness and 72 kPa to model aged/diseased aortic wall stiffness.
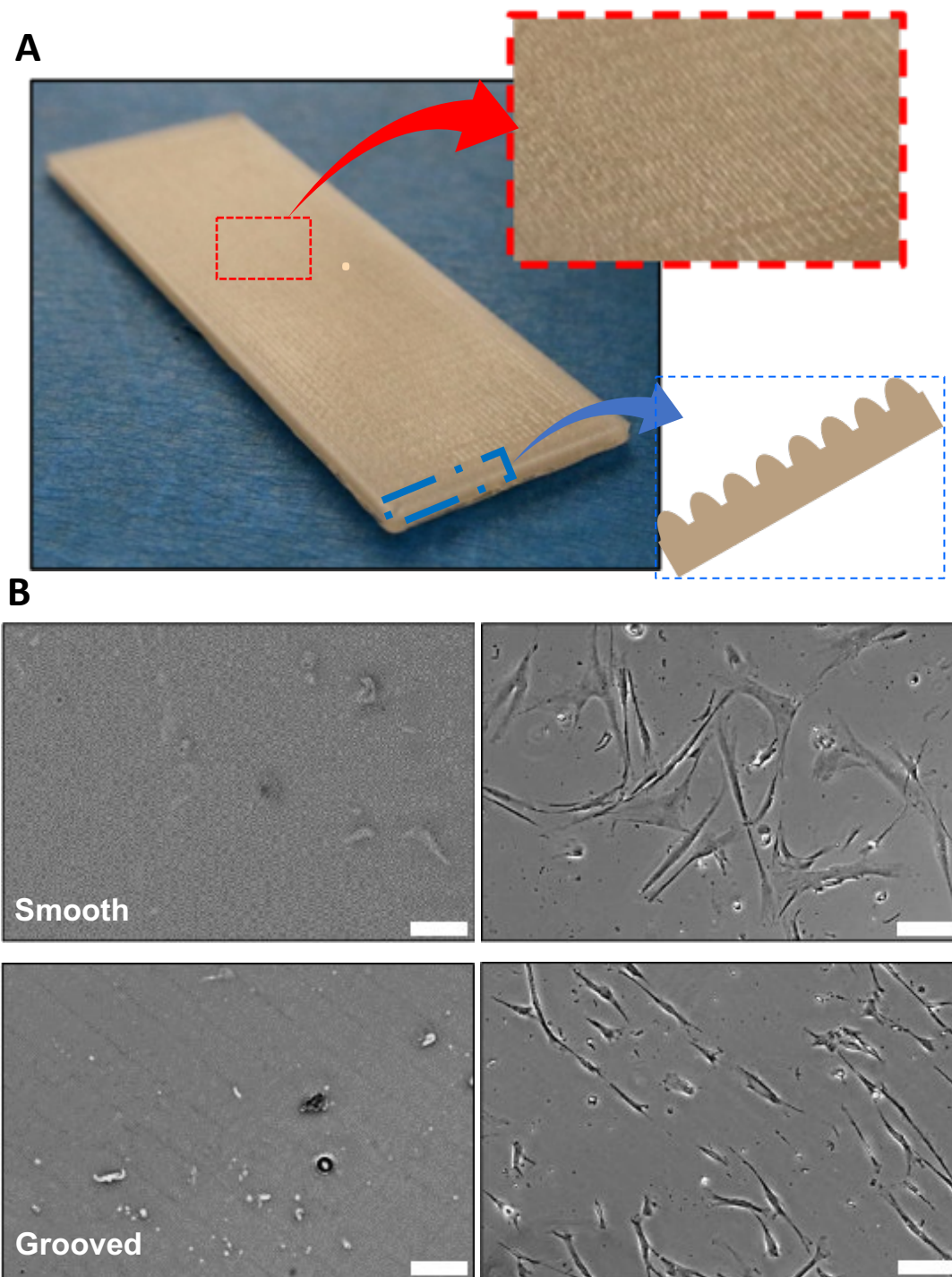
**Figure 3. 2: Fabrication of Smooth and Grooved Polyacrylamide Hydrogels: A**) The custom made, 3D printed slides on which grooved hydrogels are fabricated. Each slide is imprinted with micrometre scale indentations, top and cross-section view of grooved PAH. **B**) Smooth (top) and grooved (bottom) PAHs before (left) and after (right) being seeded with VSMCs. Scale bar represents

# 3.3 Results

## 3.3.1 VSMCs on Grooved PAHs adopt a spindle-like morphology

We set out to determine how changing the topology of PAHs would impact the morphology of VSMCs. Firstly, VSMCs were plated on smooth and grooved PAHs of 12 kPa stiffness. VSMCs were stained with Rhodamine phalloidin and lamin A/C, to visualise F-actin and the nuclear envelope respectively. Confocal immunofluorescence microscopy was performed to capture z-stacks of individual VSMCs. Analysis revealed that VSMCs on grooved PAHs displayed a reduction in cell area and cell volume, compared to their counterparts on smooth PAHs (Figure 3.3 A-C). These changes were mirrored in the nucleus, with VSMCs on grooved hydrogels possessing nuclei with reduced area and volume (Figure 3.3 A, D and E) than those plated on to smooth PAHs.
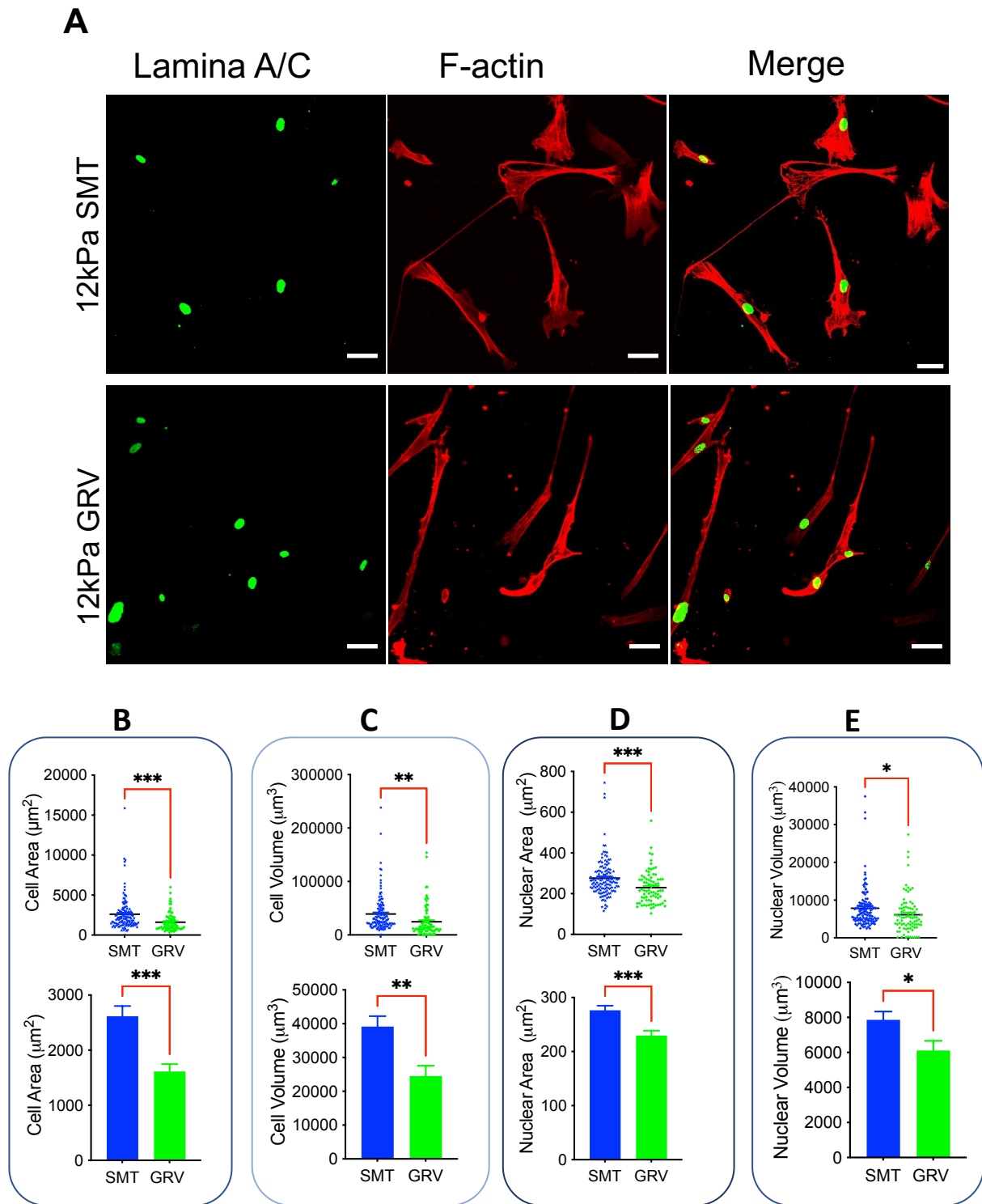
**Figure 3. 3 VSMCs seeded on grooved PAHs adopt a spindle-shaped morphology: A)** Representative images of VSMCs seeded on 12 kPa Smooth or Grooved PAHs in growth media. VSMCs were stained for F-actin (Rhodamine phalloidin, red) and Lamin A/C (green). Scale bar represents 50 μm. Graphs show **B)** VSMCs area **C)** volume **D)** nuclear area and **E)** nuclear volume. Data is based on 3 independent experiments, with (n = 127 on smooth and n = 78 on grooved PAHs) VSMCs analysed. Statistical significance was determined using unpaired student t-test (* p = <0.05, ** p = <0.01 and *** p= <0.001).

Next, we analysed the data further to determine if the relationship between VSMC area and volume was altered by PAH topology. This analysis revealed that there was a moderate relationship between VSMC area and volume for both smooth ($R^2$ = 0.61) and grooved ($R^2$ = 0.50) PAHs of 12 kPa stiffness (Figure 3.4 A). These were not significantly different, suggesting that altered PAH topology is not changing the relationship between VSMC area and volume. Nuclei displayed no obvious correlation between area and volume for both 12 kPa smooth ($R^2$ = 0.054) and grooved ($R^2$ = 0.161) PAHs (Figures 3.4 A and C). There was no significant difference.
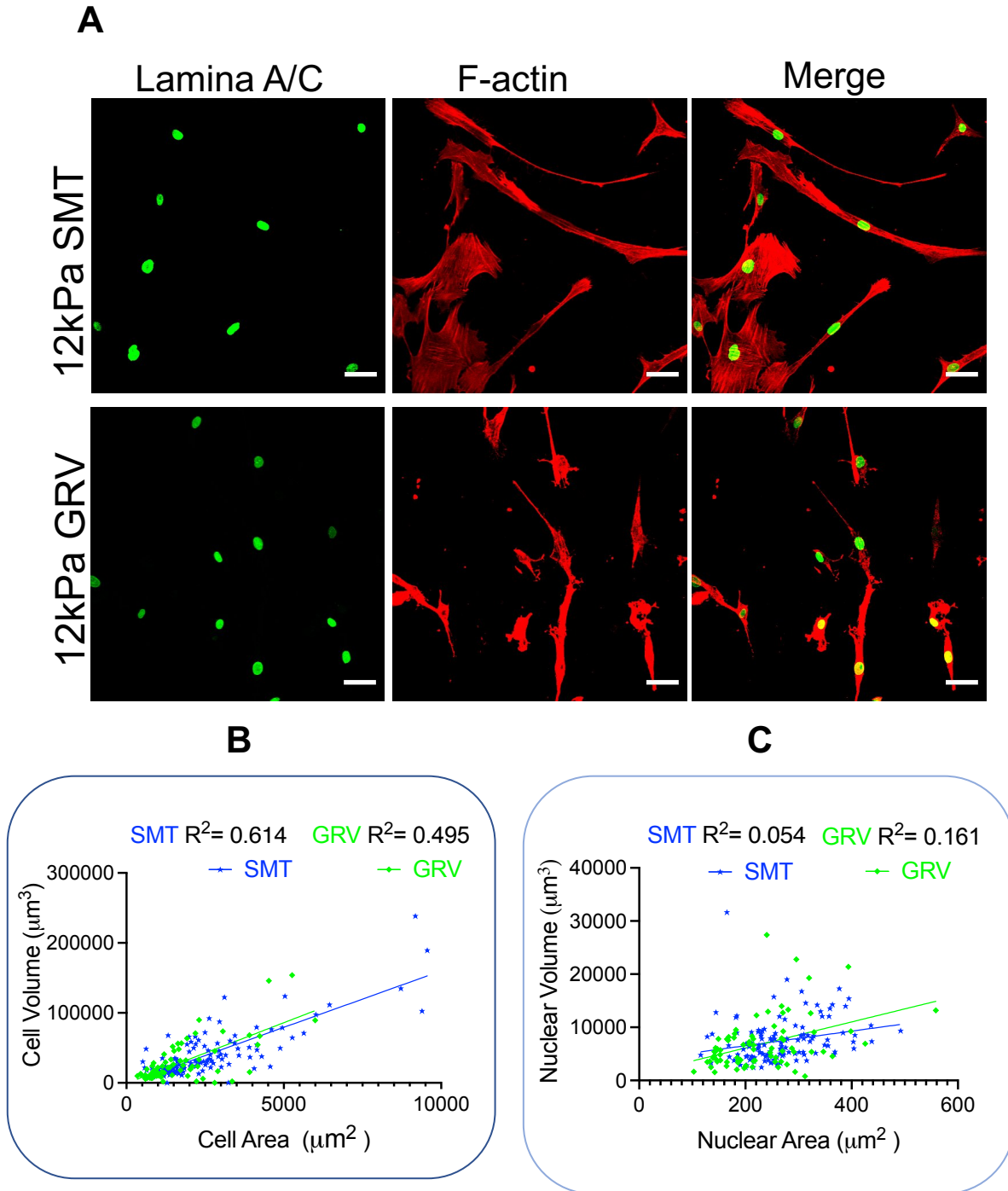
**Figure 3.4: VSMC area to volume ratio is unaltered by matrix topology**. **A)** cell volume plotted against cell area and **B)** nuclear volume plotted against nuclear area, on 12 kPa smooth and grooved PAHs. Data is based on 3 independent experiments from (n = 127 on smooth PAHs and n = 78 on grooved PAHs) VSMCs analysed.

### 3.3.2 Matrix stiffness alters the morphological response of VSMCs to grooved PAHs

The above data demonstrate that matrix topology altered VSMC morphology, promoting VSMCs to adopt a spindle shape at healthy matrix stiffness. Next, we investigated whether matrix stiffness akin to that of an aged/diseased aorta would alter the morphological response VSMCs adopt in response to hydrogel topology. VSMCs were plated on smooth and grooved 72 kPa PAHs. Confocal immunofluorescence microscopy was performed to capture z-stacks of individual VSMCs. Analysis revealed that whilst there was no change in VSMC area between smooth and grooved PAHs, VSMC volume was increased on grooved PAHs (Figures 3.5 A-C). This response was reflected in nuclear morphology, which displayed no change in area but an increase in volume (Figures 3.5 A, D and E) on grooved PAHs of aged/diseased stiffness. Furthermore, VSMCs on grooved PAHs adopted more elongated morphology.

Next, we analysed the relationship between VSMC area and volume. Analysis revealed the ratio between VSMC area and volume was altered between smooth and grooved PAHs of aged/diseased stiffness; VSMCs displayed a high correlation ($R^2$ = 0.806) between area/volume on smooth PAHs (Figure 3.6 A and B), but only a moderate correlation ($R^2$ = 0.444) on grooved PAHs (Figure 3.6 A and B). The $R^2$ values are lower than the minimum accepted significant correlation value ($R^2$ >0.5), hence the change was insignificant on smooth PAHs. Analysis of nuclear area/volume scaling revealed that VSMCs on both smooth ($R^2$ = 0.46) and grooved ($R^2$ = 0.316) PAHs displayed weak correlation (Figures 3.6 A and C).
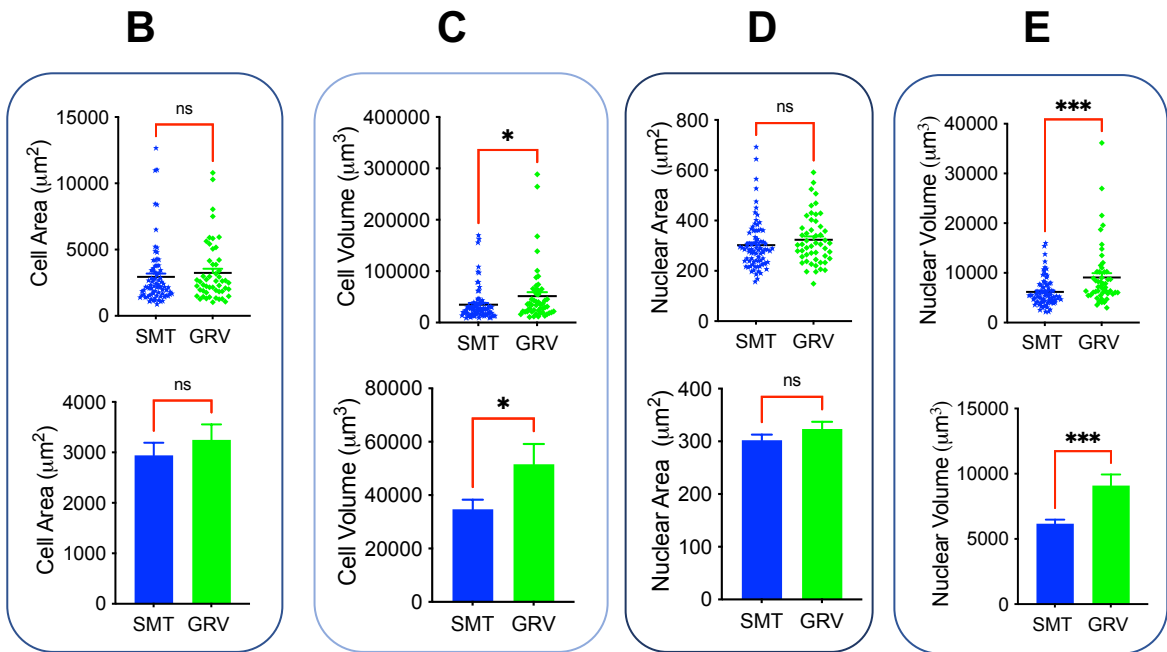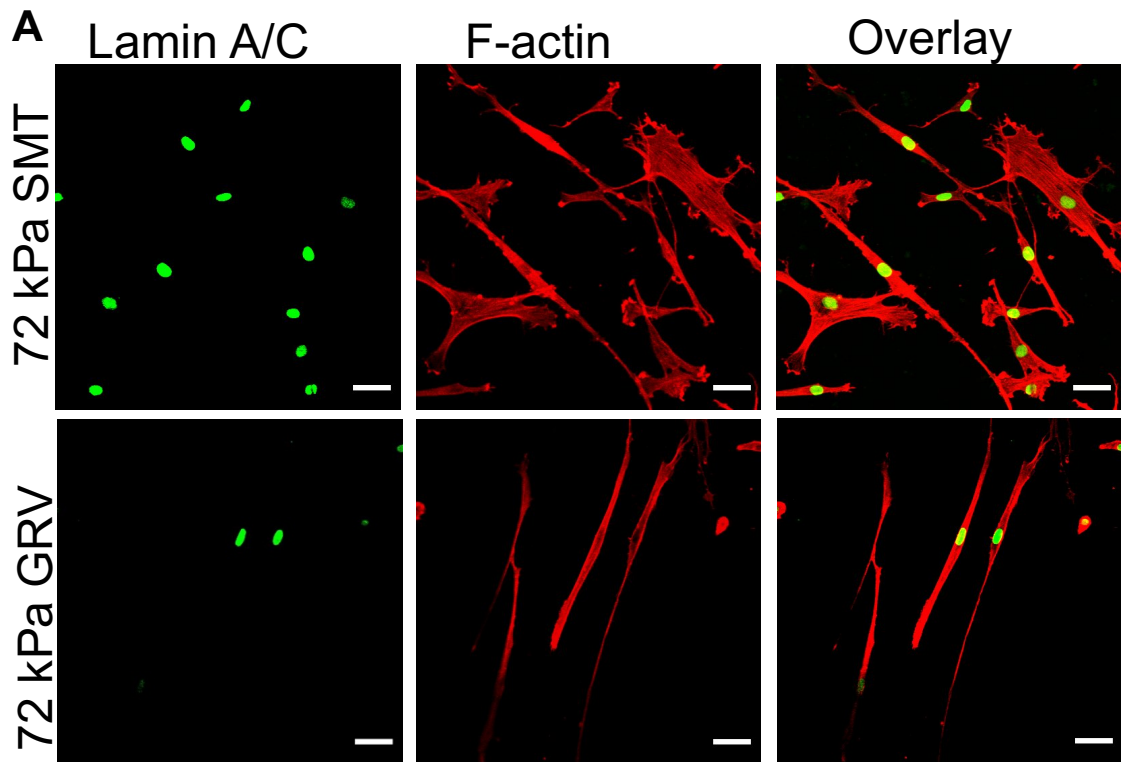
**Figure 3. 5: VSMC volume increases on grooved PAHs of enhanced stiffness. A)** Representative images of VSMCs seeded on 72 kPa Smooth or Grooved PAHs in growth media. VSMCs were stained for F-actin (Rhodamine phalloidin, red) and Lamin A/C (green). Scale bar represents 50 µm. Graphs show **B)** VSMC area, **C)** cell volume, **D**) nuclear area and **E)** nuclear volume. Data is based on 3 independent experiments from (n = 81 on smooth PAHs and n = 52 on grooved PAHs) VSMCs analysed. Statistical significance was determined using unpaired student t-test (* p = <0.05, *** p= <0.001, ns= non-significant).
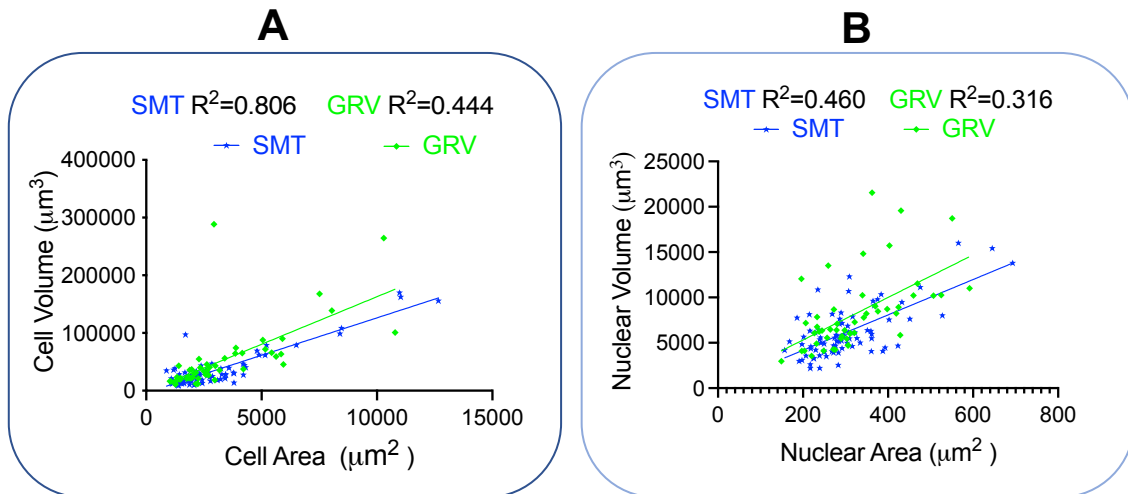
**Figure 3. 6: VSMC area to volume ratio is unaltered by matrix topology on rigid substrates.**
**A)** cell volume plotted against cell area and **B)** nuclear volume plotted against nuclear area, on 72 kPa smooth and grooved PAHs. Data is based on 3 independent experiments from (n = 81 on smooth PAHs and n = 52 on grooved PAHs) VSMCs analysed.

### 3.3.3 VSMC morphology regulates actomyosin-derived force generation under physiological stiffness

The above data shows that VSMC spreading is altered by matrix topology and stiffness. Next, we investigated whether VSMC morphology influenced actomyosin activity by directly measuring traction stresses exerted by VSMCs on the matrix. VSMCs were seeded onto smooth and grooved PAHs of 12 kPa stiffness. Traction Force Microscopy (TFM) was performed to measure actomyosin-generated traction stresses. Analysis revealed that VSMCs on grooved PAHs generated larger maximum and total (integrated) bead displacement compared to the smooth counterparts (Figures 3.7 A-C). Further analysis confirmed that VSMCs on grooved PAHs generated enhanced maximum and integrated traction stresses than the smooth control VSMCs (Figure 3.7 A, D and E).

Next, we investigated the relationship between cell area and traction stress generation. VSMC area was again observed to be smaller on grooved PAH of 12 kPa stiffness compared to those on smooth PAHs (Figure 3.8A). No difference was observed in the aspect ratio (Figure 3.8B). VSMC area was next plotted against traction stress. Analysis revealed that there was no obvious correlation between either maximal traction stress and cell area or the integrated traction stress and cell area relationship on either smooth or grooved PAHs (Figures 3.8 C and D).
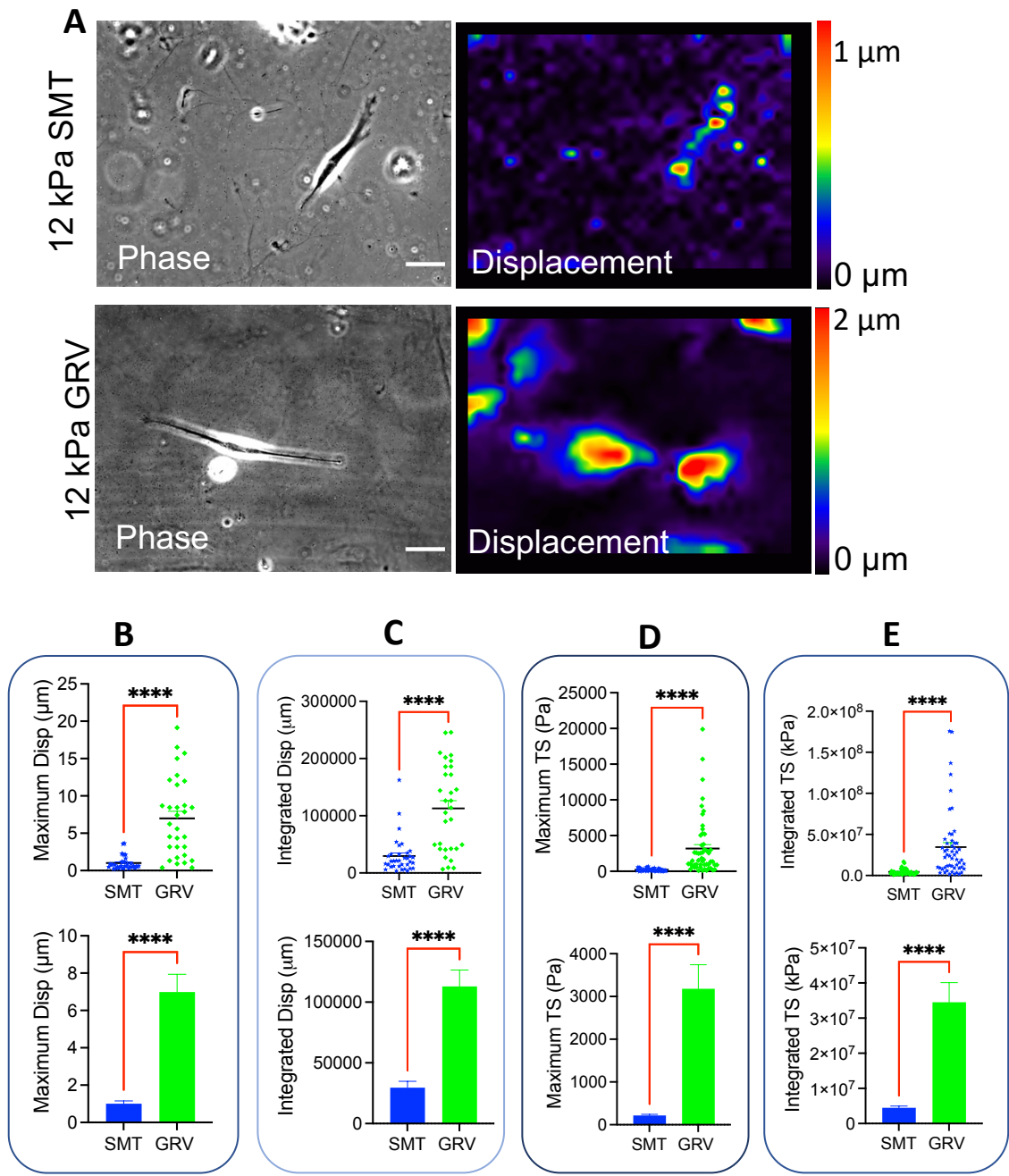
**Figure 3. 7: VSMC traction stress generation is regulated by matrix topology. A)** Representative phase and bead displacement images of VSMCs on smooth and grooved 12 kPa PAHs. Scale bar represents 50 μm. Graphs show **B)** maximum bead displacement, **C)** total bead displacement, **D)** maximum traction stress and **E)** integrated traction stress. Data is based on 4 independent experiments, from (n = 31 on smooth PAHs and n = 35 on grooved PAHs) VSMCs analysed. Statistical significance was determined using unpaired students with a t-test. (**** p= <0.0001).
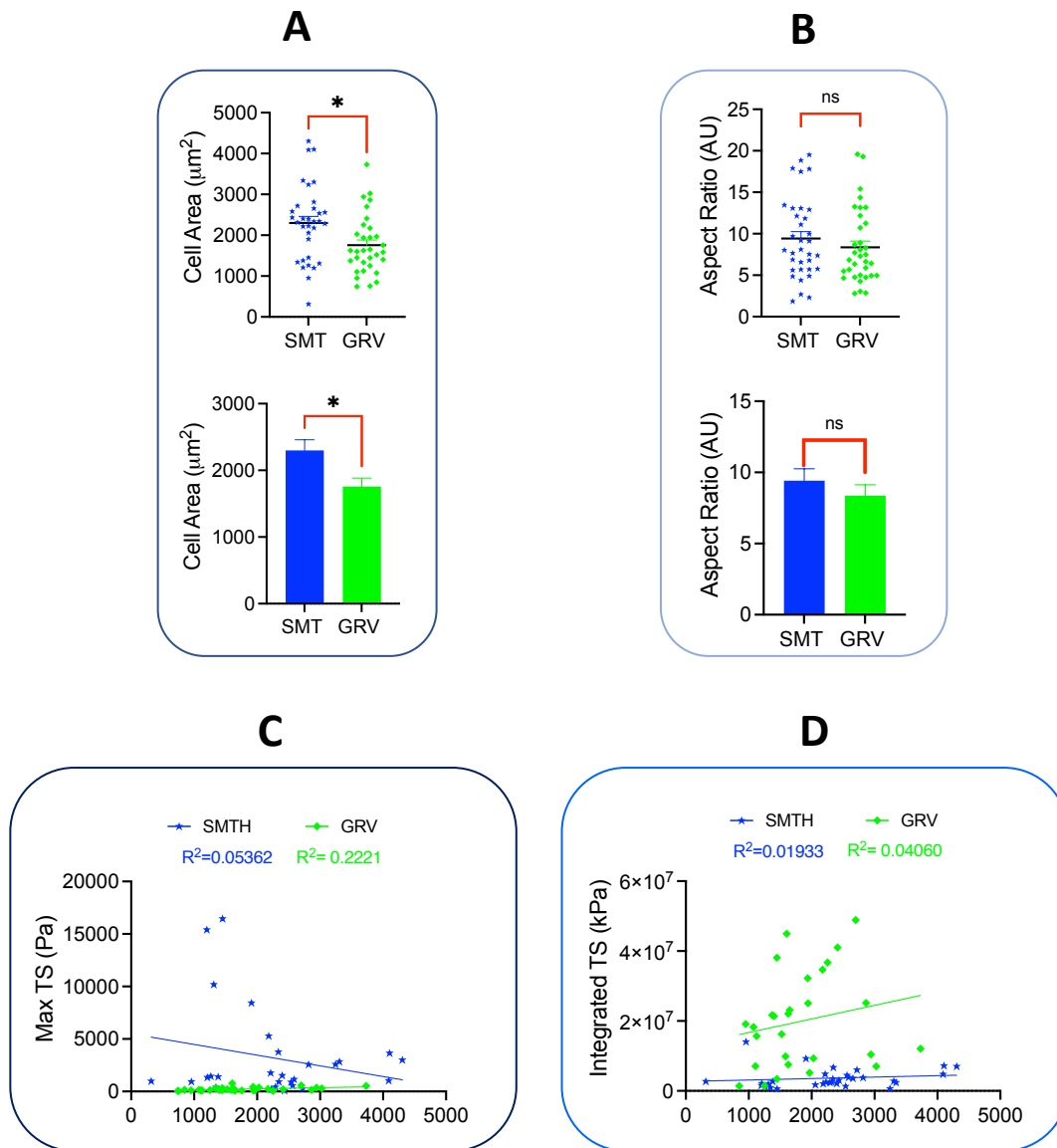
**Figure 3. 8: VMSC traction stress generation is not proportional to cell area.** VSMCs were seeded on smooth and grooved 12 kPa PAHs. Graphs show **A)** VSMC area, **B)** aspect ratio, **C)** cell area plotted against maximum traction stress and **D)** cell area plotted against integrated traction stress. Data is based on 4 independent experiments, from (n = 31 on smooth PAHs and n = 35 on grooved PAHs) VSMCs analysed. Statistical significance was determined using unpaired student t-test (* p = <0.05, ns= non-significant).

### 3.3.4 VSMC morphology regulates actomyosin-derived force generation on aged/disease stiffness

The above data shows that VSMC morphology influences traction stress generation on PAHs of physiological stiffness. Next, we investigated the influence of enhanced matrix stiffness. VSMCs were plated on smooth and grooved PAHs of 72 kPa stiffness and TFM was performed to measure the traction stress generated by VSMCs. Analysis revealed that VSMCs on grooved PAHs generated larger maximum and total (integrated) bead displacement compared to those on smooth PAHs (Figures 3.9 A-C). Further analysis showed that VSMCs on grooved PAHs generated enhanced maximum and integrated traction stress compared to those on smooth PAHs (Figure 3.9 A, D and E).

Next, we investigated the relationship between cell area and traction stress generation. This confirmed that VSMCs on grooved PAHs displayed similar areas to the smooth control VSMCs (Figure 3.10 A). VSMC area was then plotted against traction stress, however, no correlation between either maximal or integrated traction stress and cell area was observed (Figures 3.10 B and C).
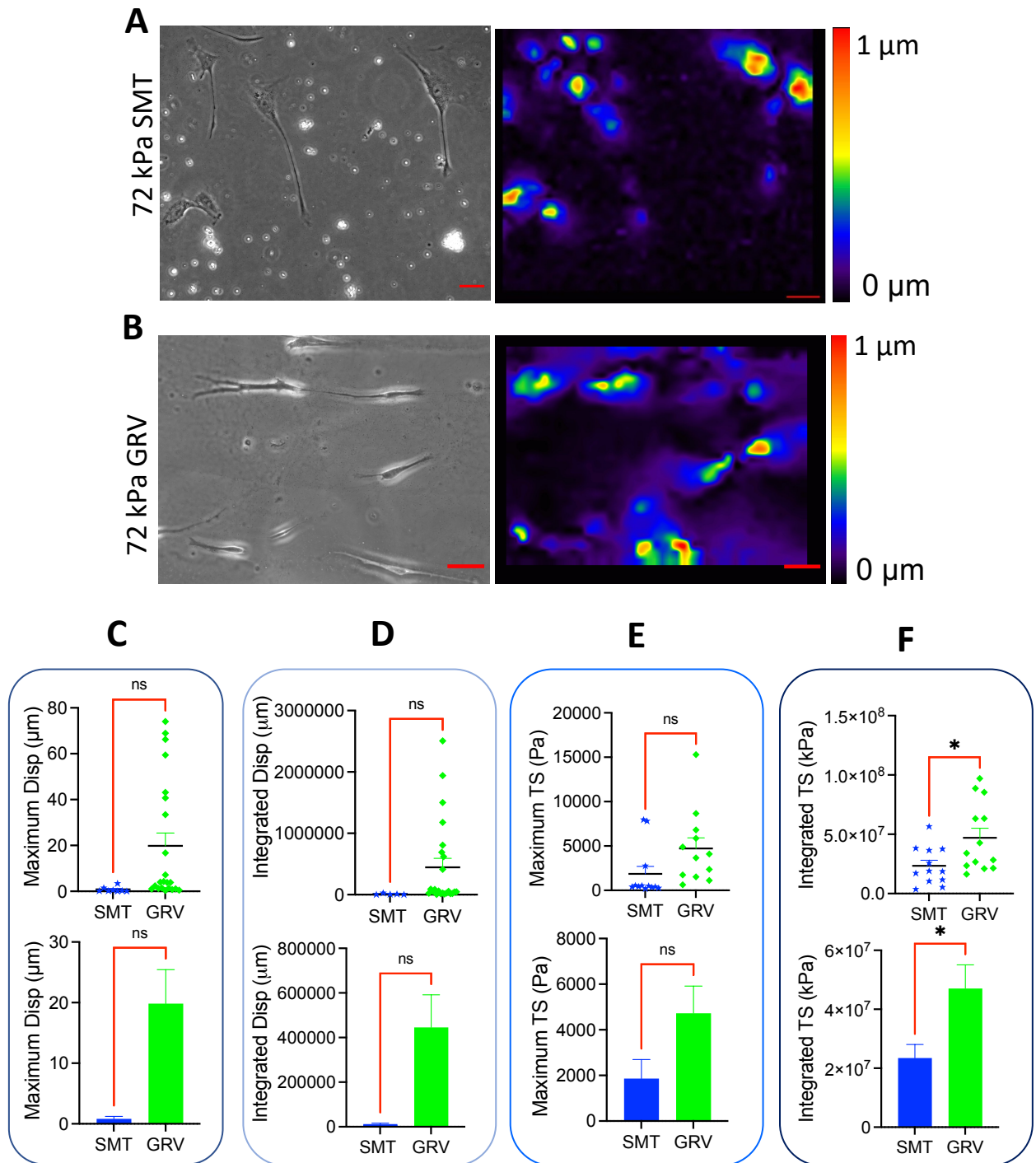
**Figure 3. 9: VSMC traction stress generation on rigid PAHs is regulated by matrix topology**. **A)** Representative phase images and bead displacement heat maps of VSMCs on smooth and grooved 72 kPa PAHs. Scale bar represents 50 µm. Graphs show **B)** maximum bead displacement, **C)** integrated displacement, **D)** maximum traction stress and **E)** integrated traction stress. Data is based on 3 independent experiments, from (n = 12 on smooth PAHs and n = 13 on grooved PAHs) VSMCs analysed. Statistical significance was determined using a unpaired student t-test (* p = <0.05, ***p= <0.01, ns= non-significant)
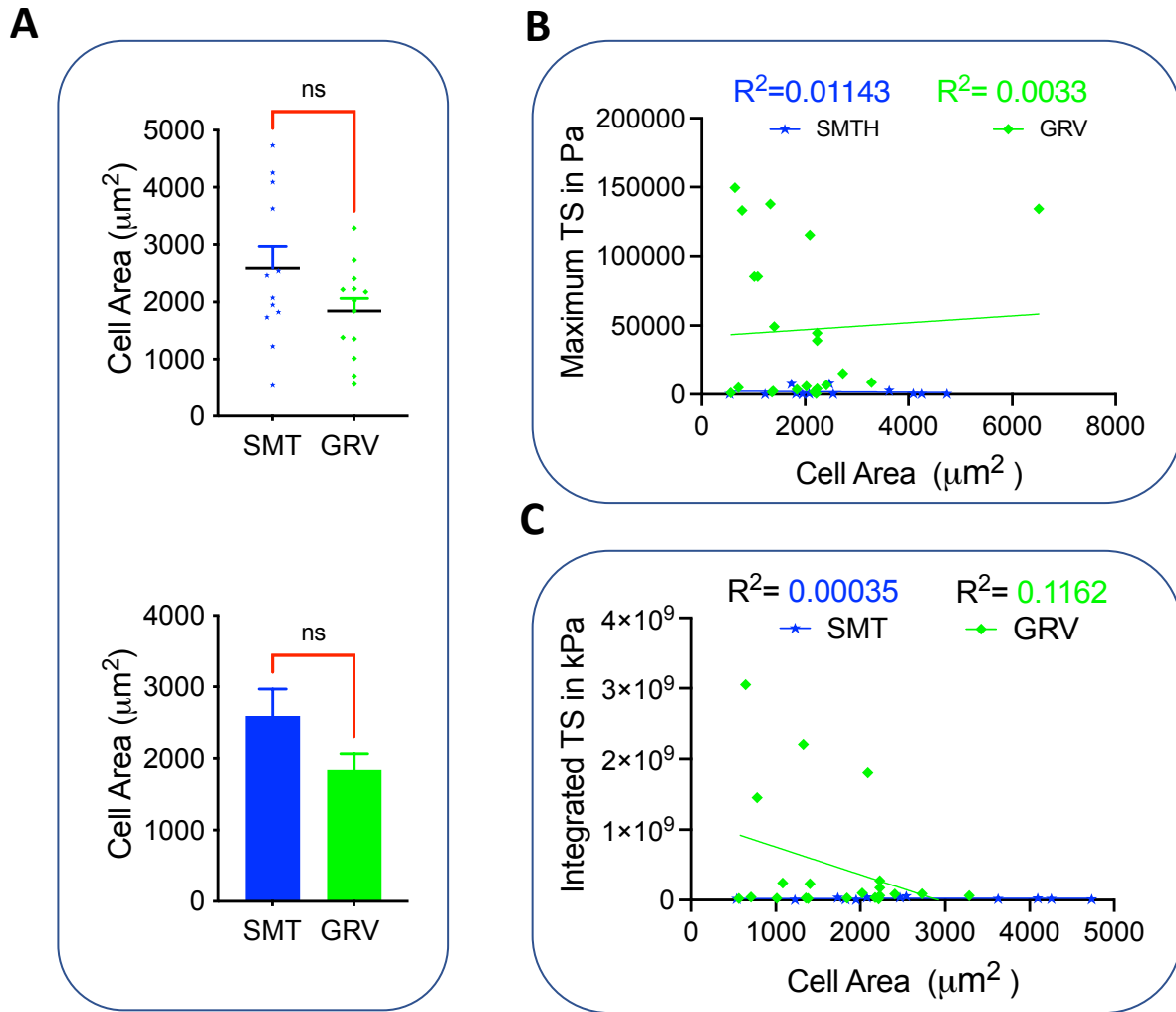
**Figure 3. 10: VSMC traction stress generation is not proportional to cell area on rigid hydrogels**. VSMCs were seeded on smooth and grooved 72 kPa PAHs. Graphs show **A)** VSMC area, **B)** VSMC area plotted against maximum traction stress and **C)** VSMC area plotted against integrated traction stress. Data is based on 3 independent experiments, from (n = 8 on smooth PAHs and n = 22 on grooved PAHs) VSMCs analysed. (ns= non-significant).

### 3.3.5 Matrix topology regulates the proliferative capacity of VSMCs

Previous studies have implicated both matrix topology and VSMC morphology as regulators of proliferation [230,231]. We therefore investigated if the topology imprinted upon our grooved PAHs would alter the proliferative capacity of VSMCs and if this regulation would be altered by matrix stiffness. VSMCs were plated on smooth and grooved PAHs of physiological and aged/diseased stiffness and left to grow overnight in the presence of BrdU. Immunofluorescence was performed to assay the number of BrdU-positive cells. Analysis revealed that on physiological and aged/diseased stiffnesses VSMCs on grooved PAHs were less proliferative than their smooth counterparts, as indicated by a decrease in the number of BrdU positive VSMCs (Figure 3.10 A). Furthermore, on grooved PAHs an increase in matrix stiffness correlated with an increase in VSMC proliferation, whilst matrix stiffness had no significant effect on VSMCs grown on smooth PAHs (Figures 3.10 B and C).

It's worth mentioning that Figure 3.11 B and C represent the same data as Figure 3. 11 A, but they have been split up to help identify the differences between VSMCs on 12 kPa and 72 kPa on smooth (Figure 3.11 B) and grooved (Figure 3.11 C) PAHs
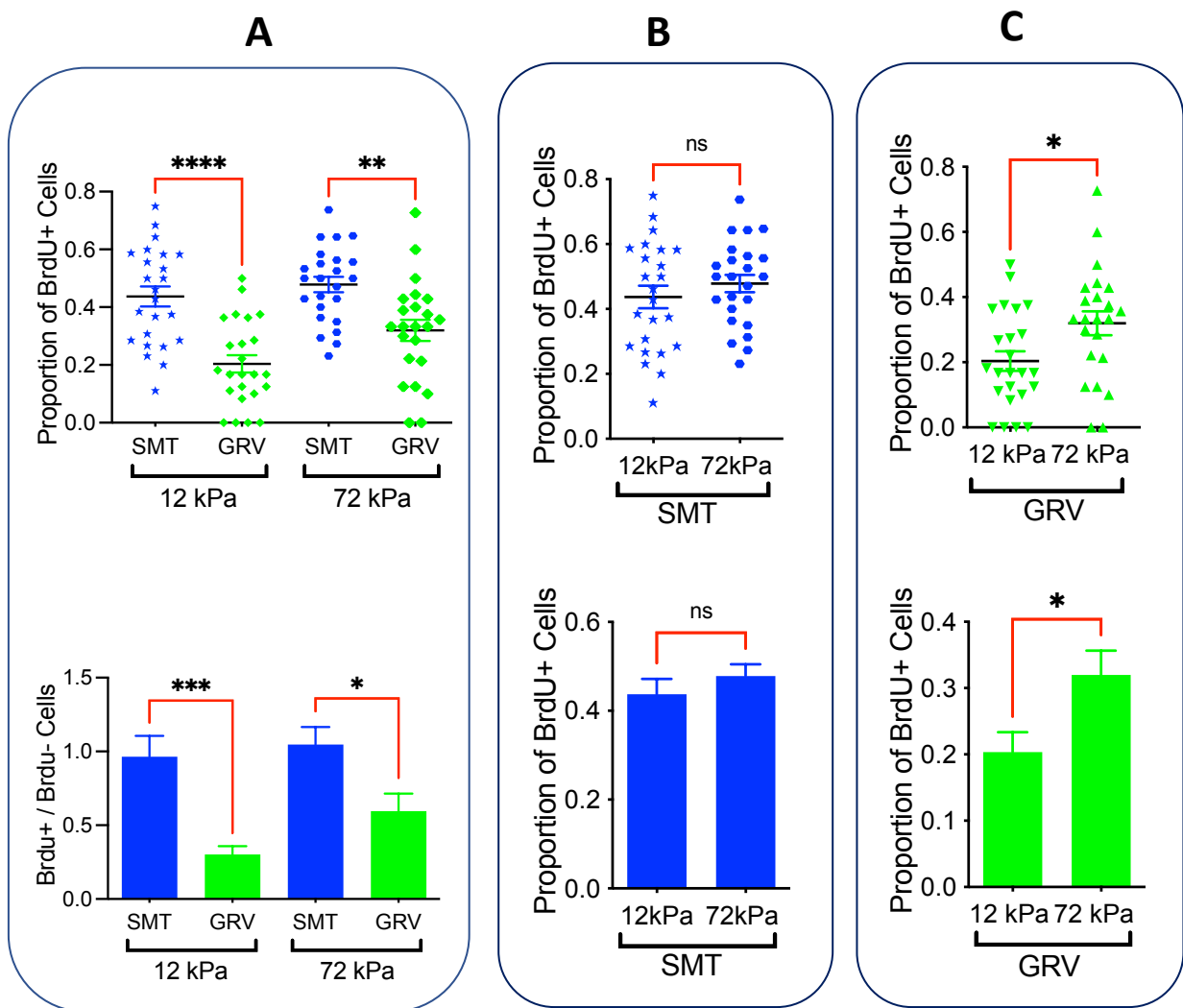
**Figure 3.11: Matrix topology regulates VSMC proliferative capacity**. VSMCs were seeded onto smooth or grooved PAHs of either 12 or 72 kPa stiffness. BrdU was added to the culture medium for 16 hours prior to BrdU incorporation being assessed by immunofluorescent microscopy. Graphs show **A)** proportion of BrdU positive VSMCs on 12 and 72 kPa smooth/grooved PAHs. **B)** proportion of BrdU positive VSMCs on 12 and 72 kPa smooth PAHs. **C)** proportion of BrdU positive VSMCs on 12 and 72 kPa grooved PAHs. Data is based on 3 independent experiments (with 6 regions of interest analysed per condition per experiment). Statistical significance was determined using one-way ANOVA (A) and unpaired t-test (B) (* $p = <0.05$, ** $p = < 0.01$ and **** $p = <0.0001$).

### 3.3.6 Matrix topology regulates the migratory capacity of VSMCs

We next investigated whether matrix topology or stiffness altered VSMC migration. VSMCs were seeded at low confluency on smooth and grooved PAHs of physiological stiffness. VSMC migration was observed using time-lapse microscopy. Analysis revealed that VSMCs on grooved PAHs migrated with an increased directionality (Figure 3.11 A and B), indicating that these cells were moving in a more persistent direction than their counterparts on smooth PAHs. Meanwhile, VSMC migration speed was reduced on grooved compared to smooth PAHs (Figure 3.11 C).

Next, we analysed the influence of matrix stiffness by plating VSMCs on smooth and grooved PAHs of aged/diseased stiffness. Analysis revealed that VSMCs again displayed an increased directionality (Figure 3.12 A and B) and a small, but significant decrease in migration speed (Figures 3.12 C) when seeded on grooved as opposed to smooth PAHs.
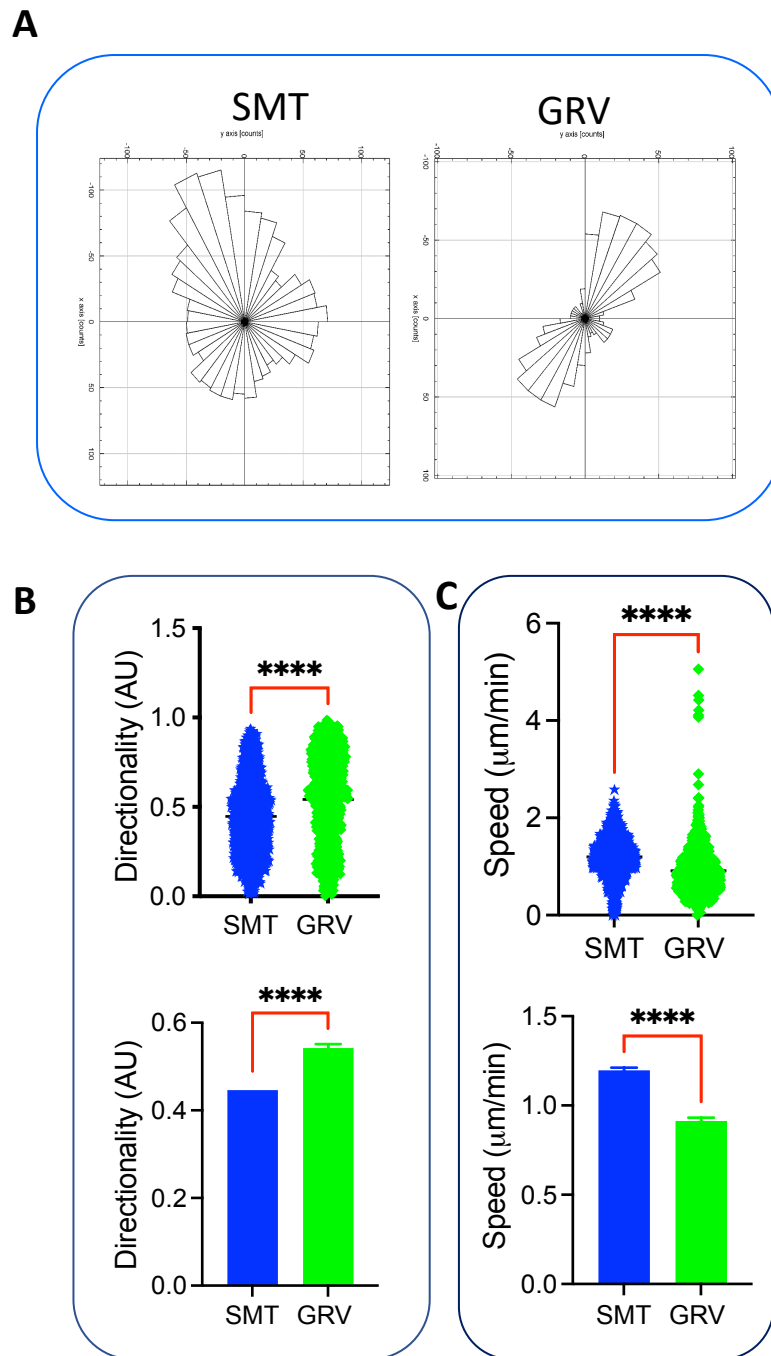
**Figure 3. 12: Matrix topology regulates VSMC migration.** VSMCs were seeded onto smooth or grooved PAH of 12 kPa, with their subsequent migration observed using time-lapse microscopy over a 12 hour period. **A)** Representative Rose plots of VSMC migration- images used are representative only. Graphs show **B)** Directionality (measured in arbitrary units) and **C)** speed of VSMC migration. Data is based on 3 independent experiments, from (n = 905 on smooth PAHs and n = 773 on grooved PAHs) VSMCs analysed. Statistical significance was determined using an unpaired student t-test (**** p = <0.0001).
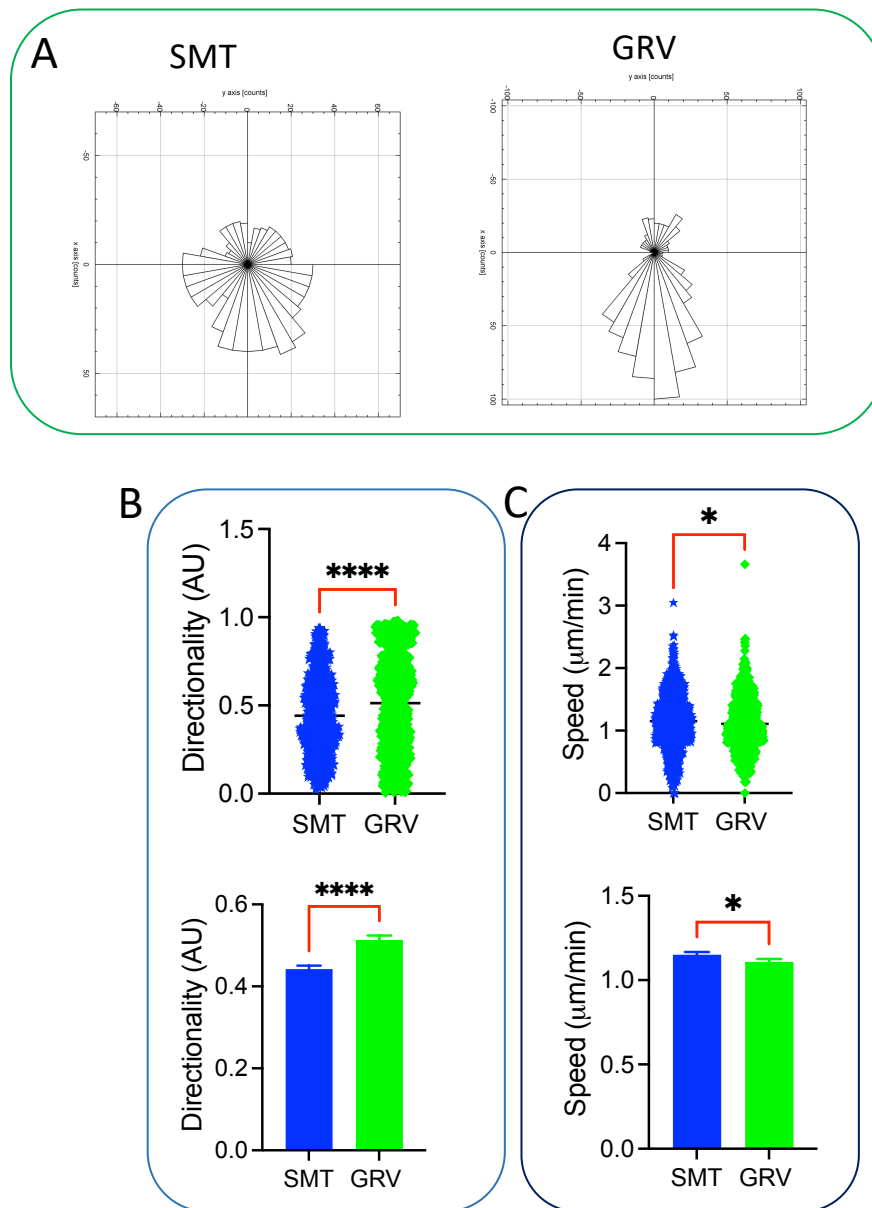
**Figure 3. 13 : Matrix topology regulates VSMC migration on rigid substrates.** VSMCs were seeded onto smooth or grooved PAH of 72 kPa, with their subsequent migration observed using time-lapse microscopy over 12 hours. **A)** Representative Rose plots of VSMC migration- images used are representative only. Graphs show **B)** Directionality (measured in arbitrary units) and **C)** speed of VSMC migration. Data is based on 3 independent experiments, from (n = 763 on smooth PAHs and n = 571 on grooved PAHs) VSMCs analysed. Statistical significance was determined using unpaired student t-test (* p = <0. 05 and **** p = <0.0001).

### 3.3.7 Matrix stiffness has no impact on VSMCs migrational capacity

The above data showed how matrix topology influence the migrational capacity of VSMCs. We next investigated whether matrix stiffness further influenced VSMC migrational capacity by comparing the 12 kPa and 72 kPa smooth and grooved migrational data presented in figures 3.14 and 3.15. Analysis revealed that VSMCs displayed no change in directionality (Figures 3.14 A, B and C) but a significant increase in migrational speed (Figures 3.15 A and C) on aged/diseased PAHs compared to VSMCs on healthy grooved PAHs. A one-way ANOVA shows that the trend of increased directionality and significantly increased speed is maintained. It also appears that matrix stiffness has no real impact on directionally smooth and grooved PHAs.

It's worth mentioning that Figure 3.14 B and C represent the same data as Figure 3. 14 A, but they have been split up to help identify the differences between VSMCs on 12 kPa and 72 kPa on smooth (Figure 3.14 B) and grooved (Figure 3.14 C) PAHs
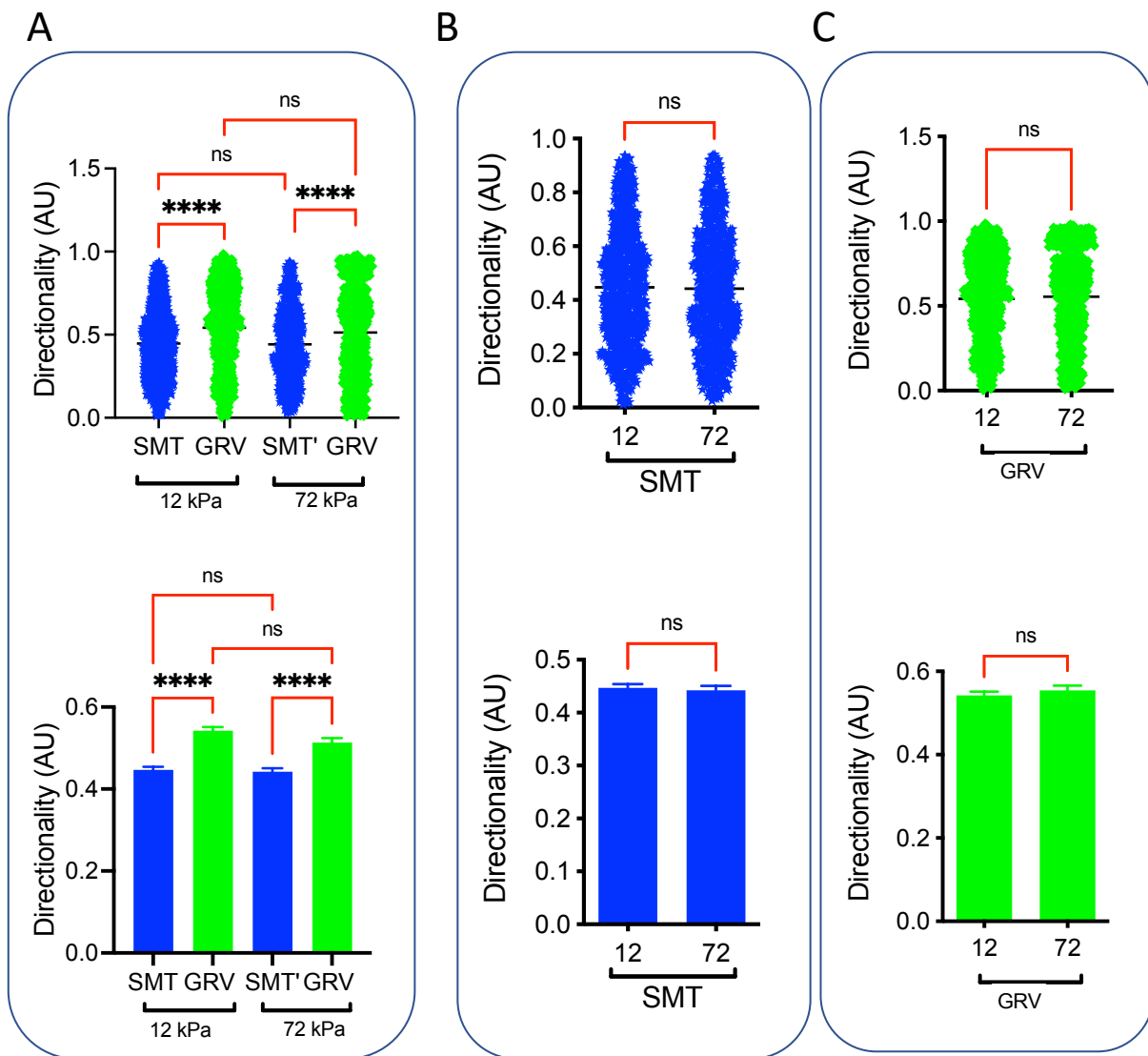
**Figure 3. 14: Matrix stiffness does not alter VSMCs migrational directionality.** VSMCs were seeded onto smooth or grooved PAH of 12 and 72 kPa, with their subsequent migration observed using time-lapse microscopy over a 12 hour period. Graphs show Directionality (measured in arbitrary units) **A)** of VSMCs on smooth and grooved 12 and 72 kPa PAHs **B)** on smooth 12 and 72 kPa PAHs and **C)** on grooved 12 and 72 kPa PAHs. Data is based on 3 independent experiments, from (n = 763 on smooth PAHs and n = 571 on grooved PAHs) VSMCs analysed. Statistical significance was determined using One way ANOVA for graph **A** and student t-test for graphs **B** and **C** (**** p = <0.0001, * p = <0. 05 and ns= non-significant).
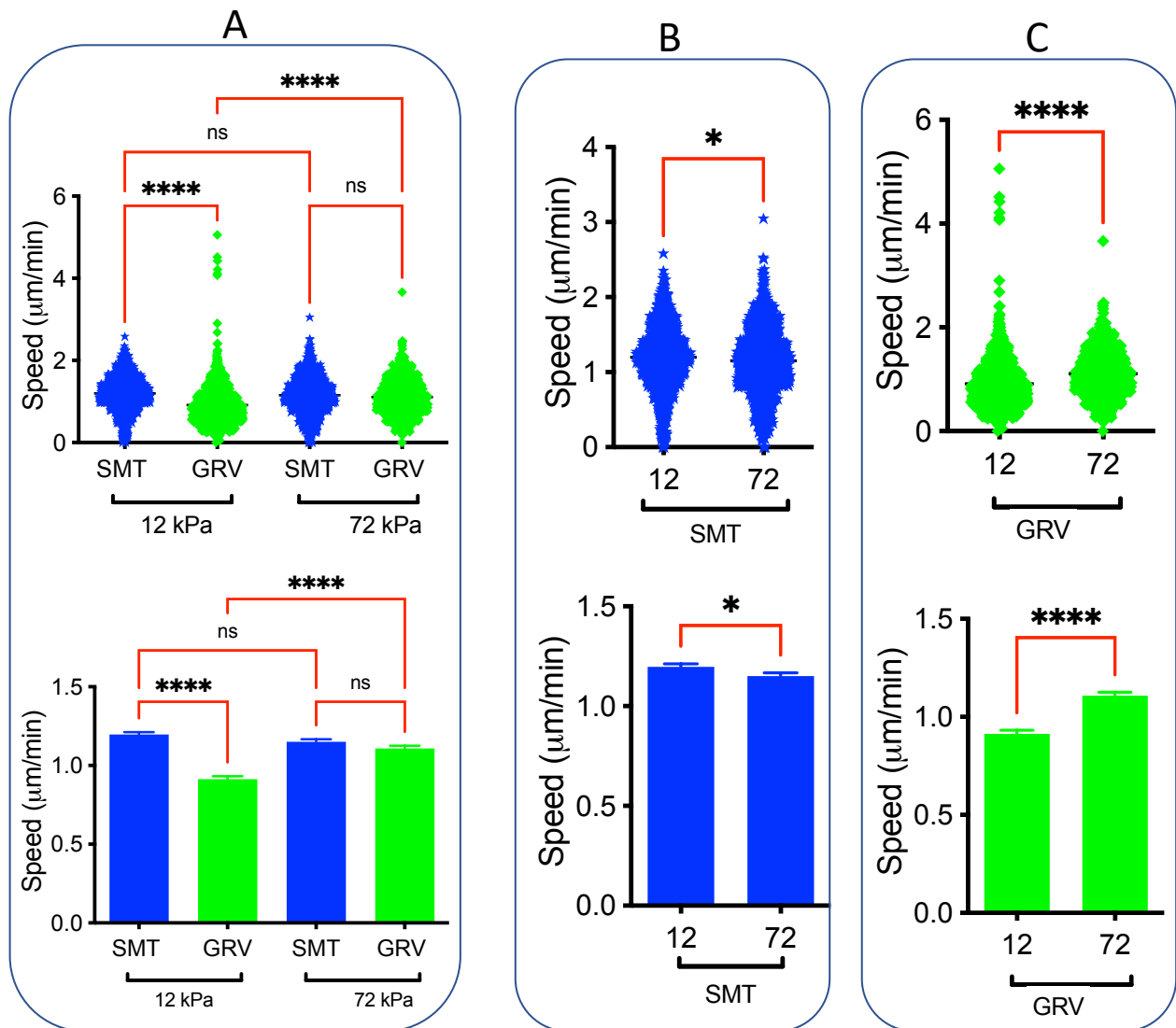
**Figure 3. 15: Matrix stiffness increased VSMCs migrational speed.** VSMCs were seeded onto smooth or grooved PAH of 12 and 72 kPa, with their subsequent migration observed using time-lapse microscopy over a 12 hour period. Graphs show VSMCs speed **A)** of VSMCs on smooth and grooved 12 and 72 kPa PAHs **B)** on smooth 12 and 72 kPa PAHs and **C)** on grooved 12 and 72 kPa PAHs. Data is based on 3 independent experiments, from (n = 763 on smooth PAHs and n = 571 on grooved PAHs) VSMCs analysed. Statistical significance was determined using One way ANOVA for graph **A** and student t-test for graphs **B** and **C** (**** $p = <0.0001$, * $p = <0.05$ and ns= non-significant).

### 3.3.8 Matrix topology does not alter VSMC response to contractile agonist stimulation

Our studies so far have used VSMC in the proliferative state. However, *in vivo* VSMCs exist in quiescent, contractile phenotype [232,233]. We next investigated whether VSMC response to contractile agonist stimulation was altered by matrix topology. To achieve this, VSMCs were plated at low density on smooth and grooved PAHs of physiological stiffness. Quiescence was induced by serum withdrawal, prior to VSMCs being stimulated with a concentration gradient of the contractile agonist, angiotensin II. Confocal immunofluorescence microscopy was used to capture morphological changes, with our lab having recently shown the contractile response of VSMCs on PAHs can be measured through changes in cell area [146]. Image analysis revealed that on both smooth and grooved PAHs VSMCs underwent a concentration-dependent decrease in cell area (Figure 3.15 A-C). Although VSMCs on grooved PAHs were initially smaller, they underwent a similar response to increasing concentrations of angiotensin II, with further analysis revealing that VSMCs on smooth PAHs displayed $EC_{50}$ values (7.9 µM) and grooved PAHs displayed $EC_{50}$ (5.2 µM) (Figure 3.15 E).

To investigate the impact of matrix stiffness, we repeated the above experiment but this time seeded VSMCs onto smooth and grooved PAHs of aged/disease stiffness. Analysis revealed that on both smooth and grooved PAHs of aged/diseased stiffness, VSMCs failed to contract and instead underwent a concentration-dependent increase in cell area (Figures 3.16 A-D). Once again, although VSMCs on grooved PAHs were initially smaller than their counterparts on smooth PAHs, further comparison of the responses revealed that the angiotensin II $EC_{50}$ values were unaltered between the two topologies (Figure3.16 E). An increase in area was larger in VSMCs on smooth hydrogels of aged/diseased stiffness (Figure 3.16 A-C). The EC50s was about 10x more VSMCs on grooved PAHs, VSMCs on smooth PAHs displayed $EC_{50}$ values (1.1 µM) and grooved PAHs displayed $EC_{50}$ (14.1 µM) (Figure 3.15 E and Figure 3.16 E).

It's worth mentioning that Figure 3.15 B and C represent the same data as Figure 3. 15 A, but they have been split up to help identify the differences between VSMCs on 12 kPa and 72 kPa on smooth (Figure 3.15 B) and grooved (Figure 3.15 C) PAHs
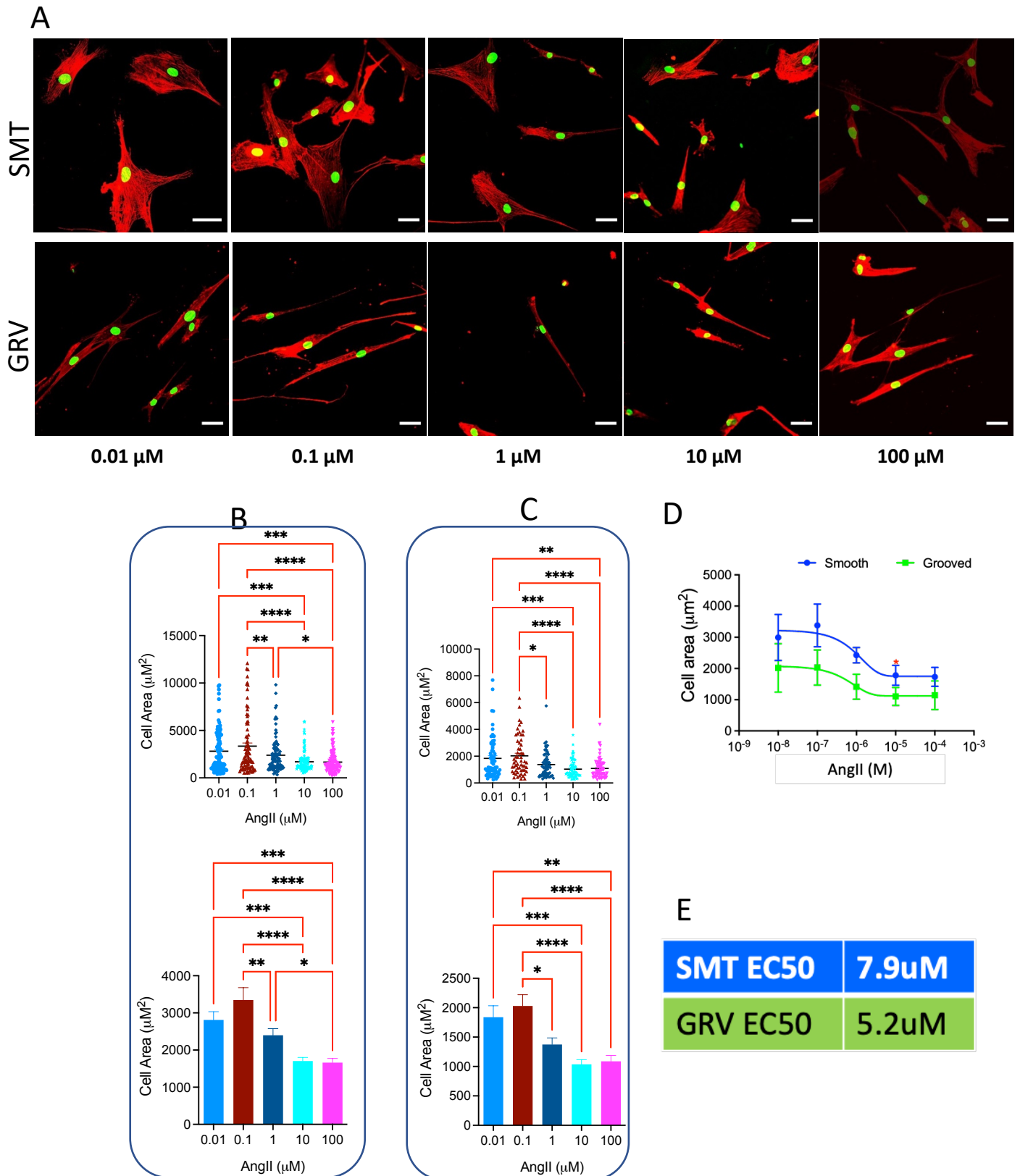
**Figure 3. 16: Angiotensin II initiates a VSMC contractile response on PAH of physiological stiffness**. VSMCs were seeded onto smooth or grooved PAHs of physiological stiffness. Quiescence was induced overnight prior to cells being stimulated with a concentration response of Angiotensin II for 30 minutes. **A)** Representative images showing Actin cytoskeleton, (Rhodamine phalloidin, red) and lamin A/C (green). Scale bar = 50 μm. **B)** VSMCs area on smooth 12 kPa PAHs, **C)** VSMCs area on grooved 12 kPa PAHs, **D)** VSMCs area on smooth vs grooved PAHs **E)** Angiotensin II EC$_{50}$ values calculated via non-linear regression. Data is representative of 3-independent experiments from ≥ 90 cells per condition on smooth and grooved 12 kPa PAHs analysed. Statistical significance was determined using a 2-way ANOVA (* p = <0.05)
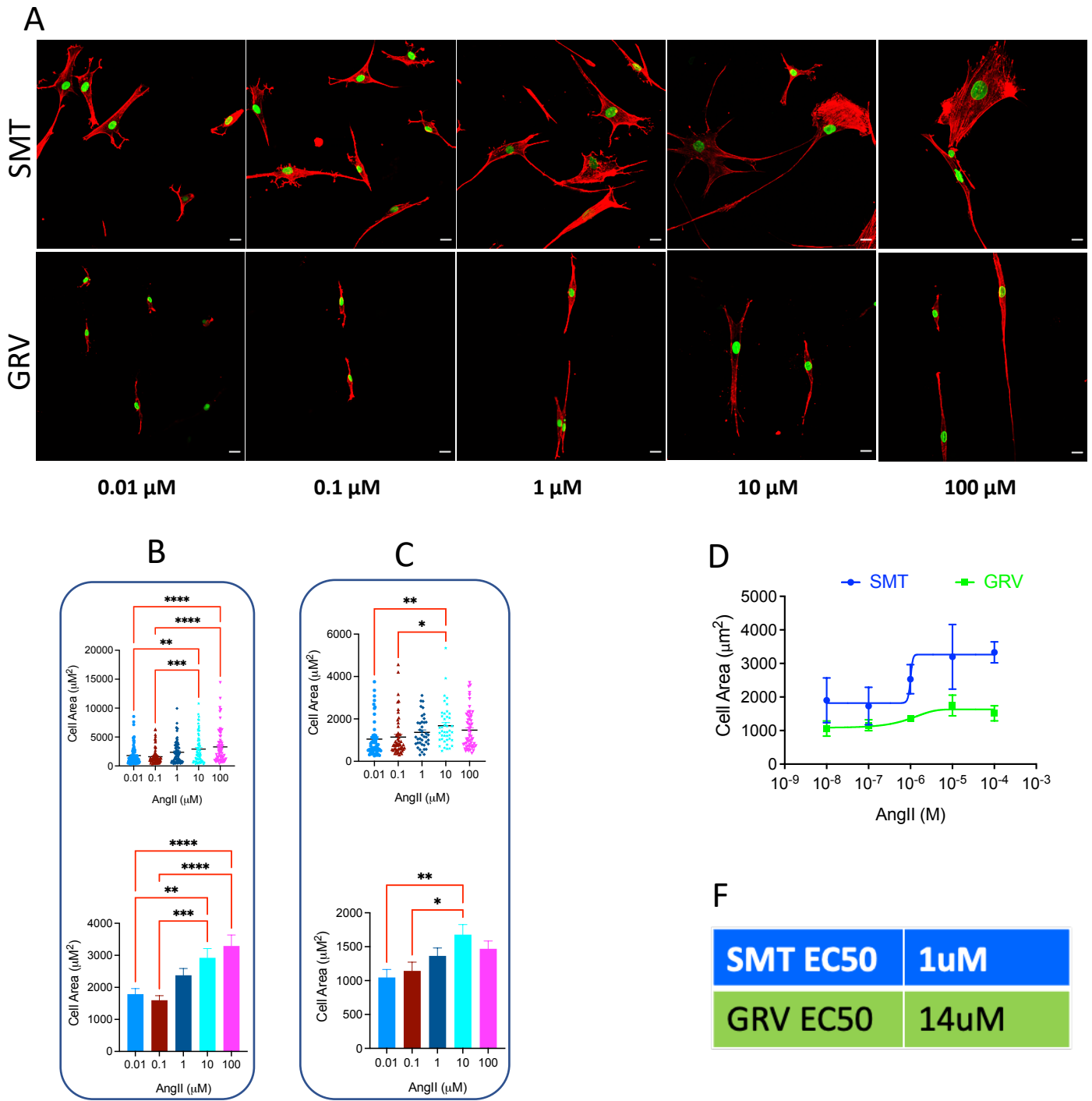
**Figure 3. 17 : Matrix stiffness prevents angiotensin II mediated VSMC contraction**. A) smooth and groove PAHs and treated with a serial dilution of angiotensin II for 30 minutes. VSMCs were seeded onto smooth or grooved PAHs of aged/diseased stiffness. Quiescence was induced overnight prior to cells being stimulated with a concentration response of Angiotensin II for 30 minutes. **A)** Representative images showing Actin cytoskeleton, (Rhodamine phalloidin, red) and lamin A/C (green). Scale bar = 50 μm. **B)** VSMCs area on smooth 12 kPa PAHs, **C)** VSMCs area on grooved 12 kPa PAHs, **D)** VSMCs area on smooth vs grooved PAHs **E)** Angiotensin II $EC_{50}$ values calculated via non-linear regression. Data is representative of 3-independent experiments ≥ 40 cells per condition on smooth and grooved 72 kPa PAHs analysed. Statistical significance and EC50 were determined using a nonlinear fit regression. (* p = <0.05)

## 3.4    Discussion and conclusion

The main role of VSMC in the arteries is to provide structural support and regulate blood vessel tone diameter, blood pressure, and flow distribution [234]. In a healthy vessel, VSMCs are in a quiescent state, and quiescent contractile protein markers are expressed including smooth muscle cell actin (ACTA2), smoothelin, SM22α, and smooth muscle cell myosin heavy chain (MYH11) [235,236] and during vessel injury, VSMCs phenotypically switch to syntactic state. VSMCs de-differentiate to synthetic state show reduced contractile protein markers and acquire macrophage markers, increased collagen III, fibronectin, matrix metalloproteinase-1 and 3 [237].

On both physiological and diseased/aged mimicking stiffnesses, we have found that imprinting a grooved topology onto our PAHs appears to encourage VSMCs to adopt a quiescent/contractile phenotype. We observe that cell and nuclear area/volume are reduced, with VSMCs adopting a more spindle-shaped appearance, as would be observed *in vivo*. VSMCs on grooved PAHs are also less proliferative and migratory, suggesting these cells are less synthetic than their counterparts on smooth PAHs. Finally, VSMCs on grooved PAHs can generate greater traction stress, and suggestion cells can generate greater actomyosin activity and in essence, are becoming more contractile.

This could be for many different reasons, including filamentous actin alignment in bundles as a result of the exposure to mechanical stress from the ECM [238]. Our lab has previously shown that a change in matrix stiffness results in a significant increase in F-actin alignments, and this was further supported by a different study that showed that actin inhibitors could decrease VSMCs rigidity induced by actomyosin activation by mechanosensing their stiff environment [239]. Previous studies have shown that matrix stiffness induces enhanced actomyosin force generation in tissue cells- including myocytes-, fibroblasts, endothelial, neurons and other cell types [240–243]. To make our investigation physiologically relevant, we tried to mimic the cell environment and study their traction stress and migration capacity. Studies on fibroblasts and human osteosarcoma cells demonstrated that the topology of the substrate has a significant impact on their cell speed, trajectory and motion [244,245]. Hence, understanding the activities of the actin cytoskeleton is of particular interest to our interrogation of the interaction of VSMCs and their environment, and how this leads to varying VSMCs morphology, contractility, motility and proliferation [246].

We gained great insight from previous work in our lab about change in matrix stiffness, we further investigated the change in the topology of 12 kPa PAHs induced a decrease in the cell area, cell volume, nuclear area, and nuclear volume of VSMCs on grooved PAHs compared

to their counterpart VSMCs on smooth PAHs (**Figure 3.3 B-E**). The cell area significantly decreased whilst the aspect ratio remained unchanged (**Figure 3.4 A and B**). At an aged/diseased stiffness (72 kPa) of ECM, the cell and nuclear volume increased on VSMCs on grooved PAH compared to VSMCs on smooth PAHs, whilst the cell and nuclear area remain the same (**Figure 3.5 B-E**).

Furthermore, the area and volume comparison between VSMCs on 12 kPa smooth PAHs and 72 kPa smooth PAHs; and on 12 kPa grooved PAHs and 72 kPa grooved PAHs shows consistent results with previous studies on matrix rigidity. This could be the effect of high localisation of the giant nesprin-1/2 on the outer nuclear membranes associated with the mechanosensitivity [247] and the linkage of LINC-complex protein components to adhesion receptors feeding it to the cell membrane and then the nuclear core [248]. Our lab has previously shown the increase of focal adhesion with increased matrix stiffness [249].

VSMCs on the smooth PAHs caused significantly lower displacement of their ECM and subsequently generating significantly lower traction stress than their counterpart VSMCs on the grooved PAHs (Figure 3.7 C-F). The observation that the spindle-shaped VSMC's ability to pull and cause deformation of ECM agrees with the structure and function of VSMCs in the healthy aorta, which is to regularly contract the vessel wall to maintain vascular tone [250].

We found that VSMCs undergo a significantly higher proliferation rate on the smooth PAHs compared to the VSMCs on the grooved PAHs. A BrdU assay also confirmed this true (Figure 3.11A). Furthermore, VSMCs on healthy stiffness grooved PAHs showed a significantly reduced proliferation rate than those on the aged/diseased PAHs. Hence, matrix topology and rigidity influences VSMCs migration and matrix topology impacts proliferation rate [251].

To understand the relationship between the change in morphology as a result of altering topology and its impact on actomyosin activity and cytoskeletal rearrangement, we conducted a contractile assay of dose-response by stimulating VSMCs with angiotensin II of serial dilution. Our finding shows that the change in morphology doesn't impact the actomyosin activity of VSMCs irrespective of their matrix stiffness (Figures 3.16 to 3.22).

## 3.5 Limitations and future work

### 3.5.1 Technical issues

During this study, we faced multiple hurdles. Our microscopes were originally operating on an ancient system but were upgraded to a new system midway through the project. Unfortunately, this new system had numerous bugs and the time taken to resolve these issues was greatly extended due to COVID-19 precautions. As such, many experiments had to be discarded as the data captured from time-lapse microscopy was unusable (combined/deconstructed images, drifting positions and file corruption, were common issues faced).

### 3.5.2 VSMCs in vivo make a monolayer

Throughout our experiments, we looked at single VSMCs. However, in the aortic wall, VSMCs make along with layers of elastic fibres make a sandwich structure. We suspect that we might miss modulating some key physical and mechanical prosperities by looking at the individual cells.

# Chapter 4: Microtubule dynamics regulate VSMC actomyosin activity and migration

## 4.1  Background

The mammalian cytoskeleton is composed of three main components that each form specific networks that perform different but interdependent functions within the cell [252]. They are actin filaments, intermediate filaments, and microtubules. Previous studies have shown that colchicine and paclitaxel have been investigated since the early 90s, and paclitaxel became a breakthrough for microtubule targeting agents [253]. Recent studies have shown that disrupting microtubules induced a significant vasoconstriction [254]. Furthermore, various studies have highlighted the importance of microtubules in VSMCs, where they are important for maintaining the cell's structural integrity, shape and motility [146,150].

Microtubules form a dynamic network, with tubules constantly growing and shrinking in a process known as dynamic instability [142]. Their unique dynamic characteristics enable microtubules to rapidly polymerization and depolymerization, thereby forming networks that suit the need of the cell at any given time. Within VSMCs, microtubules are involved in the generation of force, regulating contractility, directing actin polymerization, and driving the leading edge of migrating VSMCs [150].

In this experimental chapter, we examined the impact of disrupting microtubule dynamics on VSMCs traction stress generation and migration. This was achieved through treating VSMCs with the microtubule destabiliser colchicine (Co), the microtubule stabiliser paclitaxel (P) and demecolcine (D) whose mechanism of action varies based on its concentration but at the concentration used in this study, acts to maintain microtubule stability. Microtubule acetylation has also been implicated in regulating microtubule stability and actomyosin force generation [143,199]; therefore, in this chapter, we also utilise tubastatin (T), a HDAC6 inhibitor and remodelin (R), a NAT10 acetyltransferase inhibitor.

## 4.2 Hypothesis

We hypothesise that microtubules are essential for VSMC force generation and migration. We, therefore, predict that disruption of microtubule dynamics will alter traction force generation and the migrational capacity of VSMCs.

## 4.3 Aims

The objective of this chapter was to determine the impact of disrupting microtubule dynamics on:

1. The magnitude of VSMC traction stress generation

2. The migrational capacity of VSMCs

3. VSMC traction stress generation and migration when seeded on matrixes of different topologies and/or stiffnesses.

## 4.4 Methods

To assess traction stress generation and cell migration, VSMCs were seeded onto collagen-I coated PAHs of varying stiffness and topology. When assessing traction stress, quiescence was induced by overnight serum withdrawal, prior to pre-treating VSMCs with microtubule targeting agents (MTAs) (Table 4.1) for 30 minutes before cells were subsequently stimulated with the contractile agonist, angiotensin II (10 µM) for an additional 30 minutes. To investigate cell migration, VSMCs were maintained in growth media with MTAs added 1 hour prior to time-lapse microscopy commencing.

**Table 4.1:** Concentrations of Microtubule Targeting Agents used within this chapter.

| Microtubule targeting agent | | Colchicine (Co) | Demecolcine (D) | Paclitaxel (P) | Remodelin (R) | Tubastatin (T) |
|---|---|---|---|---|---|---|
| Concentration | | 100 nM | 10 nM | 1 nM | 1 µM | 1 µM |

# 4.5 Results

## 4.5.1 Microtubule destabilising agents increase VSMC traction stress generation.

We set out to characterise the impact of microtubule destabilisation on VSMC traction stress generation. VSMCs were pre-treated with the microtubule destabilising agent colchicine before TFM was used to determine the angiotensin II-mediated traction stress these cells could generate. Analysis revealed that colchicine pre-treatment increased both maximal and integrated (total) (Figure 4.1) traction stress generated by VSMCs seeded on smooth 12 kPa PAHs.
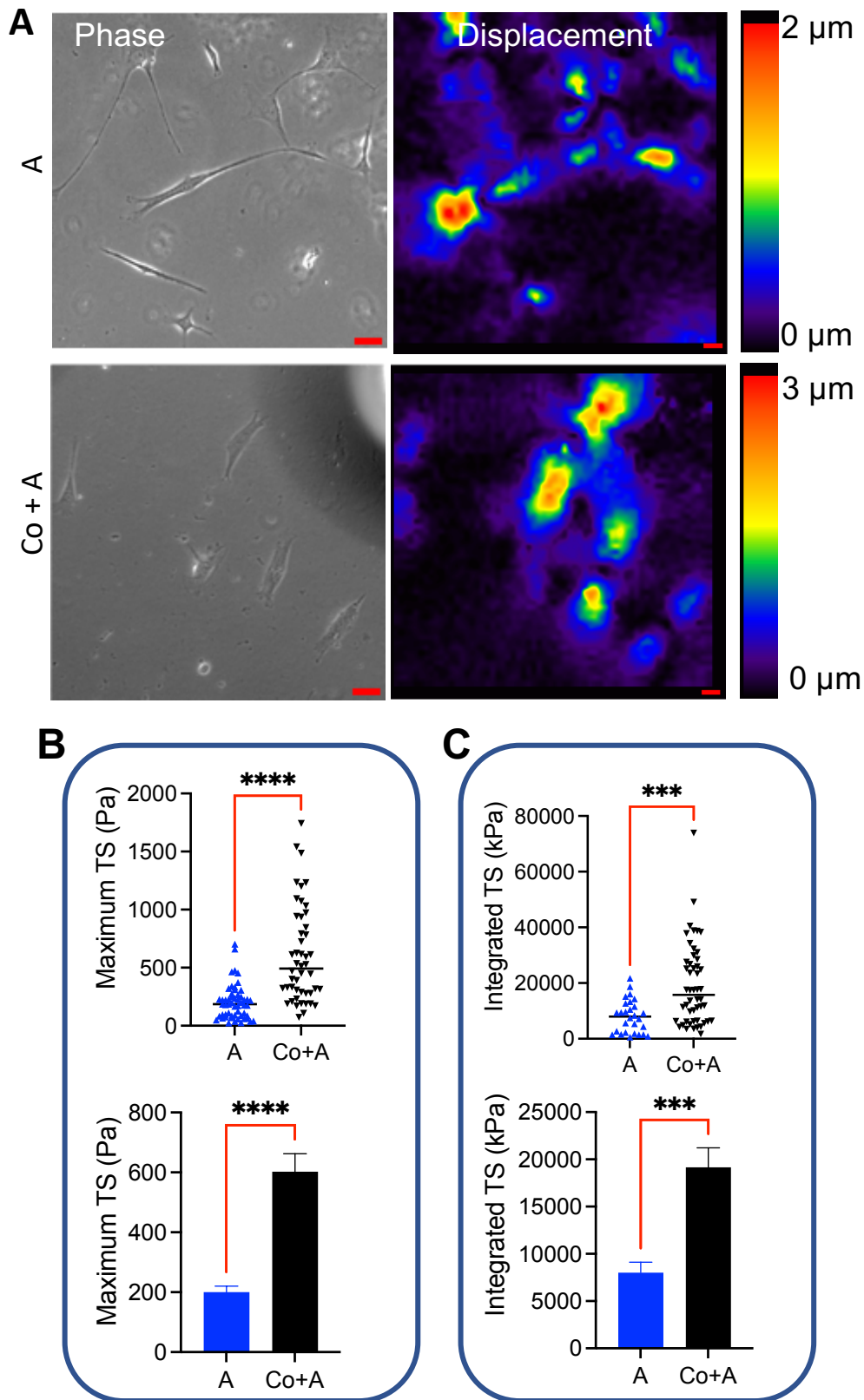
**Figure 4. 1: Microtubule destabilisation increases angiotensin II induced VSMC traction stress generation.** VSMCs were seeded onto 12 kPa Smooth PAHs and induced into quiescence by serum removal. VSMCs were colchicine (Co) pre-treated for 30 minutes, before being stimulated with the contractile agonist angiotensin II (A). **A)** Representative phase images and bead displacement heat maps. Scale bar = 50 μm. **B)** Maximum traction stress and **C)** Integrated traction stress generation. Data is representative of 3 independent experiments (n = 55 in A and n = 48 in C+A) VSMCs analysed. (*** = $p < 0.001$, **** = $p < 0.0001$).

## 4.5.2 VSMC migration is impaired by microtubule destabilisation

The above data shows that microtubule destabilisation increases actomyosin activity in VSMCs. Actomyosin activity is essential for the adhesion-based cell migration [255]. We, therefore, predicted that microtubule destabilisation would reduce the speed at which VSMCs migrate. To test this, VSMCs seeded on 12 kPa smooth PAHs were pre-treated with the microtubule destabilising agent colchicine and then tracked overnight using time-lapse microscopy. Analysis revealed that colchicine treatment reduced the directionality and speed (Figure 4.2) of VSMC migration.

In chapter 3, we showed that by altering the topology of our PAHs, VSMC migration could be reduced. We next investigated whether colchicine-driven microtubule destabilisation had the same impact on VSMCs seeded on grooved PAHs as it did on smooth. The analysis confirmed that colchicine treatment had the same impact on VSMCs migration, with colchicine reducing both the directionality and speed of migration on 12 kPa grooved PAHs (Figure 4.3.1). A look at all four conditions gives a clearer image of what is going on, where smooth C is the fastest, C+Co treatment reduced this, grooved C was slower than the smooth C and grooved C+Co is the slowest (Figure 4.3.2).
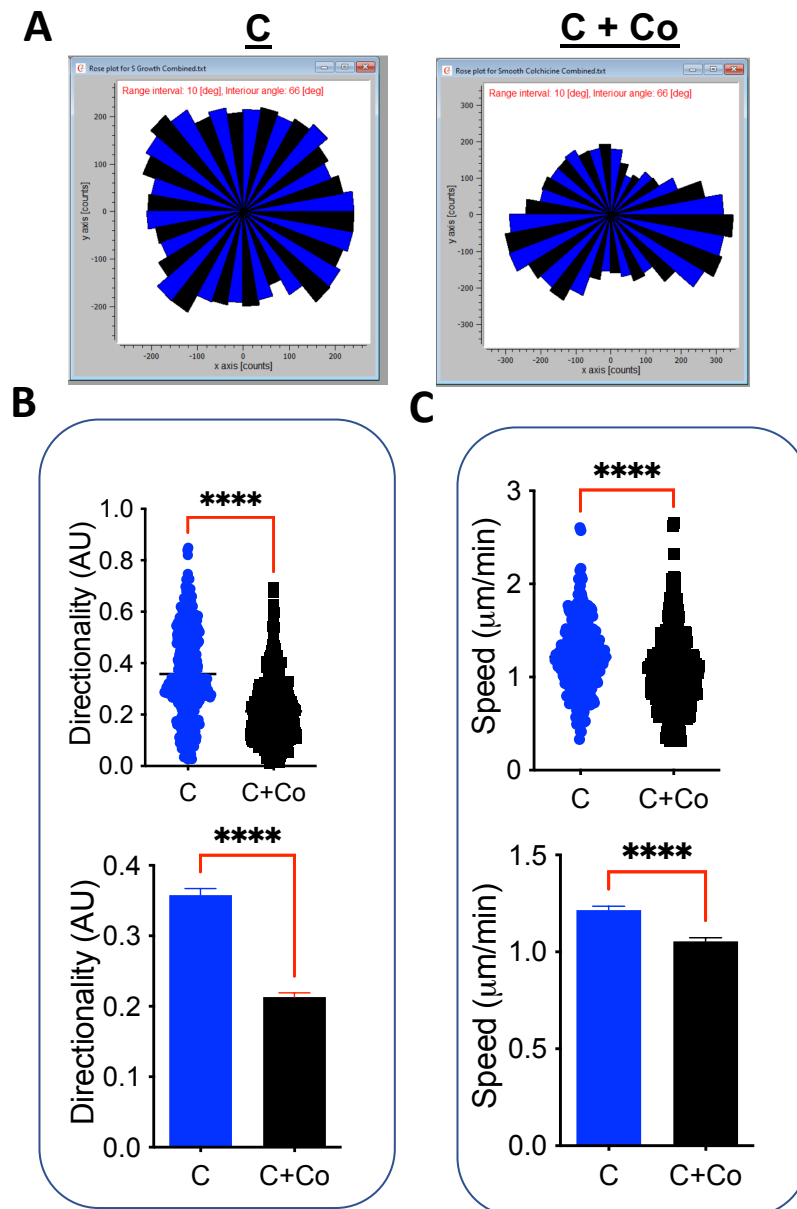
**Figure 4. 2: Microtubule destabilisation decreases the directionality and speed of VSMC migration**. VSMCs were seeded onto 12 kPa Smooth PAHs and cell migration was tracked using time-lapse microscopy over a 12 hour period. **A)** Representative rose plots of control- images used are representative only (C) and colchicine treated (C +Co) VSMCs migration. Graphs show **B)** directionality and **C)** speed of VSMC migration. Data is representative of 3 independent experiments, tracking 357 C and 397 C+Co treated VSMCs. (**** = p < 0.0001).
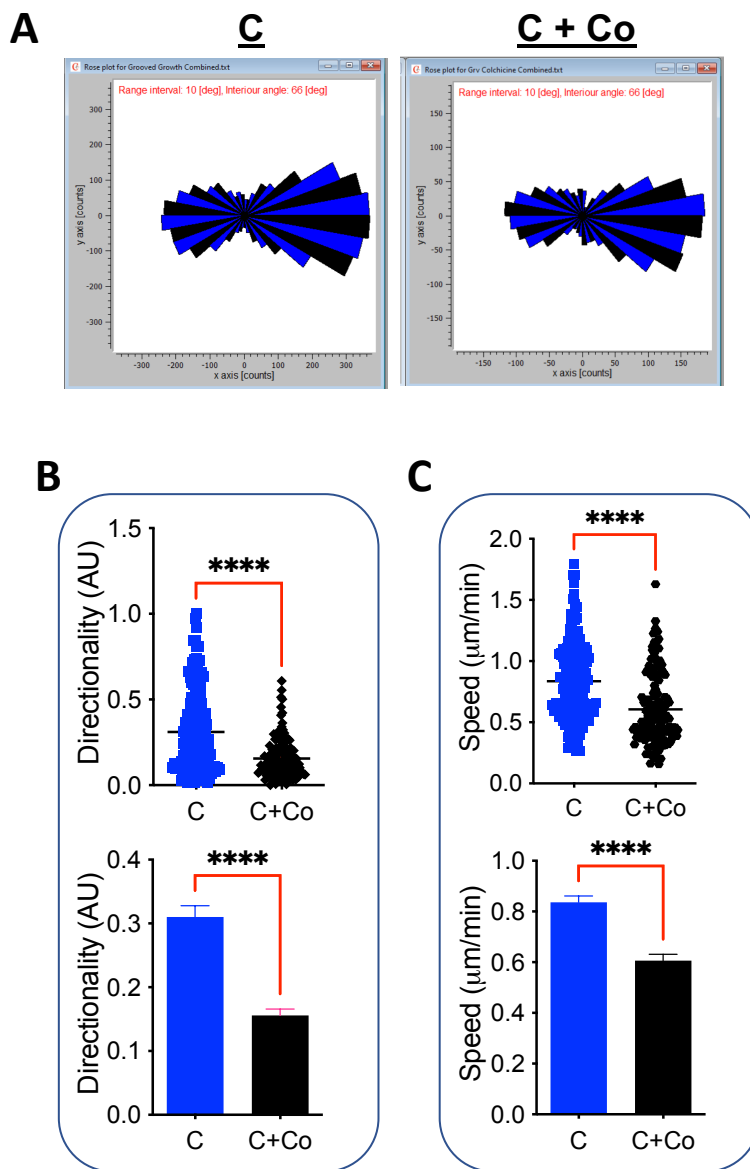
**Figure 4.3.1: Microtubule destabilisation decreases the directionality and speed of VSMC migration on grooved PAHs.** VSMCs were seeded onto 12 kPa Grooved PAHs and cell migration was tracked using time-lapse microscopy over a 12 hour period. **A)** Representative rose plots of control- images used are representative only (C) and colchicine treated (C +Co) VSMCs migration. Graphs show **B)** directionality and **C)** speed of VSMC migration. Data is representative of 3 independent experiments, tracking of 168 C and 134 C+Co treated VSMCs (**** = p < 0.0001).
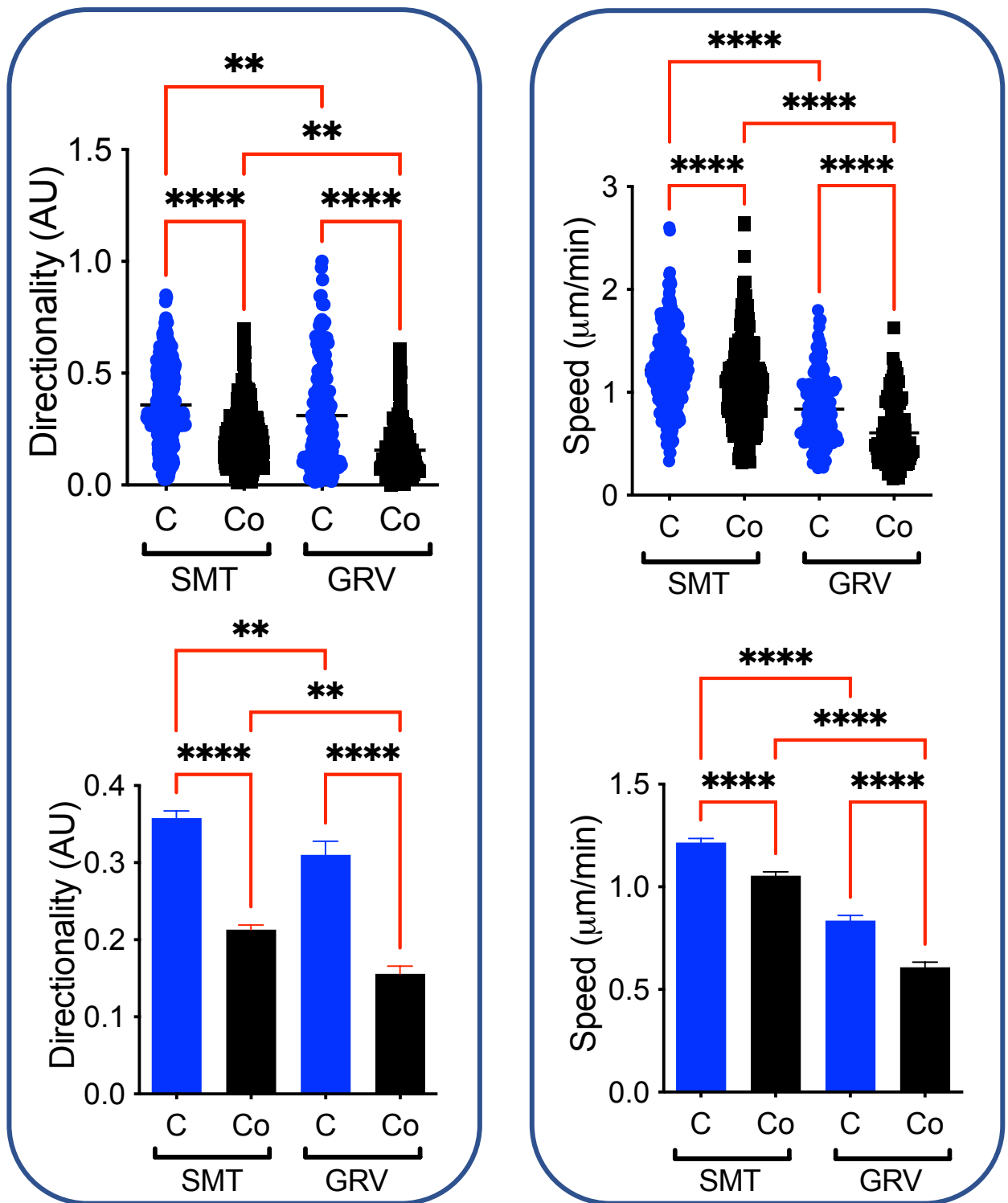
**Figure 4.3.2: Microtubule destabilisation decreases the directionality and speed of VSMC migration on both smooth and grooved PAHs.** VSMCs were seeded onto 12 kPa Grooved PAHs and cell migration was tracked using time-lapse microscopy over a 12 hour period. Graphs show **A)** directionality and **B)** speed of VSMC migration. Data is representative of 3 independent experiments, tracking 357 C, 397 C+Co treated on smooth and, 168 C and 134 C+Co treated VSMCs on grooved PAHs (**= p < 0.01). (**** = p < 0.0001).

### 4.5.3 Microtubule stabilising agents decrease VSMC traction stress generation

The above data shows that microtubule destabilisation increases traction stress generation and decreases the migrational capacity of VSMCs. We next speculated that microtubule stabilisation would reduce VSMCs traction stress generation and migrational capacity. To test this, VSMCs were pre-treated with the microtubule stabilising agent paclitaxel before TFM was used to determine the angiotensin II mediated traction stress generated by these cells. Analysis revealed that paclitaxel treatment reduced both maximal and integrated (Figure 4.4) traction stress generated by VSMCs seeded on smooth 12 kPa PAHs.

**Figure 4.4: Microtubule stabilisation decreases angiotensin II induced VSMC traction stress generation.** VSMCs were seeded onto 12 kPa Smooth PAHs and induced into quiescence by serum removal. VSMCs were paclitaxel (P) pre-treated for 30 minutes, before being stimulated with the contractile agonist angiotensin II (A). **A)** Representative phase images and bead displacement heat maps. Scale bar = 50 μm. Graphs show **B)** Maximum traction stress and **(C)** Integrate traction stress generation. Data is representative of 3 independent experiments (n = 48 in A and n = 27 P+A) VSMCs analysed (* = p < 0.05, ** = p < 0.01)

### 4.5.4 VSMC migration is impaired by microtubule stabilisation

We next looked at the effect of microtubule stabilisation on VSMC migration. To test this, VSMCs seeded on smooth 12 kPa PAHs were pre-treated with the microtubule stabilising agent paclitaxel and tracked overnight using time-lapse microscopy. Analysis revealed that paclitaxel treatment reduced both the directionality and speed (Figure 4.5) of VSMC migration. Once again, we wanted to see if the above result would be maintained when matrix topology was changed. VSMCs were therefore seeded onto 12 kPa grooved PAHs and subjected to the same experimental conditions as before. The analysis confirmed that paclitaxel treatment had the same impact on VSMCs migration on grooved as it did on smooth PAHs (Figure 4.6). Paclitaxel treatment reduced both the directionality and speed of VSMCs migration on 12 kPa grooved PAHs.
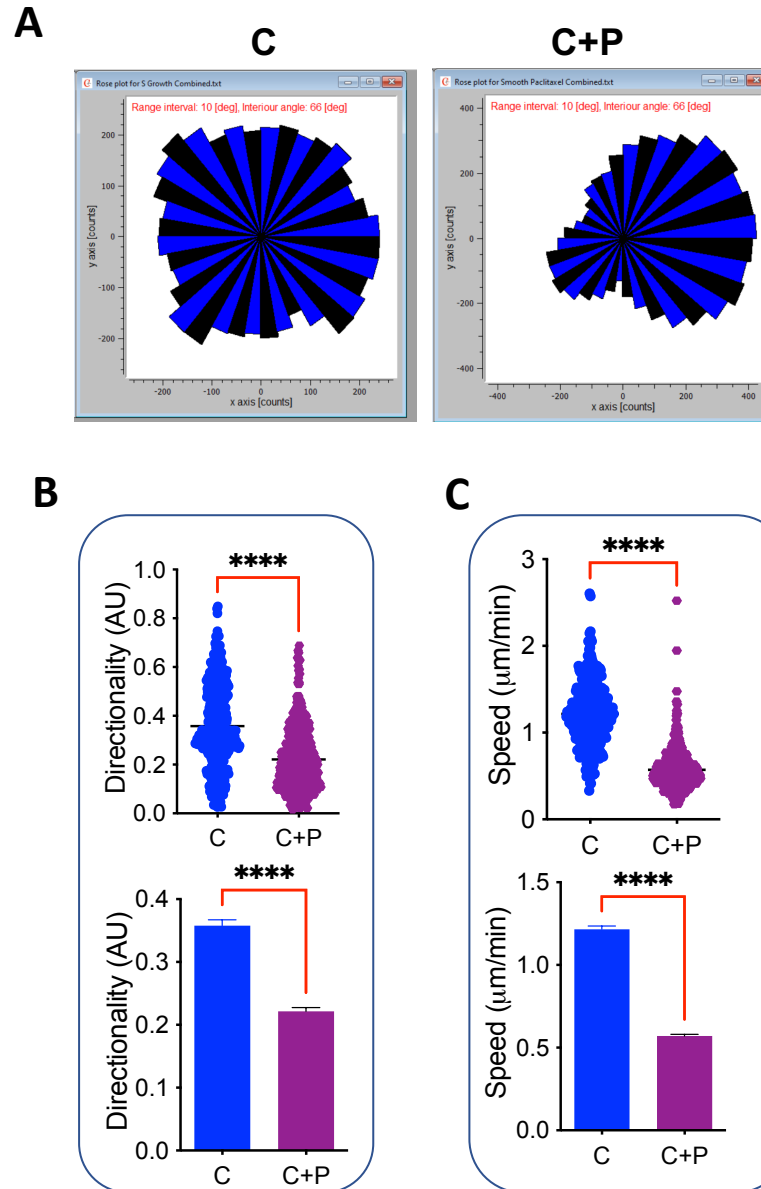
**Figure 4.5: Microtubule stabilisation decreases the directionality and speed of VSMC migration.** VSMCs were seeded onto 12 kPa smooth PAHs and cell migration was tracked using time-lapse microcopy over a 12 hour period. **A)** Representative rose plots of control- images used are representative only (C) and paclitaxel treated (C+P) VSMCs migration. Graphs show **B)** directionality and **C)** speed of VSMCs migration. Data is representative of 3 independent experiments, tracking 357 C and 494 C+P treated VSMCs. (**** = $p < 0.0001$).
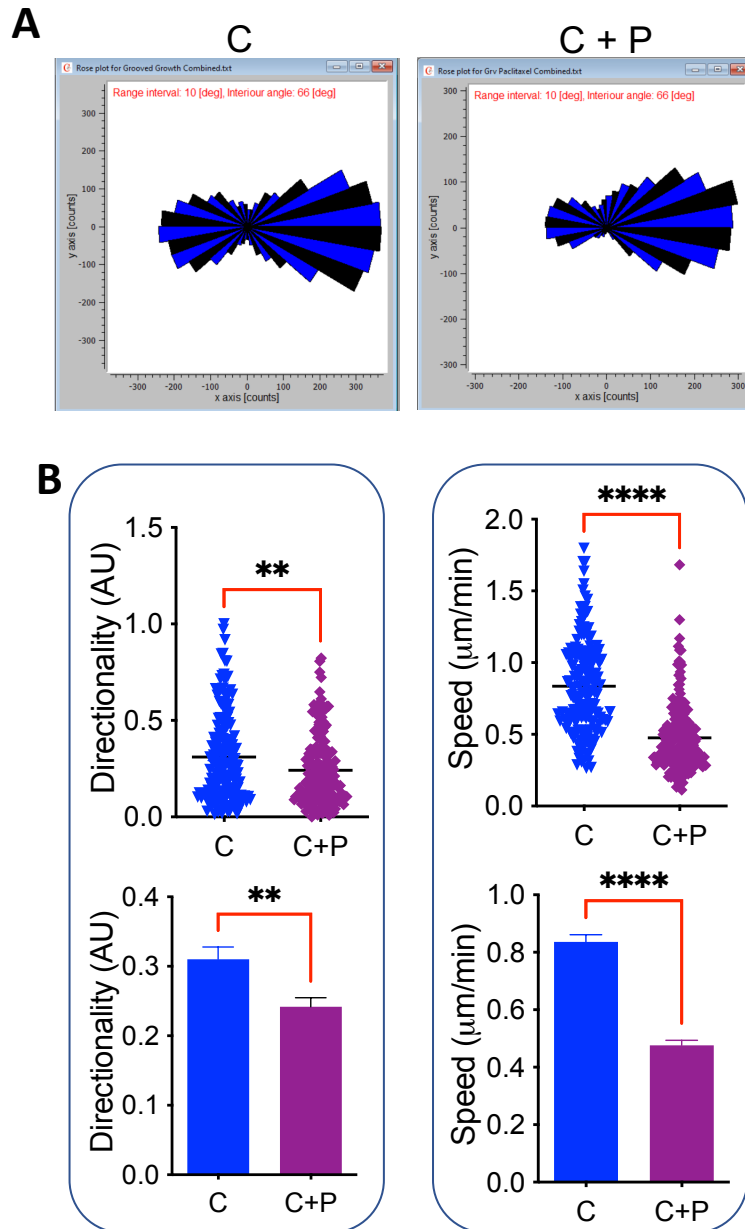
**Figure 4. 6: Microtubule stabilisation decreases the directionality and speed of VSMC migration on grooved PAHs**. VSMCs were seeded onto 12 kPa Grooved PAHs and cell migration was tracked using time-lapse microscopy over a 12 hour period. **A)** Representative rose plots of control- images used are representative only (C) and paclitaxel treated (C+P) VSMCs migration. Graphs show **B)** directionality and **C)** speed of VSMC migration. Data is representative of 3 independent experiments, tracking 168 C and 185 C+P treated VSMCs. (n = 168 control and n = 185 paclitaxel treated VSMCs). (** = $p < 0.01$, **** = $p < 0.0001$)

### 4.5.5 Microtubule stability regulates VSMC traction stress generation

The above data shows that microtubule destabilisation (via colchicine treatment) increases VSMC traction stress generation whilst microtubule stabilisation (via paclitaxel treatment) decreases traction stress generation. Meanwhile any change to microtubule stability and therefore their dynamic instability results in reduced VSMC migration. Having observed these effects, we next wanted to know the effect of another microtubule targeting agent, demecolcine. Depending on the concentration it is used at, demecolcine can both promote microtubule stability and induce microtubule catastrophe. Previous work in our lab has shown that our working concentration of demecolcine in VSMCs results in the maintenance of the total number of cold-stable microtubules. Following serum withdrawal, VSMCs seeded on smooth 12 kPa PAHs were pre-treated with demecolcine prior to undergoing angiotensin II stimulation. Traction force microscopy revealed that demecolcine treatment resulted in a slight increase in the maximum but no significant difference in the integrated traction stress generated by VSMCs (Figure 4.7).
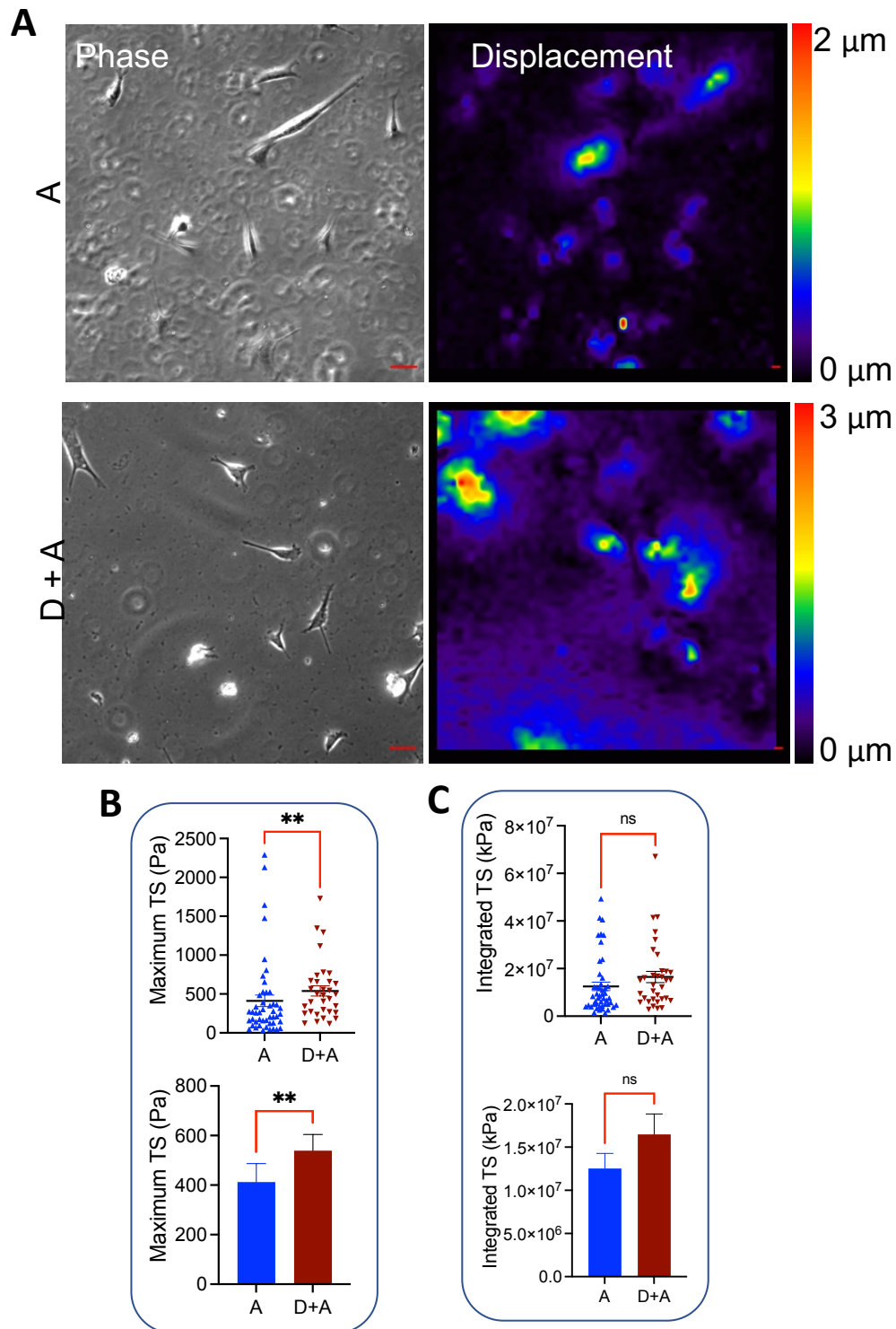
**Figure 4. 7: Demecolcine induces increased traction stress generation**. VSMCs were seeded onto 12 kPa smooth PAHs and induced into quiescence by serum removal. VSMCs were demecolcine (D) pre-treated for 30 minutes, before being stimulated with the contractile agonist angiotensin II (A). **A)** Representative phase images and bead displacement heat maps. Scale bar = 50 μm. Graphs show **B)** Maximum traction stress and **C)** Total traction stress generation. Data is representative of 3 independent experiments (with n = 47 in A and n = 34 in D+A VSMCs analysed). (n.s. = non-significant, ** = p < 0.01).

### 4.5.6 Demecolcine promotes VSMC migration.

We next wanted to observe the effect of microtubule destabilises on VSMC migration. To test this, VSMCs were seeded onto smooth 12 kPa PAHs and their migration was tracked over a 12-hour period in the presence or absence of demecolcine. Analysis revealed that demecolcine treatment had no impact on the directionality of VSMC migration, but it did promote an increase in their migration speed (Figure 4.8).
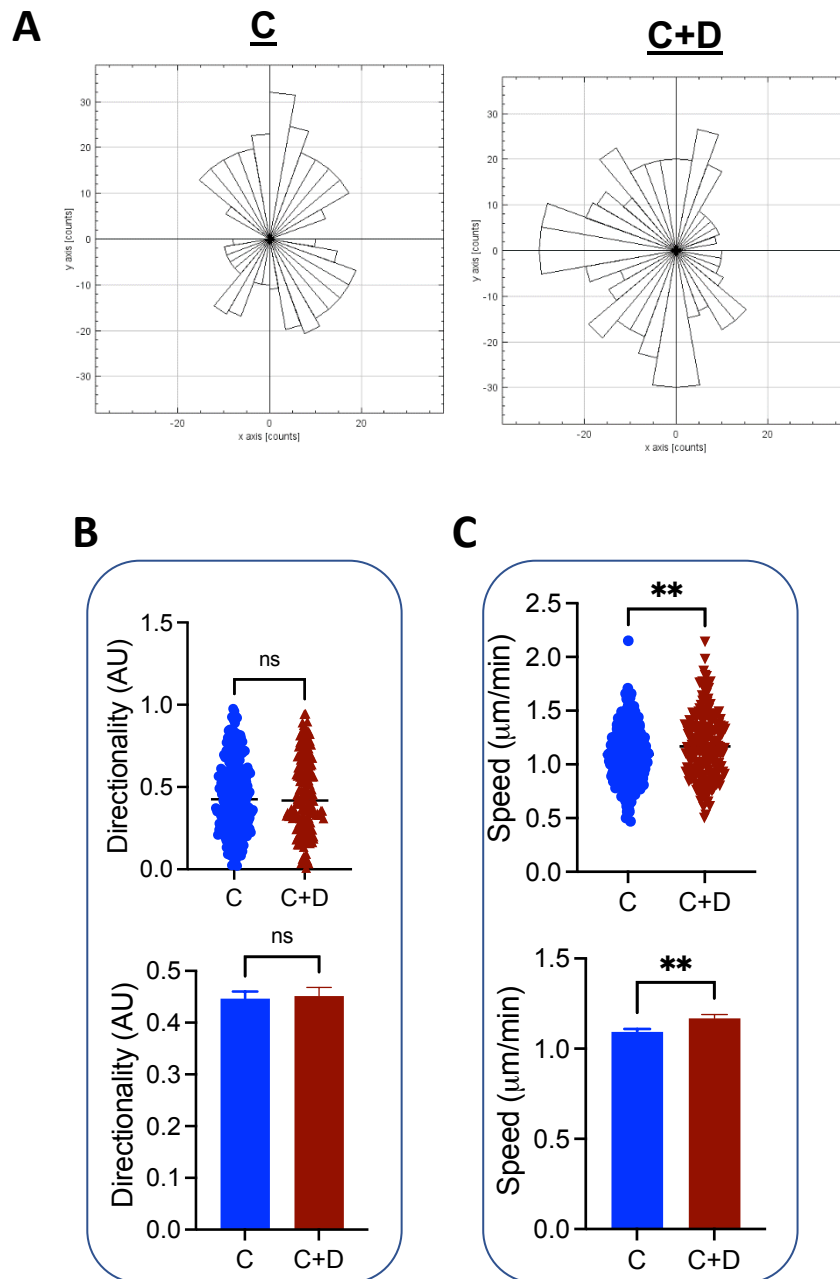
**Figure 4. 8: Demecolcine increases the speed of VSMC migration.** VSMCs were seeded onto 12 kPa smooth PAHs and cell migration was tracked using time-lapse microscopy over a 12-hour period. **A)** Representative rose plots of control- images used are representative only (C) and demecolcine treated (C+D) VSMCs migration. Graphs show **B)** directionality and **C)** speed of VSMC migration. Data is representative of 3 independent experiments, tracking 357 C and 213 C+D treated VSMCs. (n = 357 control and n = 213 demecolcine treated VSMCs tracked). (n.s. = non-significant, ** = $p < 0.01$)

### 4.5.7 Microtubule acetylation as a regulator of microtubule stability.

So far, we have investigated the effect of classical microtubule targeting agents, those that directly interact with microtubules to promote either growth or catastrophe, in their ability to regulate VSMC traction stress generation and migrational capacity. Other cytoskeletal organization key for cell motility are regulated by the RhoA activation and via acetylation of microtubule [256]. Microtubule acetylation has also been shown to regulate both microtubule dynamics and actomyosin force generation [150]. Two enzymes which regulate microtubule acetylation are NAT10 (acetylase) and HDAC6 (deacetylase). We subsequently investigated whether inhibition of those enzymes would alter VSMC actomyosin force generation or migration using their respective inhibitors, remodelin and tubastatin.

### 4.5.8 Remodelin treatment decreases VSMC traction stress generation.

We next investigated the impact of microtubule deacetylation on VSMC actomyosin force generation. To test this, VSMCs were seeded onto smooth 12 kPa PAHs and quiescence was induced by serum withdrawal. VSMCs were pre-treated with the NAT10 inhibitor, remodelin, for 30 minutes prior to angiotensin II treatment. TFM was performed to measure VSMC traction stress generation. Analysis revealed that remodelin pre-treatment produced a significant reduction in integrated VSMC traction stress generation, with maximal traction stress only trending to reduce following remodelin pre-treatment (Figure 4.9).

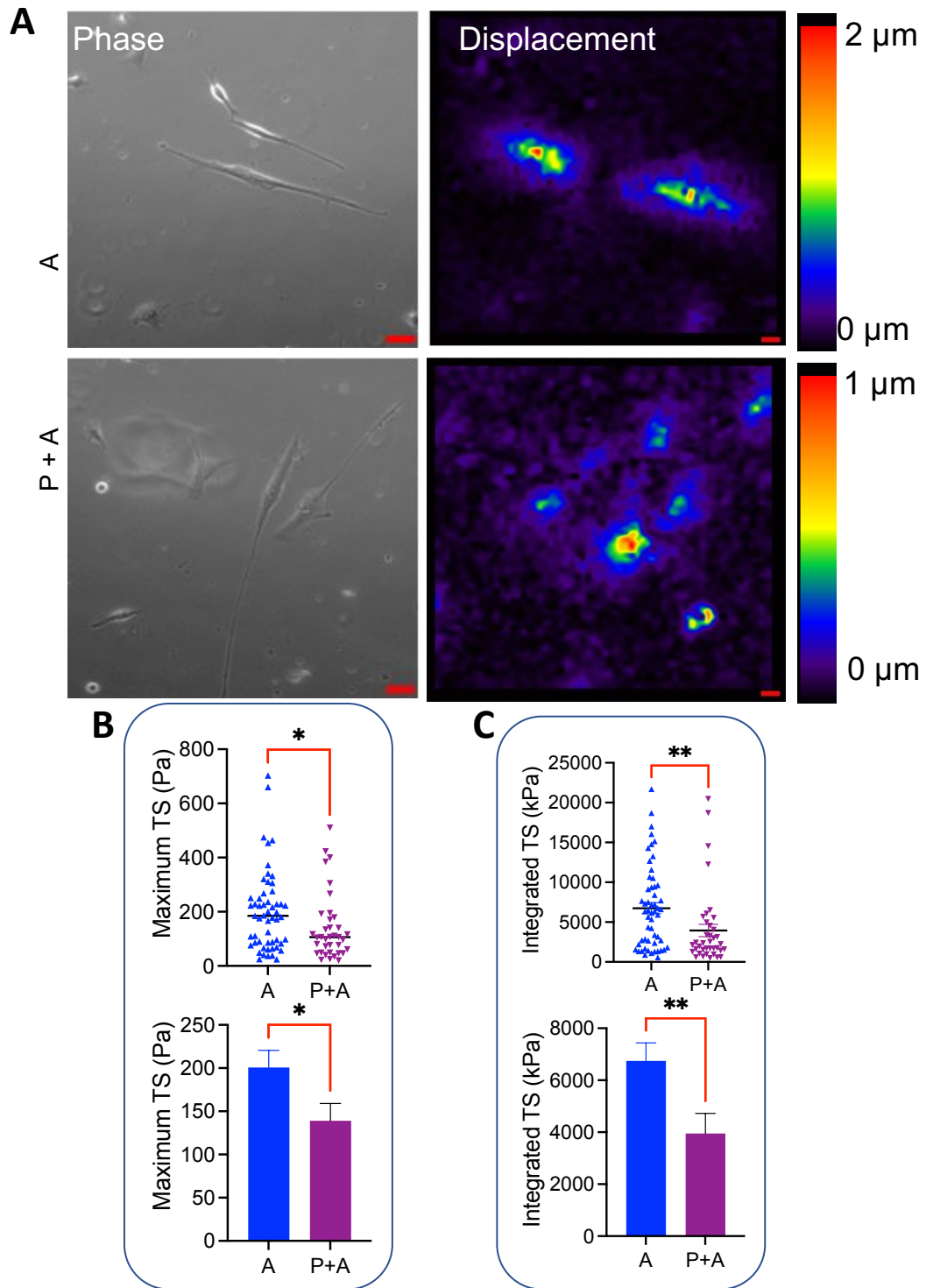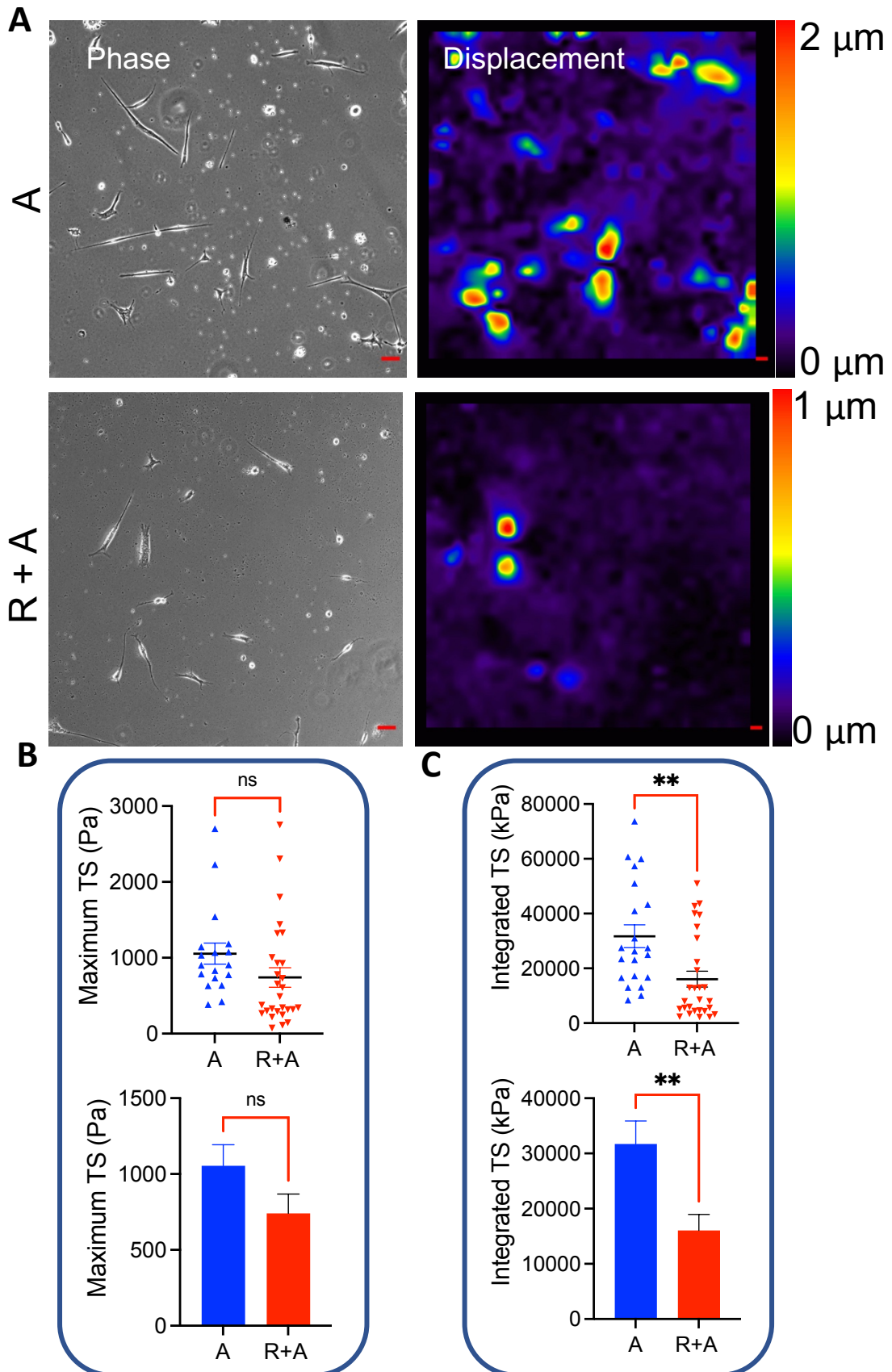**Figure 4. 9: Remodelin treatment reduces angiotensin II induced VSMC traction stress generation.** VSMCs were seeded onto 12 kPa Smooth PAHs and induced into quiescence by serum removal. VSMCs were remodelin (R) pre-treated for 30 minutes, before being stimulated with the contractile agonists angiotensin II (A). **A)** Representative phase images and bead displacement heat maps. Scale bar = 50 µm. Graphs show **B)** Maximum traction stress and **C)** Integrated traction stress generation. Data is representative of 3 independent experiments, (n=21 in A and n=28 R+A). (n.s. = non-significant, ** = $p < 0.01$).

### 4.5.9 Remodelin treatment has no effect on VSMC migration.

The data above demonstrates that NAT10 inhibition decreases actomyosin activity in VSMCs. We predicted that inhibiting the activity of NAT10 would reduce VSMC migrational capacity. To test this, VSMCs were seeded on to smooth 12 kPa PAHs and their migration was imaged over 12 hours, in the presence or absence of remodelin. Analysis revealed that remodelin treatment had no impact on either the directionality or speed of VSMC migration (Figures 4.10).

In Chapter 3 we demonstrated that matrix stiffness is a key regulator of VSMCs activity. We, therefore, speculated whether remodelin treatment may affect VSMC migration selectively in a stiffer environment. VSMCs were subsequently seeded onto smooth 72 kPa PAHs to mimic the stiffness of the aged/diseased aortic wall. VSMC migration was imaged for 12 hours in the presence or absence of remodelin. Analysis revealed that on stiffer matrixes, remodelin treatment resulted in increased VSMC migration speed but once again had no effect on directionality (Figure 4.11).
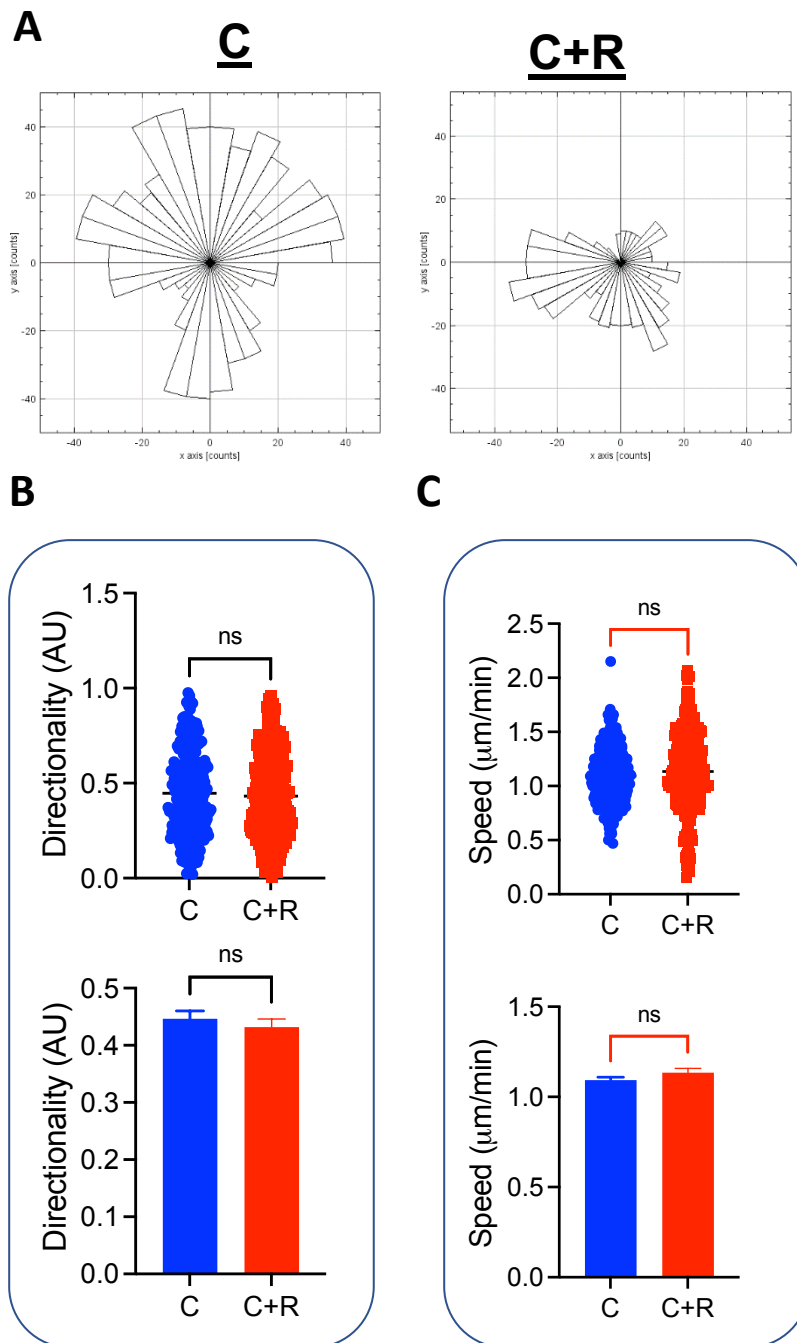
**Figure 4. 10: Remodelin treatment has no effect on VSMC migration on PAHs of physiological stiffness**. VSMCs were seeded onto 12 kPa smooth PAHs and cell migration was tracked using time-lapse microscopy over a 12 hour period. **A)** Representative rose plots of control- images used are representative only (C) and remodelin treated (C+R) VSMC migration. Graphs show **B)** directionality and **C)** speed of VSMCs migration. Data is representative of 3 independent experiments, tracking 256 C and 246 C+R treated VSMCs. (ns = non-significant)

## 4.5.10 Remodelin treatment minimally increases VSMC migrational capacity on aged/diseased stiffness

Our lab has previously proven that stiffness is a key regulator of VSMCs activity, and we have also discussed this in chapter two in great detail. So, we next investigated whether remodelin had the same impact on VSMCs seeded on a stiffness reflecting an aged/diseased environment. VSMCs were seeded onto smooth 72 kPa PAHs to mimic aged/diseased extracellular matrix. VSMC migration was imaged for 12 hours in the presence or absence of remodelin. Analysis confirmed that remodelin treatment had the same impact on VSMCs migration capacity as on the smooth 12 kPa PAHs. Remodelin treatment didn't alter directionality (Figures 4.12 A and B) while increasing the speed (Figures 4.12 A and C) of VSMCs migration on grooved PAHs.
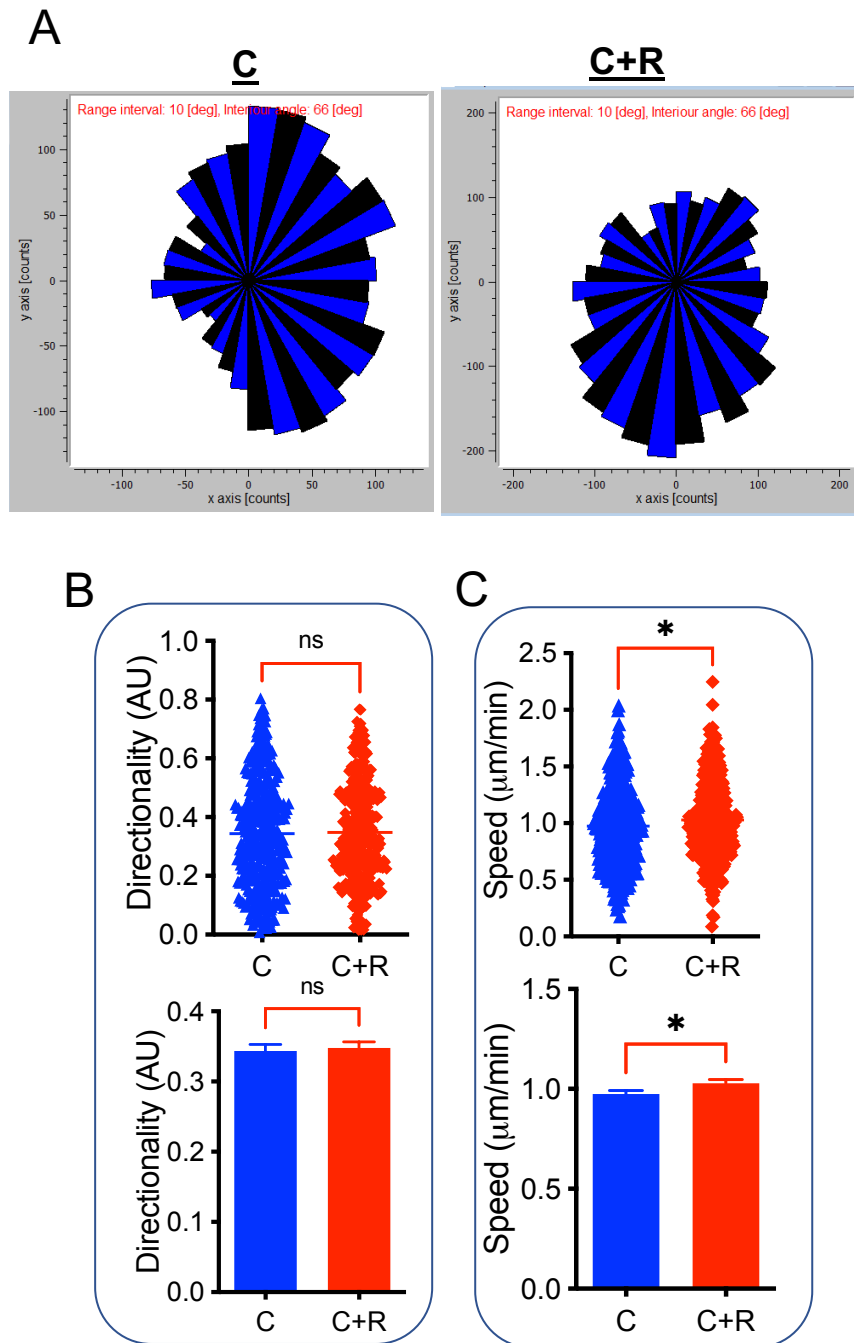
**Figure 4. 11 VSMC migration speed on stiff PAHs increases following Remodelin treatment.** VSMCs were seeded onto 72 kPa smooth PAHs and cell migration was tracked using time-lapse microscopy over a 12 hour period. **A)** Representative rose plots of control- images used are representative only (C) and remodelin treated (C+R) VSMCs migration. Graphs show **B)** directionality and **C)** speed of VSMC migration. Data is representative of 3 independent experiments, tracking 384 C and 366 C+R treated VSMCs. (ns = non-significant), (* = p < 0.05)

### 4.5.11 Microtubule hyperacetylation has no impact on VSMCs traction stress generation

Histone deacetylase 6 (HDAC6) is known to deacetylate microtubules [257,258]. We next investigated the impact of HDAC6 inhibition, thereby leading to hyperacetylation of microtubules and the effect this would have on VSMC traction force generation. VSMCs were seeded onto smooth PAHs of physiological stiffness and quiescence was induced by serum withdrawal. VSMCs were pre-treated with the HDAC6 inhibitor, tubastatin, for 30 minutes prior to angiotensin II treatment. TFM revealed that inhibition of HDAC6 had no impact on either the maximal or integrated traction stresses generated by VSMCs (Figure 4.12).
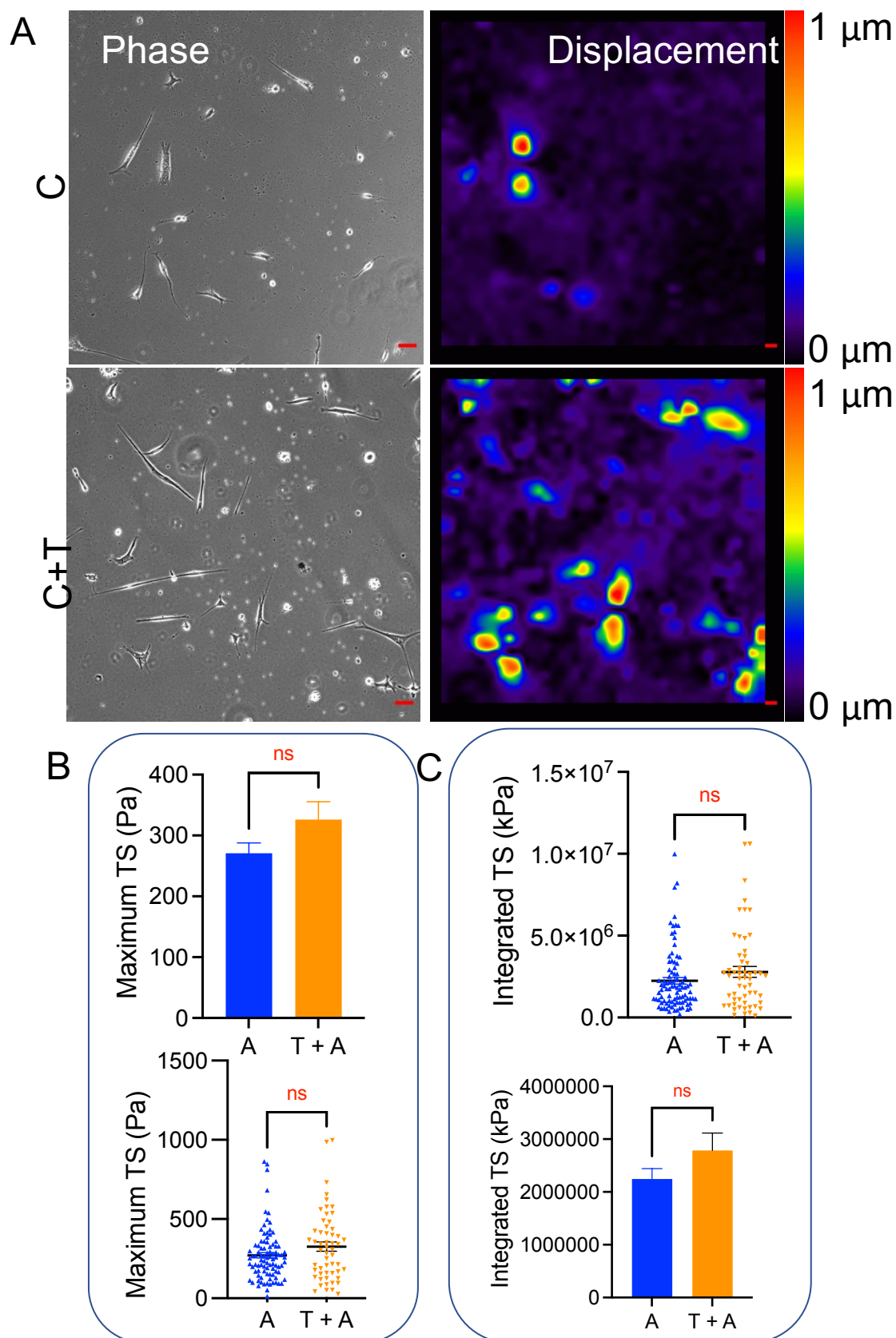
**Figure 4. 12: Microtubule hyperacetylation has no effect on angiotensin II induced VSMC traction stress generation.** VSMCs were seeded onto 12 kPa Smooth PAHs and induced into quiescence by serum removal. VSMCs were tubastatin (T) pre-treated for 30 minutes, before being stimulated with the contractile agonist angiotensin II (A). **A)** Representative phase images and bead displacement heat maps. Scale bar = 50 μm. Graphs show **B)** Maximum traction stress and **C)** integrated traction stress displative of 3 independent experiments (n=91 in A and n=56 with 91 control and 56 tubastatin treated VSMCs analysed. (n.s. = non-significant)

**4.5.12 HDAC6 inhibition has no effect on VSMC migration.**

The above data shows that tubastatin treatment had no impact on the actomyosin force generated by VSMCs on physiological matrix stiffness. From this and the other experiments performed within this chapter, we predicted that tubastatin wound not alter the migrational capacity of VSMCs. To test this, VSMCs were seeded on to smooth 12 kPa PAHs and their migration was tracked over a 12-hour period, in the presence or absence of tubustatin. Analysis confirmed that tubustatin treatment had no impact on the directionality or speed of VSMCs migration (Figure 4.13).
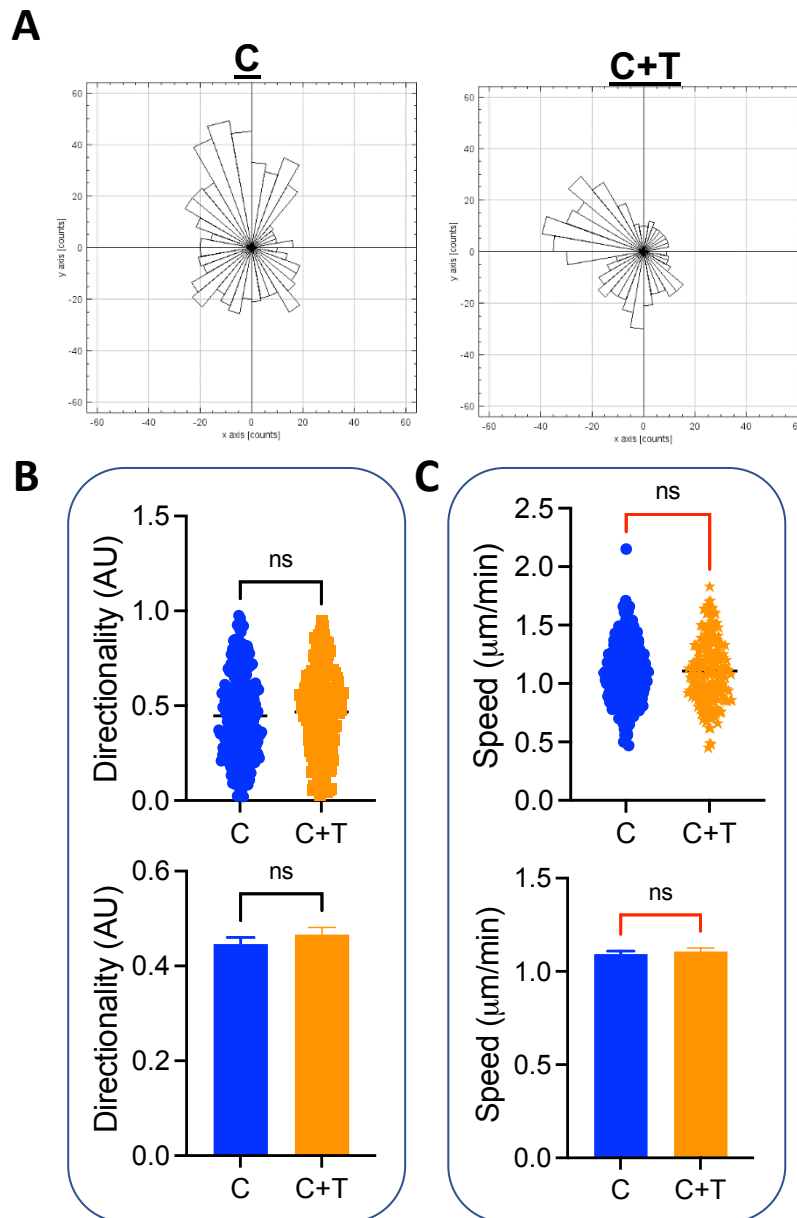
**Figure 4. 13: HDAC6 inhibition has no impact on VSMC migration.** VSMCs were seeded onto 12 kPa smooth PAHs and cell migration was tracked using time-lapse microscopy over a 12 hour period. **A)** Representative rose plots of control- images used are representative only (C) and tubustatin treated (C + T) VSMC migration. Graphs show **B)** directionality and **C)** speed of VSMC migration. Data is representative of 3 independent experiments, tracking 357 C and 205 C+T treated VSMCs. (ns = non-significant)

### 4.5.13 VSMCs generate increased traction stress following HDAC6 inhibition on aged/diseased matrix stiffness

In chapter 3 we discussed the importance of matrix stiffness and topology in regulating VSMC traction stress generation. Despite inhibition of HDAC6 having no effect on VSMC traction stress generation when cells were seeded on PAHs mimicking healthy aortic stiffness, we wanted to investigate whether the same mechanism applied to VSMCs seeded on PAHs mimicking an aged/diseased stiffness. VSMCs were therefore seeded onto smooth 72 kPa PAHs, with quiescence induced following serum withdrawal. TFM revealed that VSMCs which had been pre-treated with tubastatin, prior to angiotensin II stimulation, generated enhanced maximal and integrated traction stress on rigid PAHs (Figure 4.14).
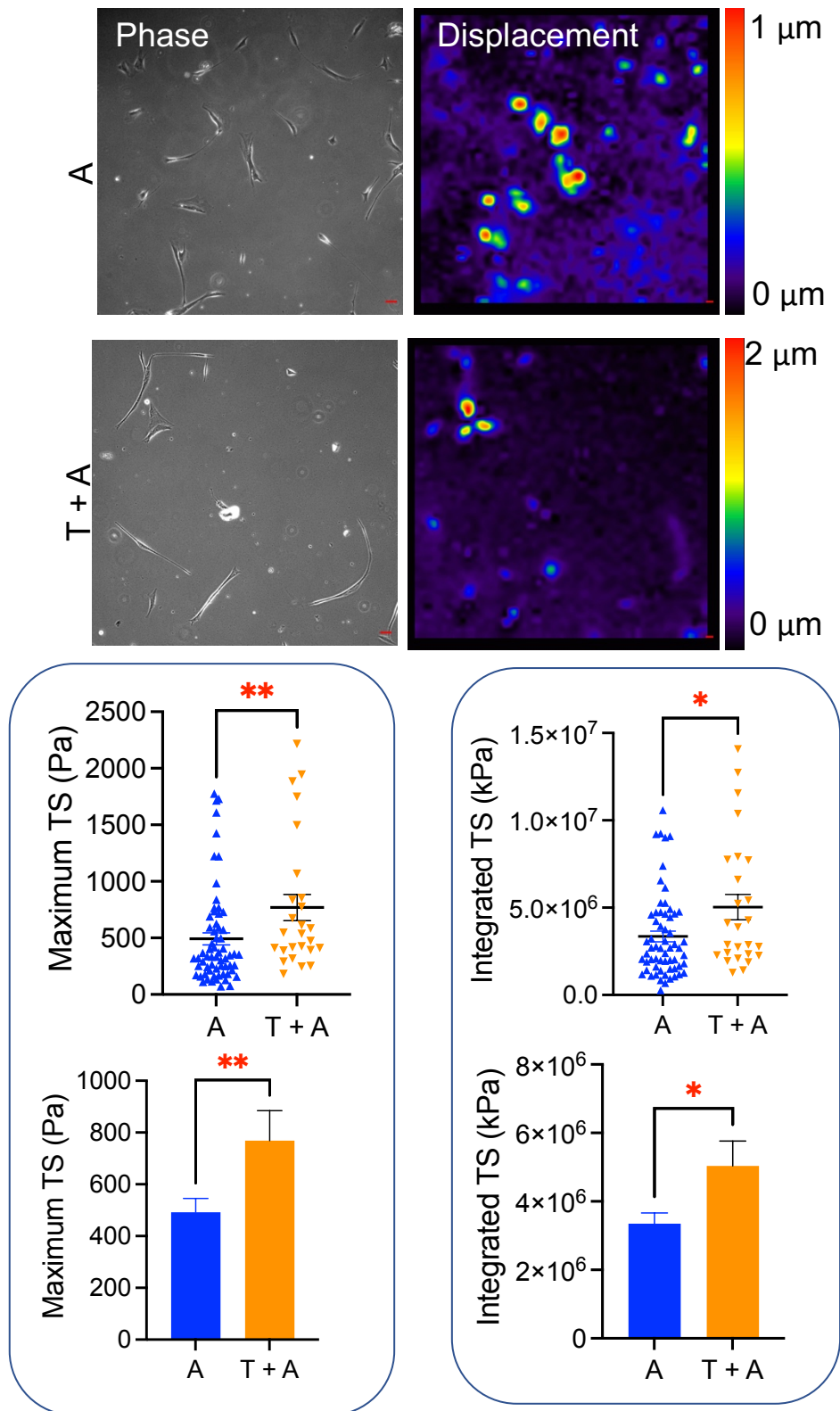
**Figure 4. 14: HDAC6 inhibition increases traction stress generated by VSMCs on 72 kPa PAHs**. VSMCs were seeded onto 72 kPa smooth PAHs and induced into quiescence by serum removal. VSMCs were tubastatin (T) pre-treated for 30 minutes, before being stimulated with the contractile agonist angiotensin II (A). **A)** Representative phase images and bead displacement heat map. Scale bar = 50 µm. Graphs show **B)** Maximum traction stress and **C)** integrated traction stress generation. Data is representative of 3 independent experiments (n = 64 in A and n = 26 in T+A VSMCs analysed). (* = $p < 0.05$, ** = $p < 0.01$).

## 4.5.14 HDAC6 inhibition reduces VSMC migration speed on PAHs mimicking aged/diseased aortic stiffness

The above data shows that tubastatin pre-treated VSMCs on aged/diseased mimicking PAHs generated significantly higher traction stress. To test if tubastatin-mediated inhibition of HDAC6 would also affect VSMC migration on aged/diseased stiffnesses, cells were seeded onto smooth 72 kPa PAHs and tracked over a 12-hour period. Analysis revealed that tubastatin treatment had no impact on the directionality of VSMC migration but resulted in a slight reduction in migration speed (Figure 4.15).
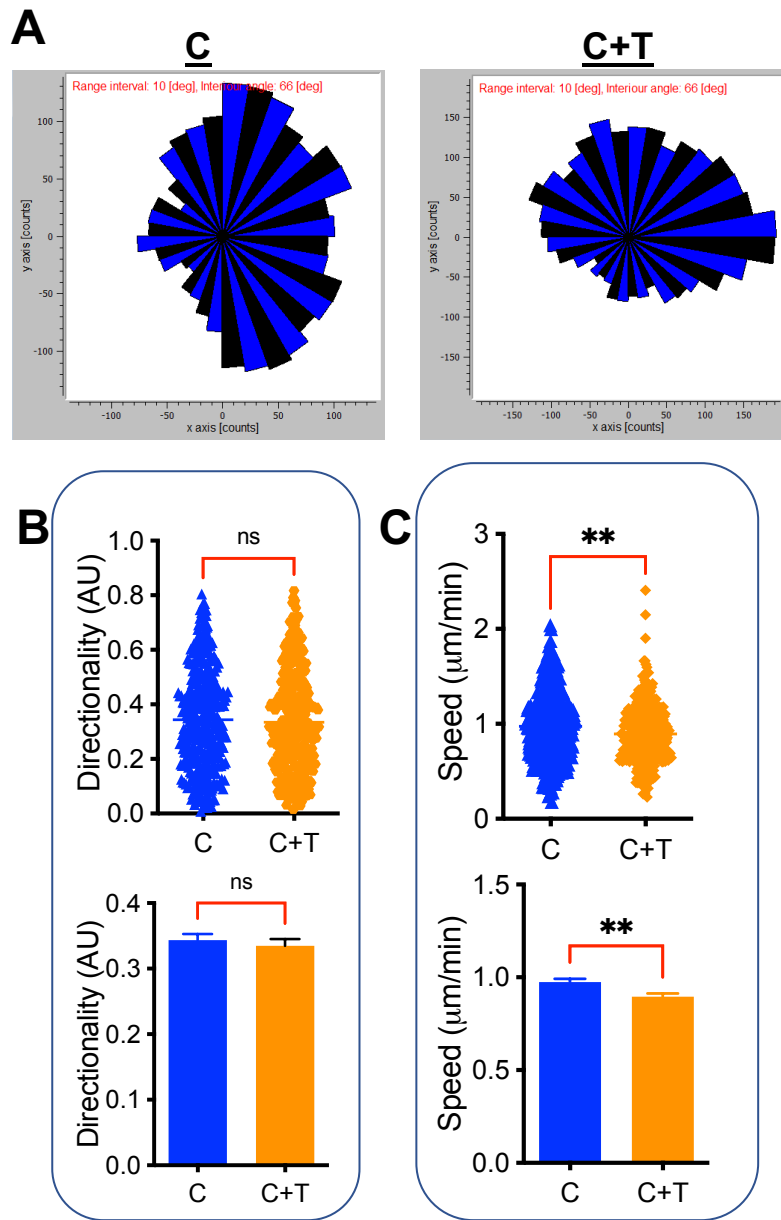
**Figure 4.15. HDAC6 inhibition reduces VSMC migration speed on PAHs mimicking aged/diseased aortic stiffness.** VSMCs were seeded onto 72 kPa smooth PAHs and cell migration was tracked using time-lapse microscopy over a 12 hour period. **A)** Representative rose plots of control- images used are representative only (C) and tubustatin treated (C + T) VSMC migration. Graphs show **B)** directionality and (**C**) speed of VSMC migration. Data is representative of 3 independent experiments, tracking 384 C and 325 C+T treated VSMCs. (ns = non-significant, ** = p < 0.01).

## 4.5.15 Comparison the impact of all drugs used on VSMC migrational capacity on aged/diseased stiffness

We next compared the migrational data for all drug treatments we used on both the aged/diseased matrix stiffness. Colchicine and paclitaxel significantly reduced the directionality of VSMC migration despite their counteracting mechanisms of action. Demecolcine, remodelin or tubastatin treatment didn't influence the directionality of VSMC migration. (Figure 4. 16 A). colchicine, paclitaxel and tubastatin reduced the migrational speed of VSMCs whilst remodelin and demecolcine had no impact (Figure 4. 16 B).
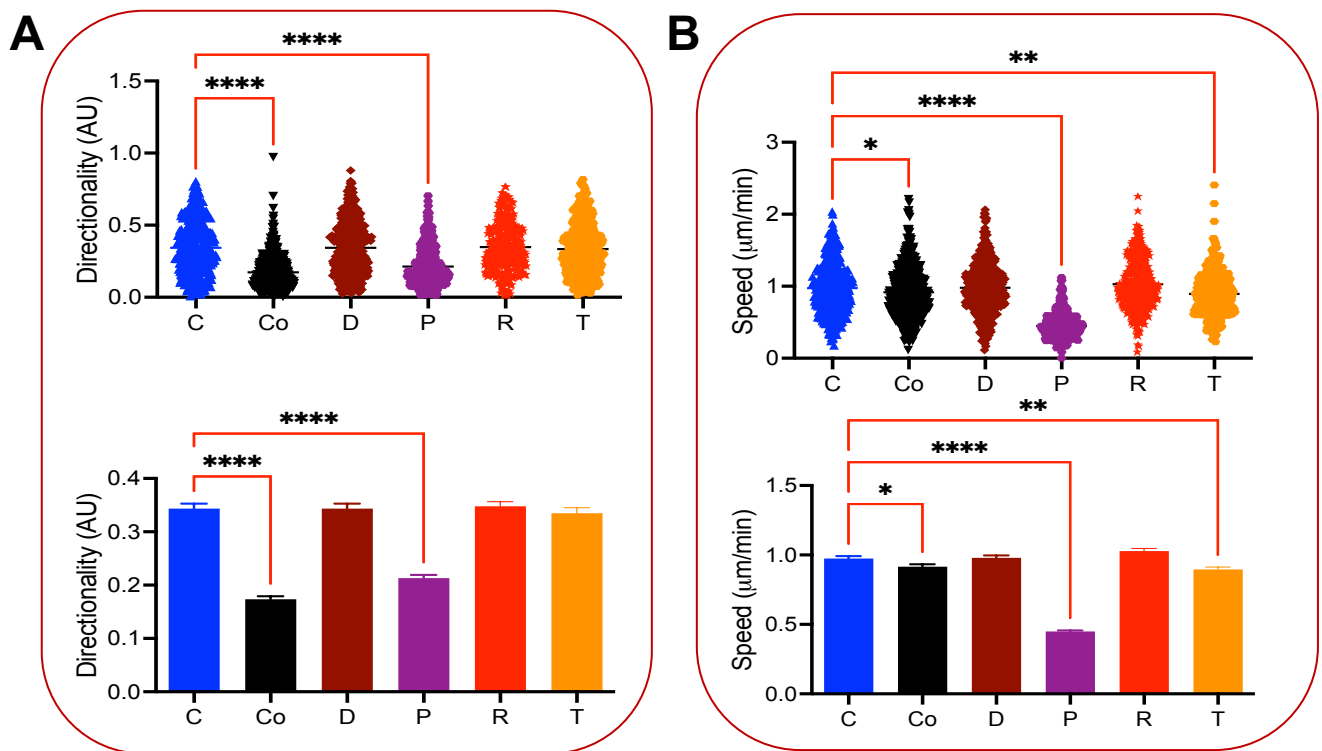
**Figure 4. 16: A comparison of microtubule targeting agents we used and their impact on migrational capacity.** Graphs show (A) directionality (B) and speed on 72 kPa PAHs. Cells were treated +/− one of the five agents (discussed in separate sections) in their corresponding concentration 30 minutes before a timelapse images were set to capture over 12 hours, on a 10-minute interval. C-control, Co-colchicine, D-demecolcine, P-paclitaxel, R- remodelin and T-tubastatin. Data is representative of 3 independent experiments with the n numbers VSMCs tracked each condition addressed on the sections 4.4.2 to 4.4.14 above. (* p = < 0.05, ** = p < 0.01, *** = p < 0.001, **** = p < 0.0001).

## 4.6 Discussion and conclusion

In this chapter, we investigated the impact of microtubule targeting compounds on VSMC traction stress generation and migration. Though many *in vitro* migration studies have been performed previously, most of these studies were carried out on plastic or glass surfaces, which are roughly a thousand-fold stiffer than the aortic wall [259]. In our recently published work [146], we validated a PAHs-based assay for screening of VSMCs contractile activity and traction stress generation. Our ability to mimic arterial wall stiffness and topology by tailoring PAHs has given us a novel way of controlling VSMCs *in vitro,* where the work we have done can be used to assess in vivo situations.

Apart from maintaining proper cell shape, the cytoskeleton function extends to facilitating the physical and mechanical interaction of the VSMCs with their surroundings. This functionality of traction stress must be properly regulated for many mechanosensing phenomena including the processes of cell migration, differentiation, growth and cell shape [260] [261].

We have previously demonstrated the impact of cell shape and substrate rigidity and topology on VSMCs functionality [51,146]. Further studies have suggested that microtubule structure and crosstalk with other cytoskeletal systems, such as actin filaments also regulate traction stress [262]. However, the mechanisms through which this happens remain under investigated. Having said that, an investigation by one research team proposed two possible pathways through which microtubule depolymerization generates increased traction stress, whilst stabilising microtubules decrease traction stress in myosin-II independent setting [263]

Whilst we also have observed that destabilising microtubules generated larger traction stress (Figure 4.1), stabilising microtubules blocked VSMCs from generating traction stress. (Figure 4.4). The mechanism through which this happens is not fully understood, however, we are using a different approach that allows us to mimic in vivo dynamics of VSMCs in vitro and our finding so far is a key insight to further studies and utilization of microtubule targeting compounds to better understand.

Microtubule targeting agents colchicine and paclitaxel significantly reduce the migration speed of VSMCs. This is due to the microtubule stabilising effect of paclitaxel, which shifts the balance of microtubules to assembly, leading to numerous unorganised and decentralized microtubules inside the cytoplasm [170]. It's worth mentioning that whilst both colchicine and paclitaxel inhibit cell division at the M phase, they involve different biological mechanisms [264,265]. Previous studies using wire myography have reported that microtubule destabilisation increased VSMC force generation [266]. Another study showed colchicine used

to test the contractile performance of hypertrophied neonatal cardiocytes through its microtubule depolymerization effect [267]

Furthermore, some studies suggest that microtubule stabilising agents inhibit proliferation and migration as a result of some sort of microtubule-mediated sequestering and release mechanism [143,173,268].

Through our experiments in this chapter, we found out that the migratory function of VSMCs significantly decreased with the disruption of microtubule instability dynamics (colchicine and paclitaxel) (Figures 4.2, 4.3, 4.5 and 4.6), and this suggests that microtubules are important components of VSMCs migration.

Comparing microtubule destabilisers and stabilisers' impact on traction stress migration: when pre-treated with colchicine, a microtubule destabilisation following angiotensin II stimulated VSMCs generated significantly larger maximum and integrated traction stress (Figure 4.7). This impact of microtubules in actomyosin activity agrees with previous observations reported as the mechanical borne of the cytoskeleton also known as tensegrity model [269,270]. However, the paclitaxel showed no influence on maximum traction stress and caused angiotensin II stimulated VSMCs to generate significantly smaller integrated traction stress (Figure 4.9).

This observation is different from the interplay between traction stress and the cell area, where cells generated increased traction stress show reduced cell area as shown in chapter 3. This could be explained by the microtubule agents' uncouple area and traction stress relationship, and that was confirmed via confocal microscopy [271].

Some recent studies are shedding light on the crosstalk between microtubules and actin of the cytoskeleton, that microtubule depolymerization activates myosin II-dependent mechanisms through FAK-independent pathways. Hence cells can generate more force without changing their shape and form. Some studies observed that there were significant changes in the focal adhesion driving proteins like focal adhesion kinases [262].

Demecolcine, a microtubule destabilising agent, depending on the concentration, depolymerizes microtubules at higher concentrations and stabilizes microtubule dynamics at lower constatation. When colchicine binds to microtubule ends or soluble tubulin for a poorly reversible tubulin-colchicine complex [272], which is central to colchicine mechanism of action in regulating the cytoskeletal function [273] and it has been reported that colchicine attenuates SMC

proliferation and migration [146,273].

N-acetyltransferase 10 (NAT10) is identified as a regulator of many cellular activities such as RNA stability and the translation process [274]. Targeting NAT10 promotes cell cycle progression through a proposed mechanism of the cyclinD1/CDK2/p21 axis [185] and is also shown to prevent DNA damage [186,275].

NAT10 is a potential therapeutic target to treat different diseases for those reasons. Currently NAT10 inhibition via its specific inhibitor remodelin is used as cancer suppression prostate cancer[276]. Remodelin is a small molecule compound, which is the only known potent inhibitor of NAT10, shown to have a reverse effect on cell proliferation, cell invasion and migration [183]. Remodelin interacts with the acetyl-CoA binding pocket of human NAT10 and has shown to have a reverse effect on cell proliferation and migration in epithelial-mesenchymal transition [188].

We found out that the remodelin pre-treated VSMCs on healthy stiffness PAHs generated a trending reduced maximal traction stress (not significant) (Figures 4.9 A and B), whilst significantly reduced total traction stress (Figures 4.9 A and C). This was also true on the aged/diseased stiffness PAHs.

When VSMCs were treated with remodelin, their migrational capacity showed no change in directionality (Figure 4.10 A and B), or speed (Figure 4.10 A and C) on healthy stiffness PAHs. However, that changed when matrix stiffness increased to aged/diseased stiffness PAHs, where the migration directionality didn't alter whilst the speed significantly increased (Figure 4.12 A and B), or speed (Figure 4.12 A and C).

HDAC6 inhibitors have been explored in cancer research for their ability to restore the expression of silenced genes and have highly effective treatment benefits along with immunotherapies, such as mAbs [277]. Four nonselective HDAC6 inhibitors have already been registered in monotherapies, romidepsin and SAHA for cutaneous T-Cell lymphoma, belinostat for relapsed or refractory peripheral T-cell lymphoma, and Panobinostat for multiple myeloma [278]. Other HDAC6 inhibitors such as ricolinostat are currently in clinical trials for Hodgkin lymphoma [277].

Inhibition of HDAC6 with tubastatin is reported to enhance the microtubule acetylation [279], suppress the dynamics of microtubules, and delayed the reassembly of depolymerized microtubules. The study also found that tubastatin enhanced the binding of HDAC6 to microtubules, and hence increase the microtubule stability in MCF-7 cells [280].

We treated VSMCs to with HDAC6 inhibitor to test the impact of altering acetylation of microtubules on VSMC's traction force generation and migrational capacity. Their result revealed that tubastatin has impact on VSMCs traction stress generation (Figure 4.13 A to C) and migration capacity (Figure 4.14 A to C) on healthy stiffness. However, this changed with the change in stiffness, that on aged/diseased PAHs, the traction stress generation significantly increased (Figure 4.15 A to C) and the migrational capacity (Figure 4.16 A to C).

Based on the data presented above, we conclude that microtubules play a key role in the functionality of VSMCs. Disrupting the microtubule stability alters the actomyosin activity and migrational capacity. We still must run more experiments to test aged/diseased matrix stiffness and microtubule targeting agents to have a complete picture of the relevance of microtubule dynamic stability in different conditions, i.e healthy and aged/diseased matrix stiffness and 3-D mimicking topology.

## 4.7 Limitation and future direction

### 4.7.1 VSMCs contractile and synthetic phenotypes

VSMCs exist in quiescent contractile phenotypes and show a significant plasticity [281]. However, VSMCs also undergo a phenotypic switch to synthetic- increased migratory and proliferation rate- due to a change in gene expression of contractile protein markers [282]. In our experiment, we promote quiescence by serum withdrawal and that is not enough to withdraw other plenty factors that VSMCs get subjected to that can alter their true contractile nature.

### 4.7.2 Microtubule targeting agents and dose sensitivity

Another key point worth addressing is the sensitivity of the microtubule agent concentration used - demecolcine. At different concentrations, demecolcine has different implications and due to time constrain, we didn't get to validate the effect of the demecolcine at higher concentrations.

### 4.7.3 Inadequate knowledge of the mechanism of microtubules on traction stress

Microtubule and actomyosin crosstalk are an exciting concept that has yet to be investigated substantially. Understanding the mechanisms of this interplay is likely to set a new direction of interest to illuminate microtubule engagement in vascular diseases and its potential for future therapeutic targets. In the future, we would investigate the proteins involved in facilitating the cross-talk of actin-microtubules on traction force generation, such as GEF-H1 and MACF1 proteins [283].

# Chapter 5: Novel regulators of VSMC function

## 5.1 Background

Understanding novel regulators of VSMC migration in vitro is key to extrapolating to in vivo situations and studying live cells' behaviours. In the previous chapters, we focused on addressing how matrix topology and microtubule stability influence VSMC traction force generation, migration, and proliferation. In this chapter, we will explore the influence of statins as other novel regulators of VSMCs and the influence of stretch activation channels in VSMC's function.

Though statins are drugs that are primarily used to reduce hyperlipidaemia, they have also been shown to have beneficial anti-inflammatory properties, act as antioxidants and stabilise atherosclerotic plaques [284,285]. Statins are reported to reduce VSMC migration and proliferation, and in doing so prevent the development of atherosclerosis [286,287]. In this experiment we will use the most commonly prescribed - simvastatin, mevastatin and atorvastatin- model statins. A study found that simvastatin and atorvastatin inhibit DNA synthesis reducing proliferation on VSMCs [288], which implies that statins may be able to regulate the phenotypic switch of VSMCs.

The primary focus of this chapter was to test the reported effects of statins whilst VSMCs were cultured on PAHs that mimicked either physiological or aged/diseased aortic stiffness. Additionally, we also investigated the effect of statins when VSMCs were cultured on PAHs of 2 kPA stiffness which is a representative model of diseased soft arterial wall. In this chapter, we compared three different statins, highly lipophilic simvastatin, and less lipophilic atorvastatin.

We also started to investigate the role of mechanosensitive ion channels in regulating VSMC migration. One of those families is the piezo (1 and 2) nonselective cation channels. Electron microscopy has reviled that piezo1 is expressed with in VSMCs  and endothelial cells in the blood vessel development and structural maintenance [289,290]. Blocking Piezo1 activity altered VSMC morphology and actomyosin force generation. Research has shown that treatment with GsMTx-4, a mechanosensitive ion channel blocker, abolishes the induction of cell currents within HEK293 cells, including those generated by Piezo1 [119]. Our lab has recently (pending publication) identified that Piezo1 expression is upregulated in VSMCs cultured on PAHs of aged/diseased stiffness. Hence, we investigated the effect of GsMTx-4 treatment on VSMCs migration under different mechanical conditions.

## 5.2 Hypothesis

We hypothesise that treating VSMCs with statins or the mechanosensitive ion channel blocker, GsMTx4, will reduce their migration speed. We also predict that the effect of these compounds will be greater when VSMCs are migrating on PAHs mimicking an aged/diseased stiffness.

## 5.3 Aims of the chapter

The objective of our experiments was:

1. To validate the impact of statins on VSMC migrational capacity on different stiffnesses and topologies of PAHs.

2. To determine the impact of GsMTx-4 on VSMC migrational capacity.

## 5.4 Results

### 5.4.1 Simvastatin reduced VSMC migration speed on PAHs of aged/diseased stiffness

In chapter 3, we demonstrated that matrix stiffness can alter VSMCs functionality. Building from those foundations, we examined if treatment with statins could alter VSMC migration on a range of physiological/pathophysiological matrix stiffnesses. VSMCs were seeded on 12 kPa and 72 kPa smooth PAHs and their migration was tracked over a 12-hour period, in the presence or absence of simvastatin. Analysis revealed that VSMCs on 72 kPa PAHs migrated faster than their counterparts on 12 kPa PAHs. Simvastatin treatment prevented the increased VSMC migration speed observed on 72 kPa PAHs but had no effect on VSMCs seeded on other stiffnesses. The directionality of VSMC migration was unaffected on all PAH stiffnesses (Figure 5.1).
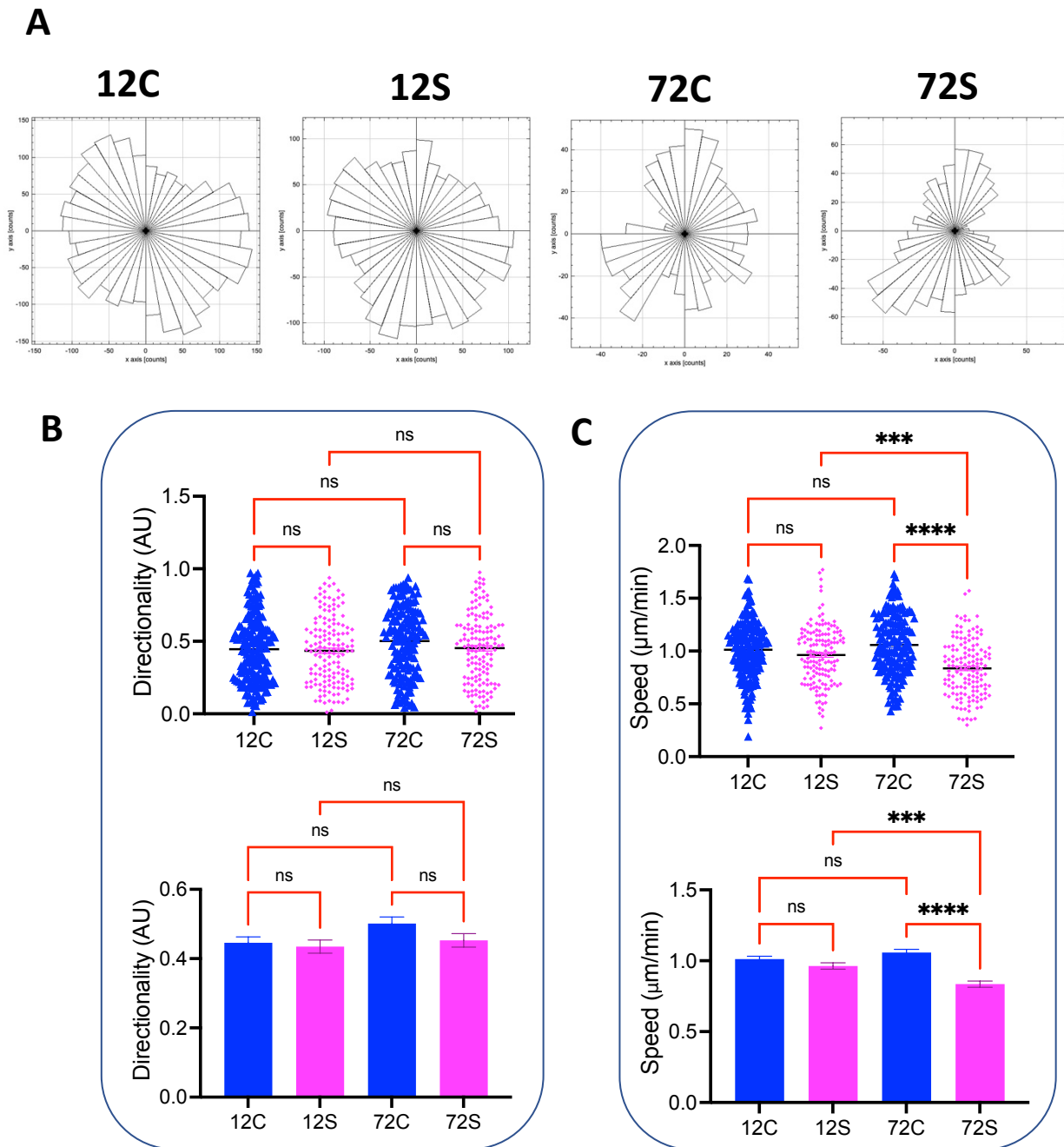
**Figure 5. 1: Simvastatin treatment reduces VSMC migration speed on 72 kPa PAHs**. VSMCs were seeded onto  12 kPa (12) or 72 kPa (72) smooth PAHs and cell migration was tracked using time-lapse microscopy over a 12 hour period. During this period cells were treated with simvastatin (S) or left untreated as a control (C). **A)** Representative rose plots of VSMC migration. Graphs show **B)** directionality and **C)** speed of VSMC migration. Data is representative of 5 independent experiments with the following number of VSMCs tracked per condition 12C (190), 12S(149), 72C(162) and 72S(145). (ns = non-significant, **** = p < 0.0001 ).

## 5.4.2 Mevastatin treatment promotes increased VSMC migration speed on PAHs of physiological stiffness.

The above data shows that simvastatin treatment prevented an increase in VSMC migration speed when cells were cultured on PAHs mimicking aged/diseased aortic stiffness. We next compared whether a structurally similar statin, mevastatin, predicting that it would have similar effects on VSMC migrational capacity as simvastatin. To test this, VSMCs were seeded onto smooth 12 kPa and 72 kPa PAHs and their migration was tracked over 12 hours, in the presence or absence of mevastatin. Analysis revealed that mevastatin treatment increased both the directionality and speed of VSMC migration on healthy stiffness (12 kPa PAHs). However, on the aged/diseased stiffness PAHs (72 kPa), mevastatin treatment reduced the directionality of VSMC migration without significant effect on the speed of their migration (Figure 5.2).
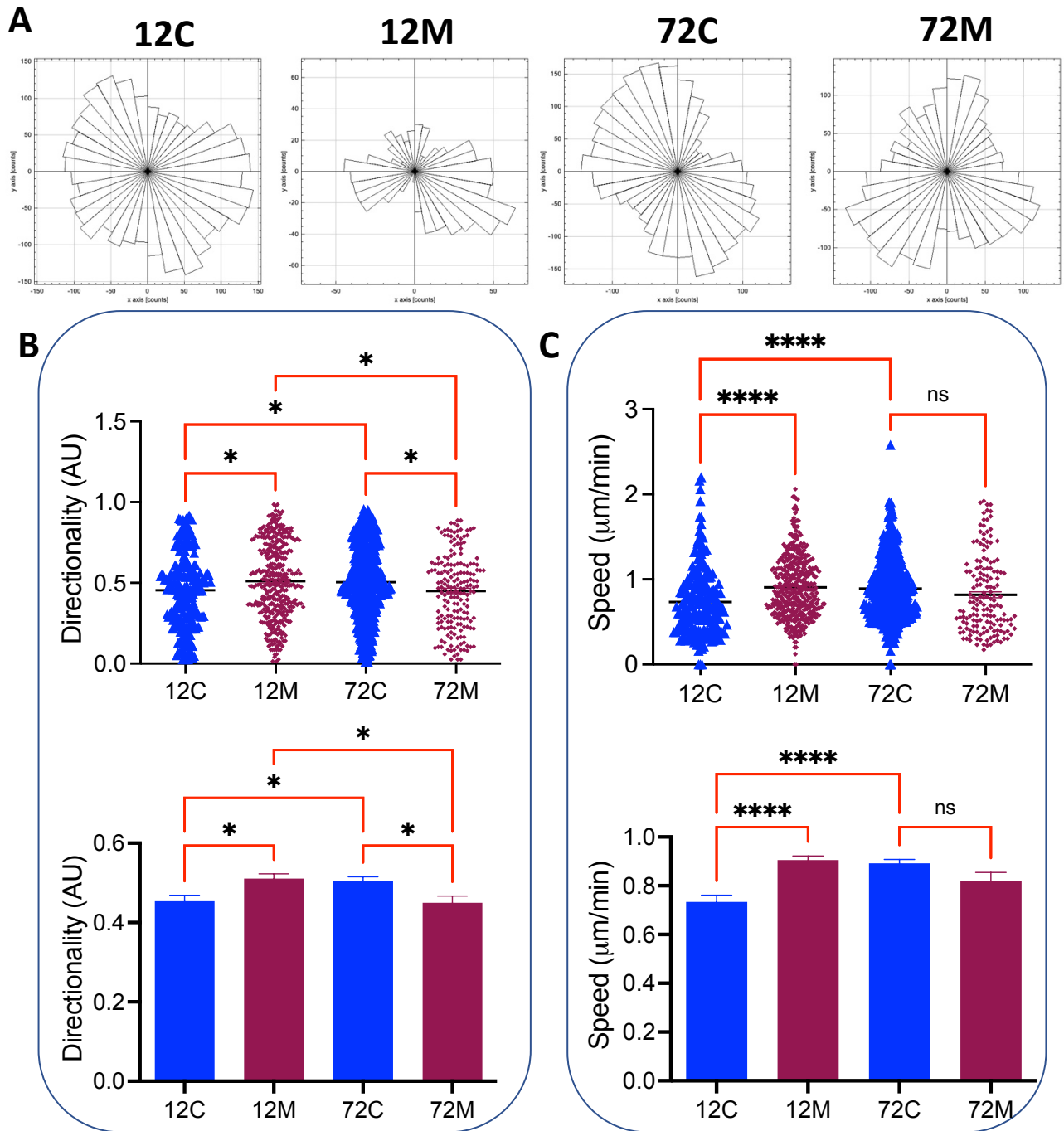
**Figure 5. 2: Mevastatin treatment promotes increased VSMC migration speed on 12 kPa PAHs.** VSMCs were seeded onto 12 kPa (12) or 72 kPa (72) smooth PAHs and cell migration was tracked using time-lapse microscopy over a 12 hour period. During this period cells were treated with mevastatin (M) or left untreated as a control (C). **A)** Representative rose plots of VSMC migration. Graphs show **B)** directionality and **C**) speed of VSMC migration. Data is representative of 3 independent experiments with the following number of VSMCs tracked per condition 12C(227), 12M(408), 72C(449) and 72M(189). (ns = non-significant, * = p < 0.05, *** = p < 0.001 , **** = p < 0.0001).

### 5.4.3 Atorvastatin treatment promotes increased VSMC migration speed on PAHs of physiological stiffness.

Next, we investigated whether the less lipophilic atorvastatin would also impact VSMC migration. To test this, VSMCs were seeded onto 12 kPa and 72 kPa PAHs and their migration was tracked over a 12-hour period, in the presence or absence of atorvastatin. Analysis revealed that atorvastatin increased both the directionality and speed of VSMC migration on PAHs of healthy stiffness (12 kPa). However, whilst atorvastatin increased the directionality of VSMC migration on PAHs of aged/diseased stiffness (72 kPa), it had no effect on the speed of their migration (Figure 5.3).
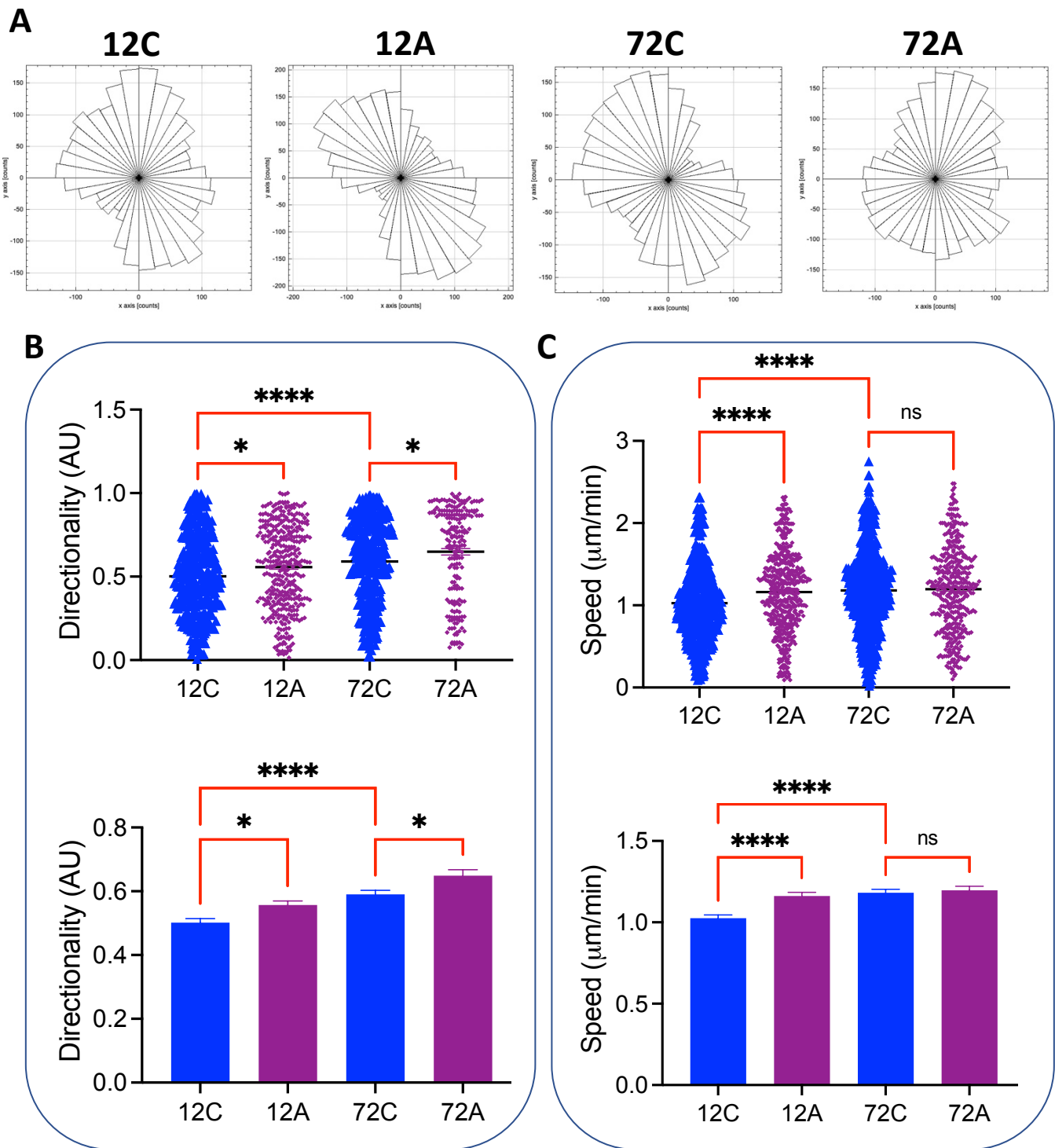
**Figure 5. 3**: **Atorvastatin treatment promotes increased VSMC migration speed on 12 kPa PAHs.** VSMCs were seeded onto 12 kPa (12) or 72 kPa (72) smooth PAHs and cell migration was tracked using time-lapse microscopy over a 12 hour period. During this period cells were treated with atorvastatin (A) or left untreated as a control (C). **A)** Representative rose plots of VSMC migration. Graphs show **B)** directionality and **C)** speed of VSMC migration. Data is representative of 4 independent experiments (n = 371 12C control, n = 393 12A, n= 380 72C and n= 212 72A treated) VSMCs tracked. (n.s. = non-significant, * = $p < 0.05$, **** = $p < 0.001$ )

### 5.4.4 Simvastatin reduces the migration speed of VSMCs on grooved PAHs of healthy stiffness.

Having assessed the impact of statins on VSMC migration when seeded on smooth PAH, we next investigated whether matrix topology may alter the observed effect statins have in regulating VSMC migration. To test this, VSMCs were seeded onto smooth and grooved 12 kPa PAHs and their migration was tracked over 12 hours, in the presence or absence of simvastatin. In agreement with our previous findings in Chapter 3, VSMC migration speed was reduced on grooved PAHs compared to their smooth counterparts (Figure 5.4). Additionally, simvastatin treatment did not alter the directionality or speed of VSMC migration on smooth PAHs of healthy stiffness, as observed earlier in this chapter (Figures 5.1 and 5.4). However, when seeded on grooved PAHs of aged/diseased stiffness, simvastatin treatment reduced the speed of VSMC migration but continued to have no effect on the directionality of their migration (Figure 5.4). Our experiments in this chapter were performed with the most commonly used statins that are lipophilic given the literature view featuring the effectiveness of different statins, though it lacks solid evidence [291].
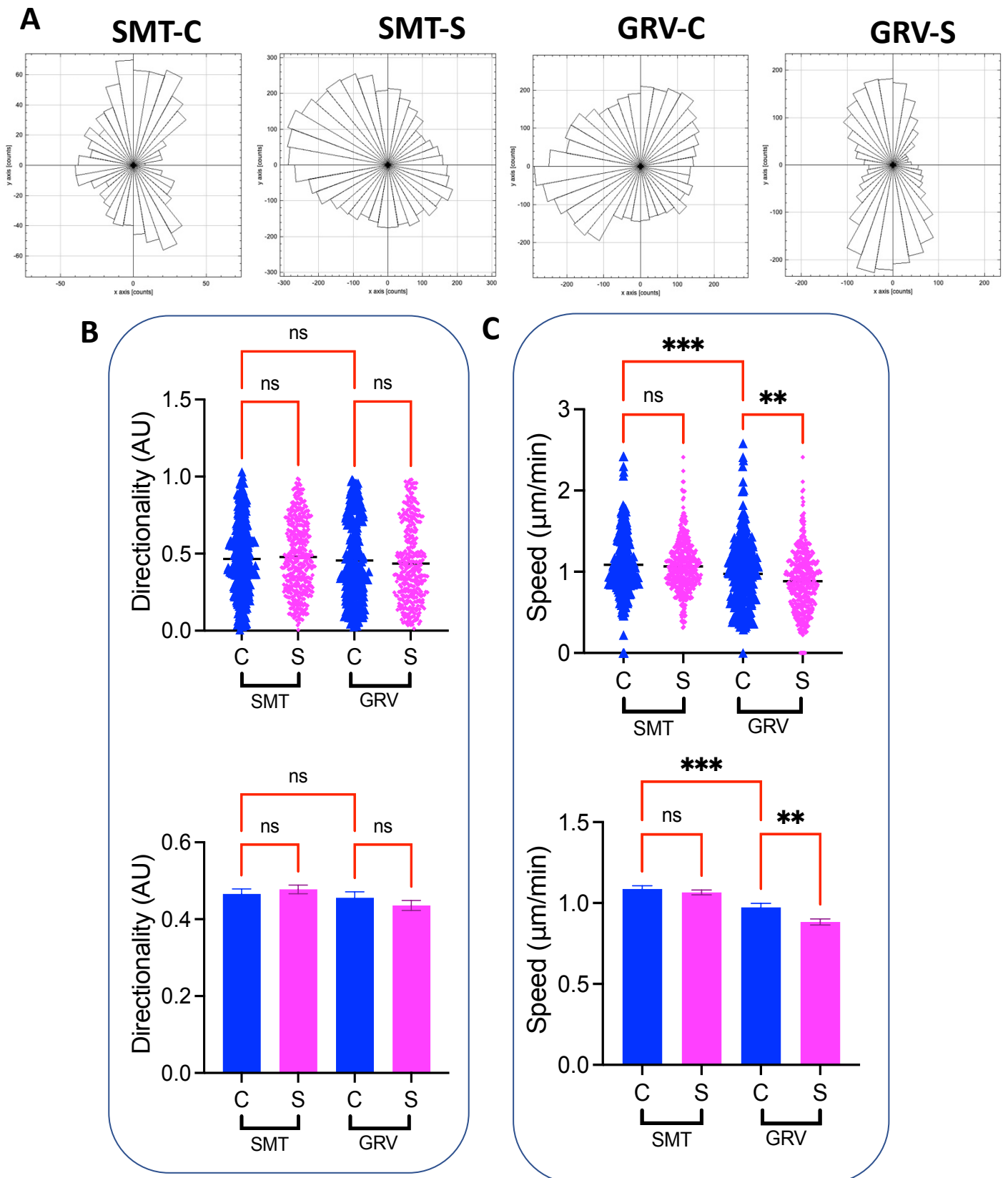
**Figure 5. 4: Simvastatin reduces the speed of VSMC migration on grooved PAHs of physiological stiffness.** VSMCs were seeded onto Smooth (SMT) or Grooved (GRV) PAHs of 12 kPa stiffness and cell migration was tracked using time-lapse microscopy over a 12 hour period. During this period cells were treated with simvastatin (S) or left untreated as a control (C). **A)** Representative rose plots of VSMC migration. Graphs show **B)** directionality and **C)** speed of VSMC migration. Data is representative of 5 independent experiments with the following number of cells tracked per condition SMT-C(315), SMT-S(437), GRV-C(282) and GRV-S(394). (n = 315 12 kPa smooth control, n = 437 12 kPa smooth simvastatin treated, n = 282 12 kPa grooved control and n= 394 12 kPa simvastatin treated grooved VSMCs tracked. (ns = non-significant, * = $p < 0.05$, ** = $p < 0.01$, **** = $p < 0.0001$).

## 5.4.5 Ion channel blockade, via GsMTx-4 treatment had no impact on VSMC migration

VSMCs migration is influenced by mechanical forces, and we explore the involvement of SAC on regulating VSMCs migrational capacity. To do that, we investigated the effect that blocking mechanosensitive ion channels, using the inhibitor GsMTx-4, had on VSMC migration on PAHs of physiological and aged/diseased stiffness. VSMCs were therefore seeded onto smooth PAHs of 12 kPa and 72 kPa stiffness and tracked over a 12-hour period, in the presence or absence of GsMTx4. Our results show that GsMTx-4 treatment had no impact on the migration speed of VSMCs on either stiffness, however, GsMTx-4 treatment did increase the directionality of VSMC migration on PAHs of aged/diseases stiffness (Figure 5.5).
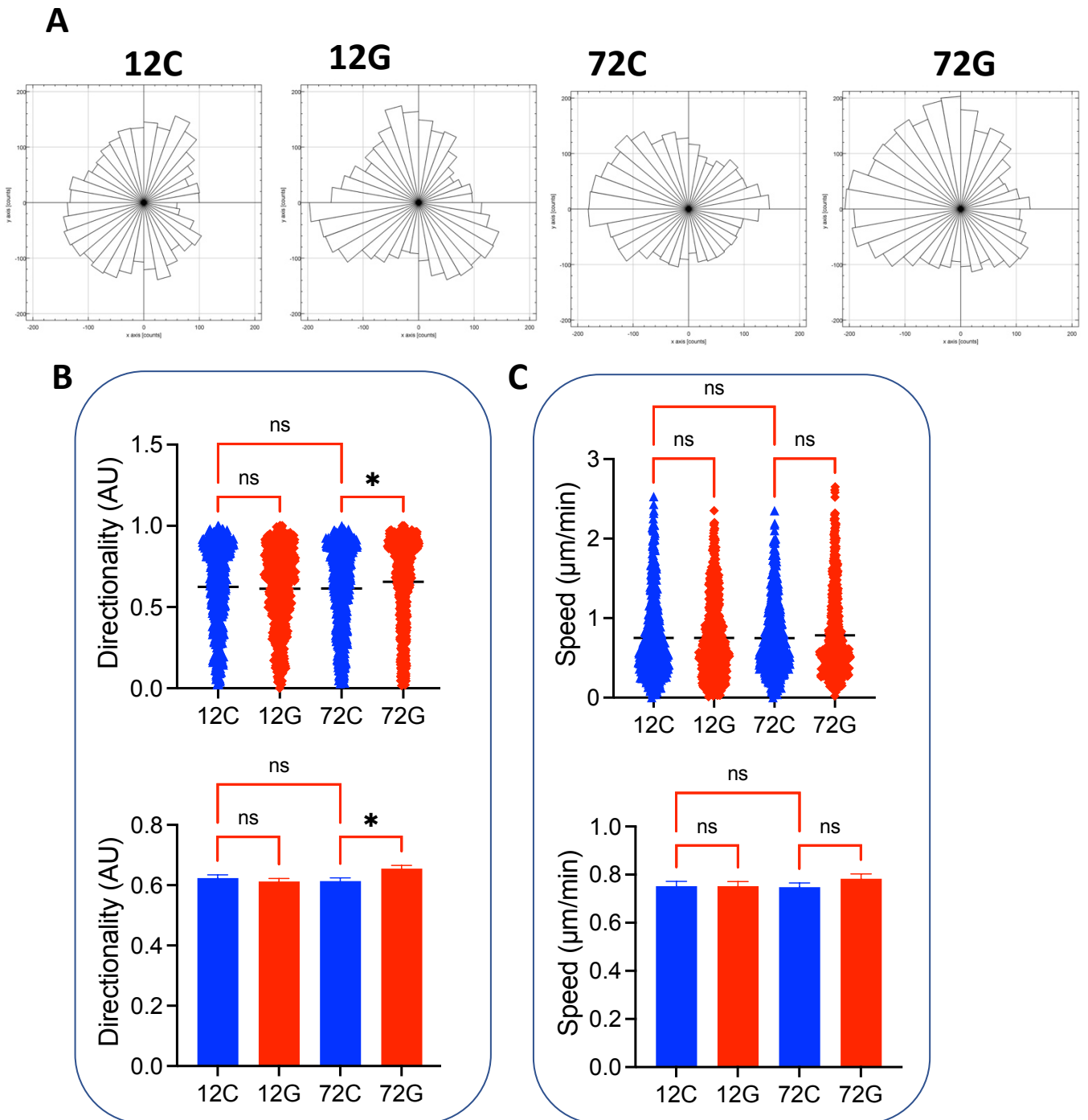
**Figure 5. 5 Ion channel blockade, via GsMTx-4 treatment, had no impact on VSMC migration.** VSMCs were seeded onto 12 kPa or 72 kPa smooth PAHs and cell migration was tracked using time-lapse microscopy over 12 hours. During this period cells were treated with GsMTx-4 (G) or left untreated as a control (C). **A)** Representative rose plots of VSMC migration. Graphs show **B)** directionality and **C**) speed of VSMC migration. Data is representative of 4 independent experiments with the following number of cells tracked per condition 12C(629), 12G(654), 72C(630) and 72G(676). (ns = non-significant, ** = p < 0.01).

**Table 5.1: Summary of the effects of statins and mechanosensitive ion channel blockers on VSMC migration**

| Treatment | Stiffness | Topology | Directionality | Speed |
|---|---|---|---|---|
| Atorvastatin 0.5 µM | 12 kPa | Smooth | increase | increase |
| | 72 kPa | Smooth | no change | no change |
| GsMTx-4  0.5 µM | 12 kPa | smooth | no change | no change |
| | 72 kPa | smooth | increase | no change |
| Mevastatin 1 µM | 12 kPa | Smooth | increase | decrease |
| | 72 kPa | Smooth | decrease | no change |
| Simvastatin 1 µM | 12 kPa | Smooth | no change | no change |
| Simvastatin 1 µM | 12 kPa | Grooved | no change | decrease |
| | 72 kPa | Smooth | no change | decrease |

## 5.5 Discussion and conclusion

In this chapter, we sought to elucidate the impact of statins on VSMC migration. Statins are beneficial to cardiovascular health and are used to prevent coronary heart disease [285,292] through their competitive inhibition of HMG-CoA) reductase . Besides their primary clinical function in lowering the build-up of circulating cholesterol [287], their pleiotropic impact on VSMCs has been reported to reduce both their proliferation and migration [287]. The primary focus of this chapter was to validate the reported effects of statins on VSMC migration when cells are cultured on our PAHs whose stiffness can mimic the physiological and aged/disease stiffness of the aorta.

Our results demonstrate that all three of the statins tested affect VSMC migration, albeit the effect they have differs depending on the statin used, as summarised in Table 5.1. Simvastatin lowers the migrational capacity of VSMCs specifically on aged/disease mimicking PAHs, with no effect on cells seeded on our PAHs of physiological stiffness. However, if we additionally alter the topology of our PAH as discussed in Chapter 3, we observed that simvastatin also lowers the migrational capacity of VSMCs on grooved PAHs of physiological stiffness. This is in alignment with previous findings that show a group of statin treatments (atorvastatin, Fluvastatin and rosuvastatin) prevented fibrous cap formation in the late stage of atherosclerosis [287].

Potentially, the effect of simvastatin on VSMC migrational capacity is via the inhibition of posttranslational modification of Ras or Rho prenylation [284,294]. Rho activity is known to increase in response to enhanced matrix stiffness. This may explain why simvastatin selectively impaired VSMC migrational capacity of PAHs of aged/disease stiffness. Furthermore, simvastatin reduced the migration capacity of VSMCs on grooved healthy PAHs, which supports our findings from the earlier experiments. This is potentially a consequence of VSMCs generating enhanced actomyosin-generated traction stresses on the grooved PAHs. This potentially stimulates enhanced RhoA activation.

Conversely, atorvastatin treated VSMCs migrated faster on PAHs of healthy stiffness, with atorvastatin not affecting those seeded on aged/diseased mimicking PAHs. A similar observation was reported with Fluvastatin, where at the early onset of atherosclerosis, statins act as pro-atherogenic by upregulating the ECM protein and fibrous caps production [287]. Hence, we speculate that this observation of atorvastatin and mevastatin on VSMCs on the healthy stiffness effect might be acting as a pro-atherogenic agent.

Finally, we also explored the effect of inhibiting mechanosensitive ion channels on

VSMC migrational capacity by using the GsMTx-4 inhibitor. Our lab has previously elucidated that the concentration of GsMTx-4 used within this study is sufficient to alter VSMC morphology and actomyosin force generation (publication pending). Whilst they have previously shown that GsMTx-4 can have a beneficial effect in preventing VSMCs from undergoing a phenotypic switch when seeded on stiffer matrixes, in this present study we find that GsMTx-4 had no impact on VSMC migrational capacity.

# Chapter 6: General discussion and conclusions

## 6.1 Arterial compliance and our PAHs models

Inside the body, under normal physiological conditions, the arterial wall is highly elastic, and that dynamicity allows it to adopt flexible constriction and dilation of the blood vessels. Those vasoconstriction/dilation involve the contractile function of VSMCs in the medial layer of the arterial wall.

The medial layer of the aortic wall, home to VSMCs, contains elastic and non-elastic ECM components [295], that cells interact differently to the change in ECM composition-leading to different stiffness- and topology [35], which resulted in the alteration of the cell morphology by reorganising the cytoskeleton and internal organelles. This two-way interplay influences VSMC's traction stress generation and migrational capacity [229,296]. In a healthy artery and physiological condition, VSMCs exist as quiescent contractile phenotypes, with spindle morphology, which are key features required for their vessel tone regulation. The spindle morphology was achieved by seeding VSMCs on grooved PAHs.

## 6.2 VSMCs morphology and traction stress generation in different ECM stiffness and topology

Our observation of the result is that VSMCs on the smooth PAHs adopt a rounded or fried egg-like structure, whilst VSMCs seeded on grooved PAHs showed reduced cell area, spindle-shaped and aligned along the micropatterns. This variation in morphology is dictated by the contact guidance that VSMCs sense on the grooved PAHs in comparison to the classical two-dimensional PAHs environment [229,297,298]. Hence, VSMCs spread better on smooth PAHs as opposed to those seeded on grooved PAHs. Our results also showed that cell on grooved PAHs deformed their surrounding matrix significantly higher than those on smooth PAHs, generating high traction stress, suggestive of their function in performing vessel tone.

We also investigated the VSMCs' actomyosin activity by treating cells with contractile agonists- Ang II. Cells were grown in basal media and treated with Ang II serial dilution ranging from **0.01** $\mu$M to **100** $\mu$M. The results revealed that VSMC seed on 12 kPa of smooth and grooved PAHs reduced in the cell area. This is an indication that the VSMCs undergo contraction and subsequently reduction in the cell area, increased traction stress leading to vasoconstriction.

Our lab has previously conducted a first-of-its-kind investigation on how a change in stiffness increased the number and size of adhesion recruitments [299]. We have seen that

VSMCs seeded on 72 kPa both smooth and groove PAHs showed an increase in VSMCs volume on the VSMCs seeded on grooved over compared to those on the smooth PAHs. That finding is being further investigated within our lab. To further understand the result of the morphological change acquired from topological alteration, we carried out the contractile stimulation of quiescent VSMCs seeded on 72 kPa smooth and groove PAHs. The setting and treatment were the same as the 12 kPa, described above. The result showed that there was a decreased cell spreading in VSMCs seeded on both smooth and groove PAHs.

Comparing the change in the cell area of VSMCs seed on the 12 kPa vs 72 kPa Smooth and 12 kPa vs 72 kPa showed that the change in morphology has a reverse relationship to the ECM stiffness on the 12 kPa PAHs. However, on the 72 kPa, VSMCs spread with increased matrix stiffness. Hence, the change in cell area is significantly influenced by both the matrix stiffness and topology.

We also speculate the changes on the 12 kPa PAHs are due to the VSMCs on grooved PAHs having concentrated and matured focal adhesions generating a sheer pulling force, that is strong enough to deform the PAHs pulling inwards [300]. The adhesion points concentration and maturation are likely to be very low with VSMCs on smooth PAHs due to the continuous effort of the cell protrusion in many directions[300].

VSMCs phenotype switch from contractile to migratory and proliferative during tissue repair after injury [35,209]. Hence, migration and proliferation are characteristics of synthetic phenotypes in VSMCs. Hence, we investigated the migrational and proliferative features of VSMCs.

## 6.3 Change in Matrix topology alters VSMCs migration

For migration to happen, cells must reorganize their shape in a dynamic and orchestrated manner [301]. This change in cell shape and its spreading regulates the distribution of the focal adhesion between the leading edge and trailing edge of a migrating cell and is governed by the biochemical switches of molecules called Rho-family GTPases . The principal regulators of those biochemical switches include Rho guanine nucleotide exchange factors (RhoGEFs) and Rho GTPase activating proteins (RhoGAPs) [303].

Other studies suggested that the cell shape is also dependent on the manner of the actin polymerization [297]. Spindle-shaped cells show a biophysically stretched elongation state and F-acting polymerization arranged on the leading edge of the cell [301,304,305].

Following our studies on ECM stiffness and VSMCs response [35], we investigated the

VSMCs migration response change to their ECM topology. In line with the previous observations, the VSMCs on smooth PAHs showed procuration in multiple directions whilst the VSMCs on the grooved PAHs aligned in the micropatterns, with spindle-shaped morphology, leading to increased directionality. Investigating the speed at which the VSMCs moved, those on the 12 kPa smooth PAHs moved at a significantly faster speed than the VSMCs on the grooved PAHs.

Our data shows that the comparison of the speed VSMCs migration between those on the smooth and grooved 72 kPa PAHs showed reversed characteristics from what we have seen on the 12 kPa PAHs. VSMCs on smooth PAHs migrate significantly faster than their counterpart on grooved PAHs.

Results from our proliferation assay also showed that VSMCs on the smooth 12 kPa PAHs have a higher proliferation rate compared to those on the grooved PAHs. This observation suggests groove PAHs have helped VSMCs to retain quiescent phenotype.

## 6.4 Novel regulators of VSMCs function

Distributing microtubules' dynamic instability of VSMCs can trigger different pathways and subsequently alter the characteristics of VSMCs in different settings. Our work interrogated the influence of microtubule targeting agents (MTA) on VSMCs traction stress generation and migration. We observed the magnitude of traction stress generated and the migrational capacity of VSMCs treated with colchicine and paclitaxel significantly reduced. A previous study in our lab investigated the morphological changes with those MTAs [146], there was an uncoupling of morphology and traction stress generated, suggesting that their influence didn't involve actomyosin pathways [146]. Demecolcine needs further characterization and finding the optimal working concentration. Colchicine and paclitaxel are both important drugs currently used in cancer treatment at a substantially higher dose. Our results suggested that both colchicine and paclitaxel could have potential therapeutic benefits in preventing major adverse cardiovascular events.

Statins are also used to investigate their influence on the regulation of the RhoA pathway on VSMC migration. Our result shows that statins work differently, a such atorvastatin didn't work at all, and simvastatin best inhibits migration on VSMC but only on the aged/diseased PAHs. Statins are currently prescribed to lower cholesterol in the body whereas the most used ones are atorvastatin and simvastatin. Statins also have additional use and functions of statins, that needs further investigation. Our data show that simvastatin reduces

the migrational capacity of VSMCs in aged/diseased stiffness, which suggests that simvastatin can be as useful as a tool to prevent further advancement of CVD.

## 6.5 General conclusion

The previous technologies to control morphology required expensive specialised training equipment. And most of the previous tissue cultures were performed on glass or plastic which is 1000s-fold in stiffness. Lots of work has been done with VSMCs proliferation but not so much with VSMCs migration. Not enough was known about VSMC function because of the limitations of plastic and glass and the lack of control of morphology.

Our lab developed a technique that allowed us to tailor the appropriate stiffness in healthy (12 kPa) and aged/diseased (72 kPa) arterial walls by using PAHs. We also used a 3D printed micropattern to develop grooved PAHs, where the micro pattern on the grooved PAHs mimics the in vivo features of the tunica media of the aortic walls.

We have now validated new approaches that we can explore the impact of matrix stiffness and topology on VSMC's morphology and function. We have got consistent results that VCMCs adopt the morphology and functions which are more similar to in vivo context. We also have shown that novel regulators of VSMC behave differently in different stiffness in terms of migration. More work needs to be done to understand how the novel regulators work in different stiffness and topology.

## 6.6  Future work

So far, we have shown that changes from mechanical cue- topology and stiffness- enhance VSMC contractility and promote VSMC phenotype switch indicative of disease- associated changes.  Comprehensive work is required to advance the 3D model of our tissue culture to mimic in vivo features of the cardiovascular system and other cell types within the structure more accurately. Further research is also required to extend our knowledge of the crosstalk of the cytoskeletal components in different conditions.

The results discussed in this thesis are a great starting point to understand and utilise microtubule targeting agents beyond their current clinical use. Current models for pre-clinical screens are low throughput, time consuming, qualitative, or inconsistent. Our model circumvents many of these issues by providing a more disease-relevant model for pre-clinical screening of microtubule-targeting drugs. This will be of clinical benefit, as this model allows much higher throughput screening which will facilitate the identification of therapeutically relevant microtubule-targeting drugs.

Concurrent with the use of anti-cancer use of microtubule targeting agents, understanding their mode of action and the appropriate concentration, there is great potential that they could be clinically used for their anti-angiogenic effect, where such effects were observed when added to endothelial cells [306].

# 7 References

1. Leloup AJA, Van Hove CE, Heykers A, Schrijvers DM, De Meyer GRY, Fransen P. Elastic and Muscular Arteries Differ in Structure, Basal NO Production and Voltage-Gated Ca2+-Channels. *Front Physiol* [Internet]. 2015

2. Augoustides JG, Cheung AT. Aneurysms and Dissections [Internet]. In: Perioperative Transesophageal Echocardiography. Elsevier; 2014 [cited 2022 Aug 16]. p. 191–217.

3. Maleszewski JJ, Veinot JP. Anatomic considerations and examina- tion of cardiovascular specimens (ex- cluding devices). :9.

4. Wang R, Yu X, Zhang Y. Mechanical and structural contributions of elastin and collagen fibers to interlamellar bonding in the arterial wall. *Biomech Model Mechanobiol*. 2021;20:93–106.

5. Pagano P, Gutterman D. The adventitia: The outs and ins of vascular disease. *Cardiovascular Research*. 2007;75:636–639.

6. Miko M, Varga I. Histologic Examination of Peripheral Nerves [Internet]. In: Nerves and Nerve Injuries. Elsevier; 2015 [cited 2022 Aug 31]. p. 79–89.

7. Ahmed S, Warren DT. Vascular smooth muscle cell contractile function and mechanotransduction. *VP*. 2018;2:36.

8. Pagidipati NJ, Gaziano TA. Estimating Deaths From Cardiovascular Disease: A Review of Global Methodologies of Mortality Measurement. *Circulation*. 2013;127:749–756.

9. Palombo C, Kozakova M. Arterial stiffness, atherosclerosis and cardiovascular risk: Pathophysiologic mechanisms and emerging clinical indications. *Vascular Pharmacology*. 2016;77:1–7.

10. Mendis S, Yach D, Bengoa R, Narvaez D, Zhang X. Research gap in cardiovascular disease in developing countries. *The Lancet*. 2003;361:2246–2247.

11. Costantino S, Paneni F, Cosentino F. Ageing, metabolism and cardiovascular disease: Mechanisms of cardiovascular ageing. *J Physiol*. 2016;594:2061–2073.

12. Roth GA, Forouzanfar MH, Moran AE, Barber R, Nguyen G, Feigin VL, Naghavi M, Mensah GA, Murray CJL. Demographic and Epidemiologic Drivers of Global Cardiovascular Mortality. *N Engl J Med*. 2015;372:1333–1341.

13. Gupta S, Gudapati R, Gaurav K, Bhise M. Emerging risk factors for cardiovascular diseases: Indian context. *Indian J Endocr Metab*. 2013;17:806.

14. Angoff R, Mosarla RC, Tsao CW. Aortic Stiffness: Epidemiology, Risk Factors, and Relevant Biomarkers. *Front Cardiovasc Med*. 2021;8:709396.

15. Zawieja DC, Gashev AA. 5.3.4.2.1 Influence of Pressure/Stretch. 2008:9.

16. Yanagisawa H, Wagenseil J. Elastic fibers and biomechanics of the aorta: Insights from mouse studies. *Matrix Biology*. 2020;85–86:160–172.

17. Grotenhuis HB, de Roos A. Structure and function of the aorta in inherited and congenital heart disease and the role of MRI. *Heart*. 2011;97:66–74.

18. Lacolley P, Regnault V, Avolio AP. Smooth muscle cell and arterial aging: basic and clinical aspects. *Cardiovascular Research*. 2018;114:513–528.

19. Jani B. Ageing and vascular ageing. *Postgraduate Medical Journal*. 2006;82:357–362.

20. McVeigh GE, Bratteli CW, Morgan DJ, Alinder CM, Glasser SP, Finkelstein SM, Cohn JN. Age-Related Abnormalities in Arterial Compliance Identified by Pressure Pulse Contour Analysis: Aging and Arterial Compliance. *Hypertension*. 1999;33:1392–1398.

21. Kopel L, Tarasoutchi F, Medeiros C, Carvalho RT, Grinberg M, Lage SG. Arterial distensibility as a possible compensatory mechanism in chronic aortic regurgitation. *Arq Bras Cardiol*. 2001;77.

22. Gardner AW, Parker DE. Association Between Arterial Compliance and Age in Participants 9 to 77 Years Old. *Angiology*. 2010;61:37–41.

23. Levy D. Echocardiographically Detected Left Ventricular Hypertrophy: Prevalence and Risk Factors: The Framingham Heart Study. *Ann Intern Med*. 1988;108:7.

24. Strait JB, Lakatta EG. Aging-Associated Cardiovascular Changes and Their Relationship to Heart Failure. *Heart Failure Clinics*. 2012;8:143–164.

25. Eichhorn J, Krissak R, Rüdiger H-J, Ley S, Arnold R, Boese J, Krug R, Gorenflo M, Khalil M, Ulmer H, Kauczor H-U, Fink C. Compliance der morphologisch unauffälligen Aorta bei Jugendlichen mit Marfan Syndrom: Vergleich von MR-Messungen der aortalen Dehnbarkeit und der Pulswellengeschwindigkeit. *Fortschr Röntgenstr*. 2007;179:841–846.

26. Westenberg JJ, van Poelgeest EP, Steendijk P, Grotenhuis HB, Jukema J, de Roos A. Bramwell-Hill modeling for local aortic pulse wave velocity estimation: a validation study with velocity-encoded cardiovascular magnetic resonance and invasive pressure assessment. *J Cardiovasc Magn Reson*. 2012;14:2.

27. Zarrinkoob L, Ambarki K, Wåhlin A, Birgander R, Carlberg B, Eklund A, Malm J. Aging alters the dampening of pulsatile blood flow in cerebral arteries. *J Cereb Blood Flow Metab*. 2016;36:1519–1527.

28. Cecelja M, Chowienczyk P. Role of arterial stiffness in cardiovascular disease. *JRSM Cardiovascular Disease*. 2012;1:1–10.

29. Glasser SP, Arnett DK, McVeigh GE, Finkelstein SM, Bank AJ, Morgan DJ, Cohn JN. Vascular Compliance and Cardiovascular Disease. 10:15.

30. Vaccarino V, Berger AK, Abramson J, Black HR, Setaro JF, Davey JA, Krumholz HM. Pulse pressure and risk of cardiovascular events in the systolic hypertension in the elderly program. *The American Journal of Cardiology*. 2001;88:980–986.

31. Townsend RR. Arterial Stiffness: Recommendations and Standardization. *Pulse*. 2016;4:3–7.

32. Shirwany NA, Zou M. Arterial stiffness: a brief review. *Acta Pharmacol Sin*. 2010;31:1267–1276.

33. Theocharis AD, Skandalis SS, Gialeli C, Karamanos NK. Extracellular matrix structure. *Advanced Drug Delivery Reviews*. 2016;97:4–27.

34. Hai C-M, editor. Vascular smooth muscle: structure and function in health and disease. New Jersey: World Scientific; 2017.

35. Afewerki T, Ahmed S, Warren D. Emerging regulators of vascular smooth muscle cell migration. *J Muscle Res Cell Motil*. 2019;40:185–196.

36. Brozovich FV, Nicholson CJ, Degen CV, Gao YZ, Aggarwal M, Morgan KG. Mechanisms of Vascular Smooth Muscle Contraction and the Basis for Pharmacologic Treatment of Smooth Muscle Disorders. *Pharmacol Rev*. 2016;68:476–532.

37. Mayet J. Cardiac and vascular pathophysiology in hypertension. *Heart*. 2003;89:1104–1109.

38. Timraz SBH, Rezgui R, Boularaoui SM, Teo JCM. Stiffness of Extracellular Matrix Components Modulates the Phenotype of Human Smooth Muscle Cells in Vitro and Allows for the Control of Properties of Engineered Tissues. *Procedia Engineering*. 2015;110:29–36.

39. Gemma L. Basatemur, Helle F. Jorgensen, Murray C. H. Clarke, Martin R. Bennet. VSMCs in the pathogenesis of atherosclerosis. Nature. 2019; 16, 727-744.

40. Zhang F, Guo X, Xia Y, Mao L. An update on the phenotypic switching of vascular smooth muscle cells in the pathogenesis of atherosclerosis. *Cell Mol Life Sci*. 2022;79:6.

41. Shanahan CM, Weissberg PL. Smooth Muscle Cell Heterogeneity :6.

42. Davis-Dusenbery BN, Wu C, Hata A. Micromanaging Vascular Smooth Muscle Cell Differentiation and Phenotypic Modulation. *ATVB*. 2011;31:2370–2377.

43. Chappell J, Harman JL, Narasimhan VM, Yu H, Foote K, Simons BD, Bennett MR, Jørgensen HF. Extensive Proliferation of a Subset of Differentiated, yet Plastic, Medial Vascular Smooth Muscle Cells Contributes to Neointimal Formation in Mouse Injury and Atherosclerosis Models. *Circ Res*. 2016;119:1313–1323.

44. Sprague AH, Khalil RA. Inflammatory cytokines in vascular dysfunction and vascular disease. *Biochemical Pharmacology*. 2009;78:539–552.

45. Mogi M. Could Management of Blood Pressure Prevent Dementia in the elderly? *Clin Hypertens*. 2019;25:27.

46. Brown IAM, Diederich L, Good ME, DeLalio LJ, Murphy SA, Cortese-Krott MM, Hall JL, Le TH, Isakson BE. Vascular Smooth Muscle Remodeling in Conductive and Resistance Arteries in Hypertension: VSMC in hypertension. 2019;36.

47. Savoia C, Sada L, Zezza L, Pucci L, Lauri FM, Befani A, Alonzo A, Volpe M. Vascular Inflammation and Endothelial Dysfunction in Experimental Hypertension. *International Journal of Hypertension*. 2011;2011:1–8.

48. Yamin R, Morgan KG. Deciphering actin cytoskeletal function in the contractile vascular smooth muscle cell: Actin cytoskeleton and smooth muscle function. *The Journal of Physiology*. 2012;590:4145–4154.

49. Iyemere VP, Proudfoot D, Weissberg PL, Shanahan CM. Vascular smooth muscle cell phenotypic plasticity and the regulation of vascular calcification. *J Intern Med*. 2006;260:192–210.

50. Safar M, Frohlich ED, editors. Atherosclerosis, large arteries and cardiovascular risk. Basel ; New York: Karger; 2007.

51. Johnson RT, Solanki R, Warren DT. Mechanical programming of arterial smooth muscle cells in health and ageing. *Biophys Rev*. 2021;13:757–768.

52. Heidari M, Mandato CA, Lehoux S. Vascular smooth muscle cell phenotypic modulation and the extracellular matrix. *ARTRES*. 2015;9:14.

53. Freedman BR, Bade ND, Riggin CN, Zhang S, Haines PG, Ong KL, Janmey PA. The (dys)functional extracellular matrix. *Biochimica et Biophysica Acta (BBA) - Molecular Cell Research*. 2015;1853:3153–3164.

54. Wagenseil JE, Mecham RP. Vascular Extracellular Matrix and Arterial Mechanics. *Physiological Reviews*. 2009;89:957–989.

55. Ahmed S, Mabeza P, Warren DT. A model for estimating traction force magnitude reveals differential regulation of actomyosin activity and matrix adhesion number in response to smooth muscle cell spreading. Cell Biology; 2019

56. Lacolley P, Regnault V, Segers P, Laurent S. Vascular Smooth Muscle Cells and Arterial Stiffening: Relevance in Development, Aging, and Disease. *Physiological Reviews*. 2017;97:1555–1617.

57. Minaisah R-M, Cox S, Warren DT. The Use of Polyacrylamide Hydrogels to Study the Effects of Matrix Stiffness on Nuclear Envelope Properties [Internet]. In: Shackleton S, Collas P, Schirmer EC, editors. The Nuclear Envelope. New York, NY: Springer New York; 2016. p. 233–239.

58. Kai F, Laklai H, Weaver VM. Force Matters: Biomechanical Regulation of Cell Invasion and Migration in Disease. *Trends in Cell Biology*. 2016;26:486–497.

59. Walker M, Rizzuto P, Godin M, Pelling AE. Structural and mechanical remodeling of the cytoskeleton maintains tensional homeostasis in 3D microtissues under acute dynamic stretch. *Sci Rep*. 2020;10:7696.

60. Eisenbarth E, Linez P, Biehl V, Velten D, Breme J, Hildebrand HF. Cell orientation and cytoskeleton organisation on ground titanium surfaces. *Biomolecular Engineering*. 2002;19:233–237.

61. Ciobanasu C, Faivre B, Le Clainche C. Actin Dynamics Associated with Focal Adhesions. *International Journal of Cell Biology*. 2012;2012:1–9.

62. Moradi M, Sivadasan R, Saal L, Lüningschrör P, Dombert B, Rathod RJ, Dieterich DC, Blum R, Sendtner M. Differential roles of α-, β-, and γ-actin in axon growth and collateral branch formation in motoneurons. *Journal of Cell Biology*. 2017;216:793–814.

63. Eriksson JE, Dechat T, Grin B, Helfand B, Mendez M, Pallari H-M, Goldman RD. Introducing intermediate filaments: from discovery to disease. *J Clin Invest*. 2009;119:1763–1771.

64. Sun J, Omary MB. Intermediate Filament Proteins. 1997; 439:439-448:18.

65. Knossow M, Campanacci V, Khodja LA, Gigant B. The Mechanism of Tubulin Assembly into Microtubules: Insights from Structural Studies. *iScience*. 2020;23:101511.

66. Barlan K, Gelfand VI. Microtubule-Based Transport and the Distribution, Tethering, and Organization of Organelles. *Cold Spring Harb Perspect Biol*. 2017;9:a025817.

67. Joyner MJ, Schrage WG, Eisenach JH. Control of Blood Pressure—Normal and Abnormal [Internet]. In: Neurobiology of Disease. Elsevier; 2007. p. 997–1005.

68. Brozovich FV, Nicholson CJ, Degen CV, Gao YZ, Aggarwal M, Morgan KG. Mechanisms of Vascular Smooth Muscle Contraction and the Basis for Pharmacologic Treatment of Smooth Muscle Disorders. *Pharmacol Rev*. 2016;68:476–532.

69. Murthy KS. SIGNALING FOR CONTRACTION AND RELAXATION IN SMOOTH MUSCLE OF THE GUT. *Annu Rev Physiol*. 2006;68:345–374.

70. Khalil RA. Regulation of Vascular Smooth Muscle Function.

71. Johnson JD, Snyder C, Walsh M, Flynn M. Effects of Myosin Light Chain Kinase and Peptides on Ca2+ Exchange with the N- and C-terminal Ca2+ Binding Sites of Calmodulin. *Journal of Biological Chemistry*. 1996;271:761–767.

72. Tang DD, Gerlach BD. The roles and regulation of the actin cytoskeleton, intermediate filaments and microtubules in smooth muscle cell migration. *Respir Res*. 2017;18:54.

73. Cario-Toumaniantz C. Modulation of RhoA-Rho kinase-mediated Ca2+ sensitization of rabbit myometrium during pregnancy - role of Rnd3. *The Journal of Physiology*. 2003;552:403–413.

74. Nuno DW, England SK, Lamping KG. RhoA localization with caveolin-1 regulates vascular contractions to serotonin. *American Journal of Physiology-Regulatory, Integrative and Comparative Physiology*. 2012;303:R959–R967.

75. Khromov A, Choudhury N, Stevenson AS, Somlyo AV, Eto M. Phosphorylation-dependent Autoinhibition of Myosin Light Chain Phosphatase Accounts for Ca2+ Sensitization Force of Smooth Muscle Contraction. *Journal of Biological Chemistry*. 2009;284:21569–21579.

76. Saphirstein RJ, Gao YZ, Jensen MH, Gallant CM, Vetterkind S, Moore JR, Morgan KG. The Focal Adhesion: A Regulated Component of Aortic Stiffness. *PLoS ONE*. 2013;8:e62461.

77. Qiu J, Zheng Y, Hu J, Liao D, Gregersen H, Deng X, Fan Y, Wang G. Biomechanical regulation of vascular smooth muscle cell functions: from *in vitro* to *in vivo* understanding. *J R Soc Interface*. 2014;11:20130852.

78. Lacolley P, Regnault V, Nicoletti A, Li Z, Michel J-B. The vascular smooth muscle cell in arterial pathology: a cell that can take on multiple roles. *Cardiovascular Research*. 2012;95:194–204.

79. Harding SD, Sharman JL, Faccenda E, Southan C, Pawson AJ, Ireland S, Gray AJG, Bruce L, Alexander SPH, Anderton S, Bryant C, Davenport AP, Doerig C, Fabbro D, Levi-Schaffer F, Spedding M, Davies JA, NC-IUPHAR. The IUPHAR/BPS Guide to

PHARMACOLOGY in 2018: updates and expansion to encompass the new guide to IMMUNOPHARMACOLOGY. *Nucleic Acids Research*. 2018;46:D1091–D1106.

80. van der Kant R, Vriend G. Alpha-Bulges in G Protein-Coupled Receptors. *IJMS*. 2014;15:7841–7864.

81. Meyen D, Tarbashevich K, Banisch TU, Wittwer C, Reichman-Fried M, Maugis B, Grimaldi C, Messerschmidt E-M, Raz E. Dynamic filopodia are required for chemokine-dependent intracellular polarization during guided cell migration in vivo. *eLife*. 2015;4:e05279.

82. Pándy-Szekeres G, Munk C, Tsonkov TM, Mordalski S, Harpsøe K, Hauser AS, Bojarski AJ, Gloriam DE. GPCRdb in 2018: adding GPCR structure models and ligands. *Nucleic Acids Research*. 2018;46:D440–D446.

83. Shan D, Chen L, Wang D, Tan Y-C, Gu JL, Huang X-Y. The G Protein Gα13 Is Required for Growth Factor-Induced Cell Migration. *Developmental Cell*. 2006;10:707–718.

84. Wynne BM, Chiao C-W, Webb RC. Vascular smooth muscle cell signaling mechanisms for contraction to angiotensin II and endothelin-1. *Journal of the American Society of Hypertension*. 2009;3:84–95.

85. Putney JW, Tomita T. Phospholipase C signaling and calcium influx. *Advances in Biological Regulation*. 2012;52:152–164.

86. Schwartz M. Rho signalling at a glance. *Journal of Cell Science*. 2004;117:5457–5458.

87. Ridley AJ. Rho GTPases and cell migration. *Journal of Cell Science*. 2001;114:2713–2722.

88. Owens K. Gary. Regulation of Vascular Smooth Muscle Function. 1995:76.

89. Nobes CD, Hall A. Rho, Rac, and Cdc42 GTPases regulate the assembly of multimolecular focal complexes associated with actin stress fibers, lamellipodia, and filopodia. *Cell*. 1995;81:53–62.

90. Hartmann S, Ridley AJ, Lutz S. The Function of Rho-Associated Kinases ROCK1 and ROCK2 in the Pathogenesis of Cardiovascular Disease. *Front Pharmacol*. 2015;6.

91. Yoneda A, Multhaupt HAB, Couchman JR. The Rho kinases I and II regulate different aspects of myosin II activity. *Journal of Cell Biology*. 2005;170:443–453.

92. Vega FM, Fruhwirth G, Ng T, Ridley AJ. RhoA and RhoC have distinct roles in migration and invasion by acting through different targets. *Journal of Cell Biology*. 2011;193:655–665.

93. Yamaguchi H, Kasa M, Amano M, Kaibuchi K, Hakoshima T. Molecular Mechanism for the Regulation of Rho-Kinase by Dimerization and Its Inhibition by Fasudil. *Structure*. 2006;14:589–600.

94. Liao JK, Seto M, Noma K. Rho Kinase (ROCK) Inhibitors. *Journal of Cardiovascular Pharmacology*. 2007;50:17–24.

95. Vicente-Manzanares M, Webb DJ, Horwitz AR. Cell migration at a glance. *Journal of Cell Science*. 2005;118:4917–4919.

96. Mangione CM, Barry MJ, Nicholson WK, Cabana M, Chelmow D, Coker TR, Davis EM, Donahue KE, Jaén CR, Kubik M, Li L, Ogedegbe G, Pbert L, Ruiz JM, Stevermer J, Wong JB. Statin Use for the Primary Prevention of Cardiovascular Disease in Adults: US Preventive Services Task Force Recommendation Statement. *JAMA*. 2022;328:746.

97. Merx MW, Liehn EA, Janssens U, Lütticken R, Schrader J, Hanrath P, Weber C. HMG-CoA Reductase Inhibitor Simvastatin Profoundly Improves Survival in a Murine Model of Sepsis. *Circulation*. 2004;109:2560–2565.

98. Rikitake Y, Liao JK. Rho GTPases, Statins, and Nitric Oxide. *Circulation Research*. 2005;97:1232–1235.

99. Liao JK, Laufs U. PLEIOTROPIC EFFECTS OF STATINS. *Annu Rev Pharmacol Toxicol*. 2005;45:89–118.

100. Bendall JK, Cave AC, Heymes C, Gall N, Shah AM. Pivotal Role of a gp91 [phox] - Containing NADPH Oxidase in Angiotensin II-Induced Cardiac Hypertrophy in Mice. *Circulation*. 2002;105:293–296.

101. Stine JE, Guo H, Sheng X, Han X, Schointuch MN, Gilliam TP, Gehrig PA, Zhou C, Bae-Jump VL. The HMG-CoA reductase inhibitor, simvastatin, exhibits anti-metastatic and anti-tumorigenic effects in ovarian cancer. *Oncotarget*. 2016;7:946–960.

102. Foncea R, Carvajal C, Almarza C, Leighton F. Endothelial cell oxidative stress and signal transduction. *Biol Res*. 2000

103. Garoffolo G, Pesce M. Mechanotransduction in the Cardiovascular System: From Developmental Origins to Homeostasis and Pathology. *Cells*. 2019;8:1607.

104. Geiger B, Bershadsky A, Pankov R, Yamada KM. TRANSMEMBRANE EXTRACELLULAR MATRIX– CYTOSKELETON CROSSTALK. 2001;13.

105. Kim K, Hong K-S. Transient receptor potential channel-dependent myogenic responsiveness in small-sized resistance arteries. *J Exerc Rehabil*. 2021;17:4–10.

106. Cellular Mechanotransduction Mechanisms in Cardiovascular and Fibrotic Diseases [Internet]. Elsevier; 2021.

107. Morris CE, Juranka PF. Lipid Stress at Play: Mechanosensitivity of Voltage-Gated Channels [Internet]. In: Current Topics in Membranes. Elsevier; 2007 [cited 2022 Sep 2]. p. 297–338.

108. Hayashi JM, Richardson K, Melzer ES, Sandler SJ, Aldridge BB, Siegrist MS, Morita YS. Stress-Induced Reorganization of the Mycobacterial Membrane Domain. *mBio*. 2018;9:e01823-17.

109. Goldmann WH. Mechanosensation [Internet]. In: Progress in Molecular Biology and Translational Science. Elsevier; 2014. p. 75–102.

110. Jansen KA, Atherton P, Ballestrem C. Mechanotransduction at the cell-matrix interface. *Seminars in Cell & Developmental Biology*. 2017;71:75–83.

111. Sackin H. Stretch-activated ion channels. *Kidney International*. 1995;48:1134–1147.

112. Gees M, Colsoul B, Nilius B. The Role of Transient Receptor Potential Cation Channels in Ca2+ Signaling. *Cold Spring Harbor Perspectives in Biology*. 2010;2:a003962–a003962.

113. Nishida M, Tanaka T, Mangmool S, Nishiyama K, Nishimura A. Canonical Transient Receptor Potential Channels and Vascular Smooth Muscle Cell Plasticity. *J Lipid Atheroscler*. 2020;9:124.

114. Halka AT, Turner NJ, Carter A, Ghosh J, Murphy MO, Kirton JP, Kielty CM, Walker MG. The effects of stretch on vascular smooth muscle cell phenotype in vitro. *Cardiovascular Pathology*. 2008;5.

115. Park KS, Kim Y, Lee Y-H, Earm YE, Ho W-K. Mechanosensitive Cation Channels in Arterial Smooth Muscle Cells Are Activated by Diacylglycerol and Inhibited by Phospholipase C Inhibitor. *Circulation Research*. 2003;93:557–564.

116. Zou H, Lifshitz LM, Tuft RA, Fogarty KE, Singer JJ. Visualization of Ca $^{2+}$ entry through single stretch-activated cation channels. *Proc Natl Acad Sci USA*. 2002;99:6404–6409.

117. Rudolf S, Joseph EB. Stretch-activated Cation Channels and the Myogenic Response of Small Arteries. Academia; 2005 [cited 2022 Jul 18].

118. Matsuda JJ, Volk KA, Shibata EF. Calcium currents in isolated rabbit coronary arterial smooth muscle myocytes. *The Journal of Physiology*. 1990;427:657–680.

119. Bae C, Sachs F, Gottlieb PA. The Mechanosensitive Ion Channel Piezo1 Is Inhibited by the Peptide GsMTx4. *Biochemistry*. 2011;50:6295–6300.

120. The mechano-gated channel inhibitor GsMTx4 reduces the exercise pressor reflex in decerebrate rats. The Journal of physiology.pdf.

121. Retailleau K, Duprat F, Arhatte M, Ranade SS, Peyronnet R, Martins JR, Jodar M, Moro C, Offermanns S, Feng Y, Demolombe S, Patel A, Honoré E. Piezo1 in Smooth Muscle Cells Is Involved in Hypertension-Dependent Arterial Remodeling. *Cell Reports*. 2015;13:1161–1171.

122. Gnanasambandam R, Ghatak C, Yasmann A, Nishizawa K, Sachs F, Ladokhin AS, Sukharev SI, Suchyna TM. GsMTx4: Mechanism of Inhibiting Mechanosensitive Ion Channels. *Biophysical Journal*. 2017;112:31–45.

123. Geiger B, Bershadsky A, Pankov R, Yamada Kenneth M. Assessment of extracellular matrix modulation of cell traction force by using silicon nanowire array. Molecular cell biology. 2001; 2.

124. Reilly GC, Engler AJ. Intrinsic extracellular matrix properties regulate stem cell differentiation. *Journal of Biomechanics*. 2010;43:55–62.

125. Geiger B, Bershadsky A, Pankov R, Yamada KM. TRANSMEMBRANE EXTRACELLULAR MATRIX– CYTOSKELETON CROSSTALK. 2001;13.

126. Reynolds LE, Wyder L, Lively JC, Taverna D, Robinson SD, Huang X, Sheppard D, Hynes RO, Hodivala-Dilke KM. Enhanced pathological angiogenesis in mice lacking β3 integrin or β3 and β5 integrins. *Nat Med*. 2002;8:27–34.

127. Margolin L, Fishbein I, Banai S, Golomb G, Perez LS, Da S. Metalloproteinase inhibitor attenuates neointima formation and constrictive remodeling after angioplasty in rats: augmentative effect of avb3 receptor blockade. 2002;9.

128. Changede R, Sheetz M. Integrin and cadherin clusters: A robust way to organize adhesions for cell mechanics. *BioEssays*. 2017;39:e201600123.

129. Wickström SA, Lange A, Montanez E, Fässler R. The ILK/PINCH/parvin complex: the kinase is dead, long live the pseudokinase! *EMBO J*. 2010;29:281–291.

130. Katz M, Amit I, Yarden Y. Regulation of MAPKs by growth factors and receptor tyrosine kinases. *Biochimica et Biophysica Acta (BBA) - Molecular Cell Research*. 2007;1773:1161–1176.

131. Nikolopoulos SN, Turner CE. Integrin-linked Kinase (ILK) Binding to Paxillin LD1 Motif Regulates ILK Localization to Focal Adhesions. *Journal of Biological Chemistry*. 2001;276:23499–23505.

132. Ho B, Hou G, Pickering JG, Hannigan G, Langille BL, Bendeck MP. Integrin-Linked Kinase in the Vascular Smooth Muscle Cell Response to Injury. *The American Journal of Pathology*. 2008;173:278–288.

133. Friedrich EB, Clever YP, Wassmann S, Werner N, Böhm M, Nickenig G. Role of integrin-linked kinase in vascular smooth muscle cells: Regulation by statins and angiotensin II. *Biochemical and Biophysical Research Communications*. 2006;349:883–889.

134. Kaneko Y, Kitazato K, Basaki Y. Integrin-linked kinase regulates vascular morphogenesis induced by vascular endothelial growth factor. *Journal of Cell Science*. 2004;117:407–415.

135. Sun Z, Martinez-Lemus LA, Hill MA, Meininger GA. Extracellular matrix-specific focal adhesions in vascular smooth muscle produce mechanically active adhesion sites. *American Journal of Physiology-Cell Physiology*. 2008;295:C268–C278.

136. Raines EW. The extracellular matrix can regulate vascular cell migration, proliferation, and survival: relationships to vascular disease: Extracellular matrix alters vascular cell function. *International Journal of Experimental Pathology*. 2001;81:173–182.

137. Khalili A, Ahmad M. A Review of Cell Adhesion Studies for Biomedical and Biological Applications. *IJMS*. 2015;16:18149–18184.

138. Cai X, Lietha D, Ceccarelli DF, Karginov AV, Rajfur Z, Jacobson K, Hahn KM, Eck MJ, Schaller MD. Spatial and Temporal Regulation of Focal Adhesion Kinase Activity in Living Cells. *Mol Cell Biol*. 2008;28:201–214.

139. Yang W-J, Yang Y-N, Cao J, Man Z-H, Li Y, Xing Y-Q. Paxillin regulates vascular endothelial growth factor A-induced in vitro angiogenesis of human umbilical vein endothelial cells. *Molecular Medicine Reports*. 2015;11:1784–1792.

140. Slack-Davis JK, Eblen ST, Zecevic M, Boerner SA, Tarcsafalvi A, Diaz HB, Marshall MS, Weber MJ, Parsons JT, Catling AD. PAK1 phosphorylation of MEK1 regulates fibronectin-stimulated MAPK activation. *Journal of Cell Biology*. 2003;162:281–291.

141. Desai A, Mitchison TJ. MICROTUBULE POLYMERIZATION DYNAMICS. *Annu Rev Cell Dev Biol*. 1997;13:83–117.

142. Zhang R, Alushin GM, Brown A, Nogales E. Mechanistic Origin of Microtubule Dynamic Instability and Its Modulation by EB Proteins. *Cell*. 2015;162:849–859.

143. Gudimchuk NB, McIntosh JR. Regulation of microtubule dynamics, mechanics and function through the growing tip. *Nat Rev Mol Cell Biol*. 2021;22:777–795.

144. Shao Y, Mann JM, Chen W, Fu J. Global architecture of the F-actin cytoskeleton regulates cell shape-dependent endothelial mechanotransduction. *Integr Biol*. 2014;6:300.

145. Dominguez R, Holmes KC. Actin Structure and Function. *Annu Rev Biophys*. 2011;40:169–186.

146. Ahmed S, Johnson RobertT, Solanki R, Afewerki T, Wostear F, Warren DerekT. Using Polyacrylamide Hydrogels to Model Physiological Aortic Stiffness Reveals that Microtubules Are Critical Regulators of Isolated Smooth Muscle Cell Morphology and Contractility. *Front Pharmacol*. 2022;13:836710.

147. Selig M, Lauer JC, Hart ML, Rolauffs B. Mechanotransduction and Stiffness-Sensing: Mechanisms and Opportunities to Control Multiple Molecular Aspects of Cell Phenotype as a Design Cornerstone of Cell-Instructive Biomaterials for Articular Cartilage Repair. *IJMS*. 2020;21:5399.

148. Bidaud-Meynard A, Binamé F, Lagrée V, Moreau V. Regulation of Rho GTPase activity at the leading edge of migrating cells by p190RhoGAP. *Small GTPases*. 2019;10:99–110.

149. Zhang J, Guo W-H, Wang Y-L. Microtubules stabilize cell polarity by localizing rear signals. *Proc Natl Acad Sci USA*. 2014;111:16383–16388.

150. Garcin C, Straube A. Microtubules in cell migration. *Essays in Biochemistry*. 2019;63:509–520.

151. Kaverina I, Straube A. Regulation of cell migration by dynamic microtubules. *Seminars in Cell & Developmental Biology*. 2011;22:968–974.

152. Fukata M, Watanabe T, Noritake J, Nakagawa M, Yamaga M, Kuroda S, Matsuura Y, Iwamatsu A, Perez F, Kaibuchi K. Rac1 and Cdc42 Capture Microtubules through IQGAP1 and CLIP-170. *Cell*. 2002;109:873–885.

153. Straube A, Merdes A. EB3 Regulates Microtubule Dynamics at the Cell Cortex and Is Required for Myoblast Elongation and Fusion. *Current Biology*. 2007;17:1318–1325.

154. Wittmann T, Bokoch GM, Waterman-Storer CM. Regulation of leading edge microtubule and actin dynamics downstream of Rac1. *Journal of Cell Biology*. 2003;161:845–851.

155. Niethammer P, Bastiaens P, Karsenti E. Stathmin-Tubulin Interaction Gradients in Motile and Mitotic Cells. *Science*. 2004;303:1862–1866.

156. Etienne-Manneville S. Microtubules in Cell Migration. *Annu Rev Cell Dev Biol*. 2013;29:471–499.

157. Salaycik KJ, Fagerstrom CJ, Murthy K, Tulu US, Wadsworth P. Quantification of microtubule nucleation, growth and dynamics in wound-edge cells. *Journal of Cell Science*. 2005;118:4113–4122.

158. Gundersen GG. Evolutionary conservation of microtubule-capture mechanisms. *Nat Rev Mol Cell Biol*. 2002;3:296–304.

159. Wittmann T, Bokoch GM, Waterman-Storer CM. Regulation of Microtubule Destabilizing Activity of Op18/Stathmin Downstream of Rac1. *Journal of Biological Chemistry*. 2004;279:6196–6203.

160. Daub H, Gevaert K, Vandekerckhove J, Sobel A, Hall A. Rac/Cdc42 and p65PAK Regulate the Microtubule-destabilizing Protein Stathmin through Phosphorylation at Serine 16. *Journal of Biological Chemistry*. 2001;276:1677–1680.

161. Perez de Castro I, Malumbres M. Mitotic Stress and Chromosomal Instability in Cancer: The Case for TPX2. *Genes & Cancer*. 2012;3:721–730.

162. Yoon D-S, Wersto RP, Zhou W, Chrest FJ, Garrett ES, Kwon TK, Gabrielson E. Variable Levels of Chromosomal Instability and Mitotic Spindle Checkpoint Defects in Breast Cancer. *The American Journal of Pathology*. 2002;161:391–397.

163. Gambino G, Rizzo V, Giglia G, Ferraro G, Sardo P. Microtubule Dynamics and Neuronal Excitability: Advances on Cytoskeletal Components Implicated in Epileptic Phenomena. *Cell Mol Neurobiol*. 2022;42:533–543.

164. Chen D. HIV-1 Tat targets microtubules to induce apoptosis, a process promoted by the pro-apoptotic Bcl-2 relative Bim. *The EMBO Journal*. 2002;21:6801–6810.

165. Haglund CM, Welch MD. Pathogens and polymers: Microbe–host interactions illuminate the cytoskeleton. *Journal of Cell Biology*. 2011;195:7–17.

166. Jordan M. Ann, Wilson Leslie. Microtubules as a target for anticancer drugs. Nat Rev Cancer. 2004; 253-265.

167. Mukhtar E, Adhami VM, Mukhtar H. Targeting Microtubules by Natural Agents for Cancer Therapy. *Mol Cancer Ther*. 2014;13:275–284.

168. Rizzelli F, Malabarba Maria Grazia, Mapelli Marina. The crosstalk between microtubules, actin and membranes shapes cell division. *Open Biology*. 2020; 10:2046-2441.

169. Greene LM, Meegan MJ, Zisterer DM. Combretastatins: More Than Just Vascular Targeting Agents? *J Pharmacol Exp Ther*. 2015;355:212–227.

170. Herdeg C, Oberhoff M, Siegel-Axel DI, Baumbach A, Blattner A, Küttner A, Schröder S, Karsch KR. Paclitaxel: Ein Chemotherapeutikum zur Restenoseprophylaxe? Experimentelle Untersuchungen in vitro und in vivo. *Z Kardiol*. 2000;89:390–397.

171. Jordan MA, Wilson L. Microtubules as a target for anticancer drugs. *Nat Rev Cancer*. 2004;4:253–265.

172. Ding A, Sanchez E, Nathan CF. Taxol shares the ability of bacterial lipopolysaccharide to induce tyrosine phosphorylation of microtubule-associated protein kinase. *Journal of Immunology*. :8.

173. Gundersen GG, Cook TA. Microtubules and signal transduction. 1999;11:81–94:14.

174. Kwon D-H, Ryu J, Kim Y-K, Kook H. Roles of Histone Acetylation Modifiers and Other Epigenetic Regulators in Vascular Calcification. *IJMS*. 2020;21:3246.

175. Wang R, Tan J, Chen T, Han H, Tian R, Tan Y, Wu Y, Cui J, Chen F, Li J, Lv L, Guan X, Shang S, Lu J, Zhang Z. ATP13A2 facilitates HDAC6 recruitment to lysosome to promote autophagosome–lysosome fusion. *Journal of Cell Biology*. 2019;218:267–284.

176. Glon D, Vilmen G, Perdiz D, Hernandez E, Beauclair G, Quignon F, Berlioz-Torrent C, Maréchal V, Poüs C, Lussignol M, Esclatine A. Essential role of hyperacetylated microtubules in innate immunity escape orchestrated by the EBV-encoded BHRF1 protein. *PLOS PATHOGENS*. :29.

177. Lopes da Rosa J, Boyartchuk VL, Zhu LJ, Kaufman PD. Histone acetyltransferase Rtt109 is required for *Candida albicans* pathogenesis. *Proc Natl Acad Sci USA*. 2010;107:1594–1599.

178. Ouyang C, Li J, Zheng X, Mu J, Torres G, Wang Q, Zou M-H, Xie Z. Deletion of *Ulk1* inhibits neointima formation by enhancing KAT2A/GCN5-mediated acetylation of TUBA/α-tubulin *in vivo*. *Autophagy*. 2021;17:4305–4322.

179. Rao R, Fiskus W, Ganguly S, Kambhampati S, Bhalla KN. HDAC Inhibitors and Chaperone Function. In: Advances in Cancer Research. Elsevier; 2012. p. 239–262.

180. Hubbert C, Guardiola A, Shao R, Kawaguchi Y, Ito A, Nixon A, Yoshida M, Wang X-F, Yao T-P. HDAC6 is a microtubule-associated deacetylase. *Nature*. 2002;417:455–458.

181. Valenzuela-Fernández A, Cabrero JR, Serrador JM, Sánchez-Madrid F. HDAC6: a key regulator of cytoskeleton, cell migration and cell–cell interactions. *Trends in Cell Biology*. 2008;18:291–297.

182. Johnson R, Ahmed S, Solanki R, Wostear F, Afewerki T, Warren D. BS18 Enhanced matrix stiffness prevents vsmc contractility: how calcium signalling and microtubule stability regulate vascular compliance during ageing. In: Basic science. BMJ Publishing Group Ltd and British Cardiovascular Society; 2022. p. A155.1-A155.

183. Dalhat MH, Altayb HN, Khan MI, Choudhry H. Structural insights of human N-acetyltransferase 10 and identification of its potential novel inhibitors. *Sci Rep*. 2021;11:6051.

184. Tsai K, Jaguva Vasudevan AA, Martinez Campos C, Emery A, Swanstrom R, Cullen BR. Acetylation of Cytidine Residues Boosts HIV-1 Gene Expression by Increasing Viral RNA Stability. *Cell Host & Microbe*. 2020;28:306-312.e6.

185. Oh T-I, Lee Y-M, Lim B-O, Lim J-H. Inhibition of NAT10 Suppresses Melanogenesis and Melanoma Growth by Attenuating Microphthalmia-Associated Transcription Factor (MITF) Expression. *IJMS*. 2017;18:1924.

186. Liu H, Ling Y, Gong Y, Sun Y, Hou L, Zhang B. DNA damage induces N-acetyltransferase NAT10 gene expression through transcriptional activation. *Mol Cell Biochem*. 2007;300:249–258.

187. Shen Q, Zheng X, McNutt MA, Guang L, Sun Y, Wang J, Gong Y, Hou L, Zhang B. NAT10, a nucleolar protein, localizes to the midbody and regulates cytokinesis and acetylation of microtubules. *Experimental Cell Research*. 2009;315:1653–1667.

188. Ma R, Chen J, Jiang S, Lin S, Zhang X, Liang X. Up regulation of NAT10 promotes metastasis of hepatocellular carcinoma cells through epithelial-to-mesenchymal transition. 2016;9.

189. Tan Y, Zheng J, Liu X, Lu M, Zhang C, Xing B, Du X. Loss of nucleolar localization of NAT10 promotes cell migration and invasion in hepatocellular carcinoma. *Biochemical and Biophysical Research Communications*. 2018;499:1032–1038.

190. Sanger Mouse Genetics Project, Balmus G, Larrieu D, Barros AC, Collins C, Abrudan M, Demir M, Geisler NJ, Lelliott CJ, White JK, Karp NA, Atkinson J, Kirton A, Jacobsen M, Clift D, Rodriguez R, Adams DJ, Jackson SP. Targeting of NAT10 enhances healthspan in a mouse model of human accelerated aging syndrome. *Nat Commun*. 2018;9:1700.

191. Wu J, Zhu H, Wu J, Chen W, Guan X. Inhibition of N-acetyltransferase 10 using remodelin attenuates doxorubicin resistance by reversing the epithelial-mesenchymal transition in breast cancer. 2018;10:9.

192. Mitchison T, Kirschner M. Dynamic instability of microtubule growth. 1984;6.

193. Requena S, Sánchez-Madrid F, Martín-Cófreces NB. Post-translational modifications and stabilization of microtubules regulate transport of viral factors during infections. *Biochemical Society Transactions*. 2021;49:1735–1748.

194. Zeng J, Xi J, Li B, Yan X, Dai Y, Wu Y, Xiao Y, Pei Y, Zhang M. Microtubules play a crucial role in regulating actin organization and cell initiation in cotton fibers. *Plant Cell Rep*. 2022;41:1059–1073.

195. Kim JM. Molecular Link between DNA Damage Response and Microtubule Dynamics. *IJMS*. 2022;23:6986.

196. Guo X, Fang Z-M, Wei X, Huo B, Yi X, Cheng C, Chen J, Zhu X-H, Bokha AOKA, Jiang D-S. HDAC6 is associated with the formation of aortic dissection in human. *Mol Med*. 2019;25:10.

197. Seetharaman S, Etienne-Manneville S. Cytoskeletal Crosstalk in Cell Migration. *Trends in Cell Biology*. 2020;30:720–735.

198. Hohmann, Dehghani. The Cytoskeleton—A Complex Interacting Meshwork. *Cells*. 2019;8:362.

199. Dogterom M, Koenderink GH. Actin–microtubule crosstalk in cell biology. *Nat Rev Mol Cell Biol*. 2019;20:38–54.

200. Rizzelli F, Malabarba MG, Sigismund S, Mapelli M. The crosstalk between microtubules, actin and membranes shapes cell division. *Open Biol*. 2020;10:190314.

201. Clare M., Waterman-Storer, E.D. Salmon. Microtubule dynamics-Treadmilling comes around again. *Current Biology*. 1997; 7:R369-R372.

202. Gupton SL, Salmon WC, Waterman-Storer CM. Converging Populations of F-Actin Promote Breakage of Associated Microtubules to Spatially Regulate Microtubule Turnover in Migrating Cells. *Current Biology*. 2002;12:1891–1899.

203. Petrie RJ, Yamada KM. At the leading edge of three-dimensional cell migration. *Journal of Cell Science*. 2012;125:5917–5926.

204. Trepat X, Chen Z, Jacobson K. Cell Migration [Internet]. In: Terjung R, editor. Comprehensive Physiology. Wiley; 2012. p. 2369–2392.

205. Levin E. Cancer Therapy Through Control of Cell Migration. *CCDT*. 2005;5:505–518.

206. Boehm M, Nabel EG. Cell Cycle and Cell Migration: New Pieces to the Puzzle. *Circulation*. 2001;103:2879–2881.

207. Qiu J, Zheng Y, Hu J, Liao D, Gregersen H, Deng X, Fan Y, Wang G. Biomechanical regulation of vascular smooth muscle cell functions: from *in vitro* to *in vivo* understanding. *J R Soc Interface*. 2014;11:20130852.

208. Sazonova OV, Isenberg BC, Herrmann J, Lee KL, Purwada A, Valentine AD, Buczek-Thomas JA, Wong JY, Nugent MA. Extracellular matrix presentation modulates vascular smooth muscle cell mechanotransduction. *Matrix Biology*. 2015;41:36–43.

209. Louis SF, Zahradka P. Vascular smooth muscle cell motility: From migration to invasion. 2010;15:11.

210. Ridley AJ, Schwartz MA, Burridge K, Firtel RA, Ginsberg MH, Borisy G, Parsons JT, Horwitz AR. Cell Migration: Integrating Signals from Front to Back. 2003;302:7.

211. Firat-Karalar EN, Welch MD. New mechanisms and functions of actin nucleation. *Current Opinion in Cell Biology*. 2011;23:4–13.

212. Hanna S, El-Sibai M. Signaling networks of Rho GTPases in cell motility. *Cellular Signalling*. 2013;25:1955–1961.

213. Goh WI, Ahmed S. mDia1-3 in mammalian filopodia. *Communicative & Integrative Biology*. 2012;5:340–344.

214. Jäger MA, De La Torre C, Arnold C, Kohlhaas J, Kappert L, Hecker M, Feldner A, Korff T. Assembly of vascular smooth muscle cells in 3D aggregates provokes cellular quiescence. *Experimental Cell Research*. 2020;388:111782.

215. Ding Y, Xu X, Sharma S, Floren M, Stenmark K, Bryant SJ, Neu CP, Tan W. Biomimetic soft fibrous hydrogels for contractile and pharmacologically responsive smooth muscle. *Acta Biomaterialia*. 2018;74:121–130.

216. Smith E, Kanczler J, Oreffo R. A new take on an old story: chick limb organ culture for skeletal niche development and regenerative medicine evaluation. *eCM*. 2013;26:91–106.

217. Rueden CT, Schindelin J, Hiner MC, DeZonia BE, Walter AE, Arena ET, Eliceiri KW. ImageJ2: ImageJ for the next generation of scientific image data. *BMC Bioinformatics*. 2017;18:529.

218. Liu Z-Q. Scale space approach to directional analysis of images.

219. Camasão DB, Mantovani D. The mechanical characterization of blood vessels and their substitutes in the continuous quest for physiological-relevant performances. A critical review. *Materials Today Bio*. 2021;10:100106.

220. Gamble G, Zorn J, Sanders G, MacMahon S, Sharpe N. Estimation of arterial stiffness, compliance, and distensibility from M-mode ultrasound measurements of the common carotid artery. *Stroke*. 1994;25:11–16.

221. Lee H-Y, Oh B-H. Aging and Arterial Stiffness. *Circ J*. 2010;74:2257–2262.

222. Hui L, Zhang J, Ding X, Guo X, Jiang X. Matrix stiffness regulates the proliferation, stemness and chemoresistance of laryngeal squamous cancer cells. *International Journal of Oncology*. 2017;50:1439–1447.

223. Butcher DT, Alliston T, Weaver VM. A tense situation: forcing tumour progression. *Nat Rev Cancer*. 2009;9:108–122.

224. Cordoba CG, Daly CJ. The organisation of vascular smooth muscle cells; a quantitative Fast Fourier Transform (FFT) based assessment. *Translational Research in Anatomy*. 2019;16:100047.

225. Cao F, Ma S. Autophagy and Hypertension [Internet]. In: Autophagy and Cardiometabolic Diseases. Elsevier; 2018 [cited 2022 Aug 9]. p. 91–99.

226. Petsophonsakul P, Furmanik M, Forsythe R, Dweck M, Schurink GW, Natour E, Reutelingsperger C, Jacobs M, Mees B, Schurgers L. Role of Vascular Smooth Muscle Cell Phenotypic Switching and Calcification in Aortic Aneurysm Formation: Involvement of Vitamin K-Dependent Processes. *ATVB*. 2019;39:1351–1368.

227. Mitry RR, Hughes RD, editors. Human Cell Culture Protocols. Totowa, NJ: Humana Press; 2012.

228. Tse JR, Engler AJ. Preparation of Hydrogel Substrates with Tunable Mechanical Properties. *Current Protocols in Cell Biology*. 2010

229. Paul CD, Hung W-C, Wirtz D, Konstantopoulos K. Engineered Models of Confined Cell Migration. *Annu Rev Biomed Eng*. 2016;18:159–180.

230. Tsuji-Tamura K, Ogawa M. Morphology regulation in vascular endothelial cells. *Inflamm Regener*. 2018;38:25.

231. Li L, Li X, Chen L, Sun P, Hao N, Jiang B. Morphology, proliferation, alignment, and new collagen synthesis of mesenchymal stem cells on a microgrooved collagen membrane. *Journal of Biomaterials Science, Polymer Edition*. 2016;27:581–598.

232. Deftu AT. Chapter 9 - Exosomes as intercellular communication messengers for cardiovascular and cerebrovascular diseases. :40.

233. Bacakova L, Travnickova M, Filova E, Matejka R, Stepanovska J, Musilkova J, Zarubova J, Molitor M. Vascular Smooth Muscle Cells (VSMCs) in Blood Vessel Tissue Engineering: The Use of Differentiated Cells or Stem Cells as VSMC Precursors. In: Sakuma K, editor. Muscle Cell and Tissue - Current Status of Research Field. InTech; 2018

234. Deng Y, Lin C, Zhou HJ, Min W. Smooth muscle cell differentiation: Mechanisms and models for vascular diseases. *Front Biol*. 2017;12:392–405.

235. Shi Ning, Chen Shi-You. Smooth Muscle Cell Differentiation: Model Systems, Regulatory Mechanisms, and Vascular Diseases. *JOURNAL OF CELLULAR PHYSIOLOGY*. 2016;4:777-787:11.

236. Eddinger TJ, Meer DP, Miner AS, Meehl J, Rovner AS, Ratz PH. Potent Inhibition of Arterial Smooth Muscle Tonic Contractions by the Selective Myosin II Inhibitor, Blebbistatin. :6.

237. Owens, G. K. Regulation of differentiation of vascular smooth muscle cells. Physiology. 1995:487-517

238. Choi CK, Vicente-Manzanares M, Zareno J, Mogilner A, Horwitz AR. Actin and α-actinin orchestrate the assembly and maturation of nascent adhesions in a myosin II motor-independent manner. 2010;22.

239. Qiu H, Zhu Y, Sun Z, Trzeciakowski JP, Gansner M, Depre C, Resuello RRG, Natividad FF, Hunter WC, Genin GM, Elson EL, Vatner DE, Meininger GA, Vatner SF. Short Communication: Vascular Smooth Muscle Cell Stiffness As a Mechanism for Increased Aortic Stiffness With Aging. *Circ Res*. 2010;107:615–619.

240. Deroanne C. In vitro tubulogenesis of endothelial cells by relaxation of the coupling extracellular matrix-cytoskeleton. *Cardiovascular Research*. 2001;49:647–658.

241. William Wan, Kristen K. Bjorkman, Esther S. Choi, Amanda L. Panepento, Kristi S. A. Leinwand. Cardiac myocytes respond differentially and synergistically to matrix stiffness and topography. *bioRxiv*. 2019.

242. Discher DE, Janmey P, Wang Y. Tissue Cells Feel and Respond to the Stiffness of Their Substrate. *Science, New Series*. 2005;310:1139–1143.

243. Pelham RJ, Wang Y-L. Cell Locomotion and Focal Adhesions are Regulated by Substrate Flexibility. *Proceedings of the National Academy of Sciences of the United States of America*. 1997;94:13661–13665.

244. Raman PS, Paul CD, Stroka KM, Konstantopoulos K. Probing cell traction forces in confined microenvironments. *Lab Chip*. 2013;13:4599.

245. Mahmud G, Campbell CJ, Bishop KJM, Komarova YA, Chaga O, Soh S, Huda S, Kandere-Grzybowska K, Grzybowski BA. Directing cell motions on micropatterned ratchets. *Nature Phys*. 2009;5:606–612.

246. Fletcher DA, Mullins RD. Cell mechanics and the cytoskeleton. *Nature*. 2010;463:485–492.

247. Warren DT, Zhang Q, Weissberg PL, Shanahan CM. Nesprins: intracellular scaffolds that maintain cell architecture and coordinate cell function? *Expert Reviews in Molecular Medicine*. 2005;7:1–15.

248. Wang N, Tytell JD, Ingber DE. Mechanotransduction at a distance: mechanically coupling the extracellular matrix with the nucleus. *Nat Rev Mol Cell Biol*. 2009;10:75–82.

249. Ahmed S. A model for estimating traction force magnitude reveals differential regulation of actomyosin activity and matrix adhesion number in response to smooth muscle cell spreading. 2019:18.

250. Kraning-Rush CM, Califano JP, Reinhart-King CA. Cellular Traction Stresses Increase with Increasing Metastatic Potential. *PLoS ONE*. 2012;7:e32572.

251. Yu Y, Ren L-J, Liu X-Y, Gong X-B, Yao W. Effects of substrate stiffness on mast cell migration. *European Journal of Cell Biology*. 2021;100:151178.

252. Lundin VF, Leroux MR, Stirling PC. Quality control of cytoskeletal proteins and human disease. *Trends in Biochemical Sciences*. 2010;35:288–297.

253. Steinmetz MO, Prota AE. Microtubule-Targeting Agents: Strategies To Hijack the Cytoskeleton. *Trends in Cell Biology*. 2018;28:776–792.

254. Zhang D, Wang Z, Jin N, Li L, Rhoades RA, Yancey W, Swartz DR. Microtubule disruption modulates the Rho-kinase pathway in vascular smooth muscle. :8.

255. Plaza GR, Uyeda TQP. Contraction speed of the actomyosin cytoskeleton in the absence of the cell membrane. *Soft Matter*. 2013;9:4390.

256. Ulu A, Frost JA. Regulation of RhoA activation and cytoskeletal organization by acetylation. *Small GTPases*. 2016;7:76–81.

257. Hubbert C, Guardiola A, Shao R, Kawaguchi Y, Ito A, Nixon A, Yoshida M, Wang X-F, Yao T-P. HDAC6 is a microtubule-associated deacetylase. *Nature*. 2002;417:455–458.

258. Zhang Y, Li N, Caron C, Matthias G, Hess D, Khochbin S, Matthias P. HDAC-6 interacts with and deacetylates tubulin and microtubules in vivo. *EMBO J*. 2003;22:1168–1179.

259. Li X, Ni Q, He X, Kong J, Lim S-M, Papoian GA, Trzeciakowski JP, Trache A, Jiang Y. Tensile force-induced cytoskeletal remodeling: Mechanics before chemistry. *PLoS Comput Biol*. 2020;16:e1007693.

260. Beningo KA, Dembo M, Kaverina I, Small JV, Wang Y. Nascent Focal Adhesions Are Responsible for the Generation of Strong Propulsive Forces in Migrating Fibroblasts. *Journal of Cell Biology*. 2001;153:881–888.

261. Pelham RJ, Wang Y. High Resolution Detection of Mechanical Forces Exerted by Locomoting Fibroblasts on the Substrate. *MBoC*. 1999;10:935–945.

262. Danowski BA. Fibroblast contractility and actin organization are stimulated by microtubule inhibitors. :11.

263. Rape A, Guo W, Wang Y. Microtubule depolymerization induces traction force increase through two distinct pathways. *Journal of Cell Science*. 2011;124:4233–4240.

264. McLoughlin EC, O'Boyle NM. Colchicine-Binding Site Inhibitors from Chemistry to Clinic: A Review. *Pharmaceuticals*. 2020;13:8.

265. Kampan NC, Madondo MT, McNally OM, Quinn M, Plebanski M. Paclitaxel and Its Evolving Role in the Management of Ovarian Cancer. *BioMed Research International*. 2015;2015:1–21.

266. Platts SH, Falcone JC, Holton WT, Hill MA, Meininger GA. Alteration of microtubule polymerization modulates arteriolar vasomotor tone. *American Journal of Physiology-Heart and Circulatory Physiology*. 1999;277:H100–H106.

267. Tsutsui H, Tagawa H, Kent RL, McCollam PL, Ishihara K, Nagatsu M, Cooper G. Role of microtubules in contractile dysfunction of hypertrophied cardiocytes. *Circulation*. 1994;90:533–555.

268. Chan A, Singh AJ, Northcote PT, Miller JH. Inhibition of human vascular endothelial cell migration and capillary-like tube formation by the microtubule-stabilizing agent peloruside A. *Invest New Drugs*. 2015;33:564–574.

269. Zhang D, Jin N, Rhoades RA, Yancey KW, Swartz DR. Infuence of microtubules on vascular smooth muscle contraction. :8.

270. Stamenović D, Wang N, Ingber DE. CELLULAR TENSEGRITY MODELS AND CELL-SUBSTRATE INTERACTIONS [Internet]. In: Principles of Cellular Engineering. Elsevier; 2006 [cited 2022 Aug 28]. p. 81–101.

271. Rape A, Guo W, Wang Y. Microtubule depolymerization induces traction force increase through two distinct pathways. *Journal of Cell Science*. 2011;124:4233–4240.

272. Hastie SB. Interactions of colchicine with tubulin. *Pharmacology & Therapeutics*. 1991;51:377–401.

273. Zhang F, He Q, Qin CH, Little PJ, Weng J, Xu S. Therapeutic potential of colchicine in cardiovascular medicine: a pharmacological review. *Acta Pharmacol Sin*. 2022

274. Li Q, Liu X, Jin K, Lu M, Zhang C, Du X, Xing B. NAT10 is upregulated in hepatocellular carcinoma and enhances mutant p53 activity. *BMC Cancer*. 2017;17:605.

275. Larrieu D, Britton S, Demir M, Rodriguez R, Jackson SP. Chemical Inhibition of NAT10 Corrects Defects of Laminopathic Cells. *Science*. 2014;344:527–532.

276. Ma N, Liu H, Wu Y, Yao M, Zhang B. Inhibition of N-Acetyltransferase 10 Suppresses the Progression of Prostate Cancer through Regulation of DNA Replication. *IJMS*. 2022;23:6573.

277. Amengual JE, Johannet P, Lombardo M, Zullo K, Hoehn D, Bhagat G, Scotto L, Jirau-Serrano X, Radeski D, Heinen J, Jiang H, Cremers S, Zhang Y, Jones S, O'Connor OA. Dual Targeting of Protein Degradation Pathways with the Selective HDAC6 Inhibitor ACY-1215 and Bortezomib Is Synergistic in Lymphoma. *Clinical Cancer Research*. 2015;21:4663–4675.

278. Gryder BE, Sodji QH, Oyelere AK. Targeted cancer therapy: giving histone deacetylase inhibitors all they need to succeed. *Future Medicinal Chemistry*. 2012;4:505–524.

279. Asthana J, Kapoor S, Mohan R, Panda D. Inhibition of HDAC6 Deacetylase Activity Increases Its Binding with Microtubules and Suppresses Microtubule Dynamic Instability in MCF-7 Cells. *Journal of Biological Chemistry*. 2013;288:22516–22526.

280. Asthana J, Kapoor S, Mohan R, Panda D. Inhibition of HDAC6 Deacetylase Activity Increases Its Binding with Microtubules and Suppresses Microtubule Dynamic Instability in MCF-7 Cells. *Journal of Biological Chemistry*. 2013;288:22516–22526.

281. Worssam MD, Jørgensen HF. Mechanisms of vascular smooth muscle cell investment and phenotypic diversification in vascular diseases. *Biochemical Society Transactions*. 2021;49:2101–2111.

282. Chang S, Song S, Lee J, Yoon J, Park J, Choi S, Park J-K, Choi K, Choi C. Phenotypic Modulation of Primary Vascular Smooth Muscle Cells by Short-Term Culture on Micropatterned Substrate. *PLoS ONE*. 2014;9:e88089.

283. Krendel M, Zenke FT, Bokoch GM. Nucleotide exchange factor GEF-H1 mediates cross-talk between microtubules and the actin cytoskeleton. *Nat Cell Biol*. 2002;4:294–301.

284. Corpataux J-M, Naik J, Porter KE, London NJM. The Effect of Six Different Statins on the Proliferation, Migration, and Invasion of Human Smooth Muscle Cells. *Journal of Surgical Research*. 2005;129:52–56.

285. Ikeda U, Shimada K. Pleiotropic Effects of Statins on the Vascular Tissue. *CDTCHD*. 2001;1:51–58.

286. Son B-K, Kozaki K, Iijima K, Eto M, Kojima T, Ota H, Senda Y, Maemura K, Nakano T, Akishita M, Ouchi Y. Statins Protect Human Aortic Smooth Muscle Cells From Inorganic Phosphate-Induced Calcification by Restoring Gas6-Axl Survival Pathway. *Circulation Research*. 2006;98:1024–1031.

287. Islam T. Impact of statins on vascular smooth muscle cells and relevance to atherosclerosis. *J Physiol*. 2020;598:2295–2296.

288. Wada H, Abe M, Ono K, Morimoto T, Kawamura T, Takaya T, Satoh N, Fujita M, Kita T, Shimatsu A, Hasegawa K. Statins activate GATA-6 and induce differentiated vascular smooth muscle cells. *Biochemical and Biophysical Research Communications*. 2008;374:731–736.

289. Ranade SS, Qiu Z, Woo S-H, Hur SS, Murthy SE, Cahalan SM, Xu J, Mathur J, Bandell M, Coste B, Li Y-SJ, Chien S, Patapoutian A. Piezo1, a mechanically activated ion channel, is required for vascular development in mice. *Proc Natl Acad Sci USA*. 2014;111:10347–10352.

290. Li J, Hou B, Tumova S, Muraki K, Bruns A, Sedo A, Hyman AJ, McKeown L, Young RS, Majeed Y, Wilson LA, Rode B, Bailey MA, Kim R, Fu Z, Carter DA, Bilton J, Imrie H, Ajuh P, Neil T, Cubbon RM, Kearney MT, Prasad RK, Evans PC, Fx J, Beech DJ. Piezo1 integration of vascular architecture with physiological force. 2015;

291. Climent E, Benaiges D, Pedro-Botet J. Hydrophilic or Lipophilic Statins? *Front Cardiovasc Med*. 2021;8:687585.

292. Lim SY. Role of Statins in Coronary Artery Disease. *Chonnam Med J*. 2013;49:1.

293. Indolfi C, Cioppa A, Stabile E, Di Lorenzo E, Esposito G, Pisani A, Leccia A, Cavuto L, Stingone AM, Chieffo A, Capozzolo C, Chiariello M. Effects of hydroxymethylglutaryl coenzyme A reductase inhibitor simvastatin on smooth muscle cell proliferation in vitro

and neointimal formation in vivo after vascular injury. *Journal of the American College of Cardiology*. 2000;35:214–221.

294. Nohria A, Prsic A, Liu P-Y, Okamoto R, Creager MA, Selwyn A, Liao JK, Ganz P. Statins inhibit Rho kinase activity in patients with atherosclerosis. *Atherosclerosis*. 2009;205:517–521.

295. Cai A, Zhou Y, Li L. Rho-GTPase and Atherosclerosis: Pleiotropic Effects of Statins. *JAHA*. 2015; 4.

296. Mierke CT. Mechanical Cues Affect Migration and Invasion of Cells From Three Different Directions. *Front Cell Dev Biol*. 2020;8:583226.

297. Sheets K, Wunsch S, Ng C, Nain AS. Shape-dependent cell migration and focal adhesion organization on suspended and aligned nanofiber scaffolds. *Acta Biomaterialia*. 2013;9:7169–7177.

298. Li C-B, Li X-X, Chen Y-G, Gao H-Q, Bao M-C, Zhang J, Bu P-L, Zhang Y, Ji X-P. Simvastatin exerts cardioprotective effects and inhibits the activity of Rho-associated protein kinase in rats with metabolic syndrome. *Clin Exp Pharmacol Physiol*. 2012;39:759–764.

299. Ahmed S, Mabeza P, Warren DT. A model for estimating traction force magnitude reveals differential regulation of actomyosin activity and matrix adhesion number in response to smooth muscle cell spreading. Cell Biology; 2019

300. Balzer EM, Tong Z, Paul CD, Hung W, Stroka KM, Boggs AE, Martin SS, Konstantopoulos K. Physical confinement alters tumor cell adhesion and migration phenotypes. *FASEB j*. 2012;26:4045–4056.

301. Trepat X, Chen Z, Jacobson K. Cell Migration. In: Terjung R, editor. Comprehensive Physiology. Wiley; 2012 [cited 2022 Mar 10]. p. 2369–2392.

302. Bretscher MS. On the shape of migrating cells — a `front-to-back' model. *Journal of Cell Science*. 2008;121:2625–2628.

303. Bergert M, Chandradoss SD, Desai RA, Paluch E. Cell mechanics control rapid transitions between blebs and lamellipodia during migration. *Proc Natl Acad Sci USA*. 2012;109:14434–14439.

304. Baskaran JP, Weldy A, Guarin J, Munoz G, Shpilker PH, Kotlik M, Subbiah N, Wishart A, Peng Y, Miller MA, Cowen L, Oudin MJ. Cell shape, and not 2D migration, predicts extracellular matrix-driven 3D cell invasion in breast cancer. *APL Bioengineering*. 2020;4:026105.

305. Tanimoto H, Sano M. A Simple Force-Motion Relation for Migrating Cells Revealed by Multipole Analysis of Traction Stress. *Biophysical Journal*. 2014;106:16–25.

306. Dumontet C, Jordan MA. Microtubule-binding agents: a dynamic field of cancer therapeutics. *Nat Rev Drug Discov*. 2010;9:790–803.